Power law diffusion in drying processes

Document Version:
Publisher's PDF, also known as Version of Record (includes final page, issue and volume numbers)

Please check the document version of this publication:

• A submitted manuscript is the version of the article upon submission and before peer-review. There can be important differences between the submitted version and the official published version of record. People interested in the research are advised to contact the author for the final version of the publication, or visit the DOI to the publisher's website.
• The final author version and the galley proof are versions of the publication after peer review.
• The final published version features the final layout of the paper including the volume, issue and page numbers.

Link to publication

POWER LAW DIFFUSION
IN
DRYING PROCESSES

W. J. COUMANS

POWER LAW DIFFUSION IN DRYING PROCESSES

POWER LAW DIFFUSION
IN
DRYING PROCESSES

door

WILHELMUS JOHANNES COUMANS

geboren te Weert

Dit proefschrift is goedgekeurd door

1^e promotor: prof.ir. K.Ch.A.M. Luyben, Technische Universiteit Delft

2^e promotor: prof.dr.ir. D. Thoenes, Technische Universiteit Eindhoven

to my mother,

Marianne and Steven

ACKNOWLEDGEMENTS

CURRICULUM VITAE

The author was born on november, 15, 1945 at Weert, the Netherlands.
After his secondary education and military service he joined Dutch State
Mines (DSM) at Geleen in 1966. As a working student he followed a study
for chemical analist. After his examination in 1969 (cum laude) he
started to work at Eindhoven University of Technology in the Polymer
Engineering Group of Prof. D. Heikens. In 1970, again as a working
student, he began his studies for chemical engineer at Eindhoven, which
he concluded in 1978 (cum laude). His graduate research in the field of
mechanical behaviour of plastic materials was performed in the group of
Prof. D. Heikens. In 1980 he became the assistant of the late Prof.
H.A.C. Thijssen, who stimulated him to start this research on drying in
1982.

SUMMARY

In solids drying the calculation of drying rates and drying times is
complicated by the concentration dependence of the diffusion coefficient
and the shrinkage of the drying bodie due to the moisture loss. The
calculation is further complicated if particles contain an internal gas
core (e.g. in spray drying), which expands or shrinks during drying. In
principle even the most complex processes can be calculated numerically.
However, the lack of known product properties (for instance the relation
between diffusion coefficient and moisture concentration) and the extre-
mely difficult and laborious programming render the numerical approach
prohibitive for practical application by process engineers and desig-
ners. It is the aim of this research to provide easily to handle *short-
cut calculation procedures*, which are applicable to slabs, massive and
hollow cylinders and spheres, irrespective of their degree of shrinkage.
Diffusion of moisture in shrinking and non-shrinking bodies of the
various geometries is described by a generalized diffusion equation.
This equation has been solved numerically for a *power law dependence* of
the diffusion coefficient on moisture concentration. Two boundary condi-
tions, which are typical for two main drying stages, are considered:
constant surface flux and *constant surface concentration*. Both drying
stages can be subdivided into a *Penetration Period* (centre concentration
hardly affected) and a *Regular Regime* (centre concentration clearly
affected).
The numerical computer output can be described by simple correlations.
For both Penetration Periods the introduction of a *G-parameter* appears
to be helpful and for both Regular Regimes the concept of *Sherwood
numbers* of the dispersed phase is of great importance. Drying times
calculated with the correlations deviate less than 5% from the "exact"
calculated values.
Moreover, a drying apparatus has been developed, to determine the weight
of a sample (thin layer) as a function of time during drying (*drying
curve*). The approximate correlations are used to evaluate the experimen-
tal drying curves for obtaining the relevant model parameters. Next the
same correlations are used to predict drying curves at different drying
conditions. Deviations between *predicted* and *experimental* drying curves
of aqueous maltodextrin solutions appear to vary from a few percent to
about 30% .

SAMENVATTING

De berekening van het drooggedrag van deeltjes is erg gecompliceerd,
omdat de diffusiecoefficient van het migrerende vocht veelal sterk
afhangt van het vochtgehalte. Een "exacte" berekening van het droogge-
drag vereist kennis van numerieke methoden, grote vaardigheid in het
programmeren en de beschikking over een main-frame computer. Bovendien
is de relatie tussen de diffusiecoefficient en het vochtgehalte meestal
onbekend en zijn moeizame experimenten noodzakelijk ter bepaling hier-
van. Proces ingenieurs en ontwerpers van droogapparatuur hebben in hun
dagelijkse praktijk behoefte aan gemakkelijk te hanteren rekenproce-
dures.

Het onderzoek beschrijft een *kortsluitrekenmethode*, welke uitgaat van
een machtsrelatie tussen de diffusiecoeffient en het vochtgehalte (*power
law diffusion*). De (cor)relaties van deze vereenvoudigde berekening zijn
gebaseerd op de "exacte" numeriek berekende oplossingen. De afwijkingen
in droogtijden, berekend volgens de "exacte methode" en de kortsluit-
methode, bedragen gemiddeld 2% en zijn maximaal 5% . De kortsluitmethode
is toepasbaar voor holle en massieve deeltjes met elke graad van krimp
(vlakke lagen, cylinders en bollen).

Bovendien is een geautomatiseerde meetopstelling ontwikkeld, waarmee het
gewicht van een monster (dunne laag) tijdens een droogproces kan worden
geregistreerd (*droogcurven*). M.b.v. de vergelijkingen van de kortsluit-
methode worden uit deze experimentele droogcurven de relevante model
parameters berekend; vervolgens wordt met de kortsluitmethode het droog-
gedrag bij andere droogcondities voorspeld. De afwijkingen tussen voor-
spelde en experimentele droogtijden van maltodextrine oplossingen vari-
ëren van enkele procenten tot 30% .

CONTENTS

CHAPTER I

INTRODUCTION

Though drying is an economical important unit operation, which is
frequently used in many branches of industry, it still is a hard to
grasp process. The design of dryers is complicated by:
- the changing conveyance properties of the material during drying
  e.g. a wet droplet may first change into a sticky material and
  eventually into a free flowing powder;
- the prediction of the required drying time, which is a rather
  difficult calculation problem, especially if drying rates are fully
  controlled by diffusion of moisture in the material.
In this thesis the attention is focussed on the latter problem.

1.1 Approximate Calculation Methods.

In solids drying mass transfer takes place from a dispersed phase
(e.g. droplet of milk) to a continuous phase (e.g. air). Interface
mass transfer processes are usually split up into mass transfer in the
continuous phase and mass transfer in the dispersed phase.
Mass transfer in the continuous phase is generally described in a
phenomenological way by means of a mass transfer coefficient (one film
model). For some situations literature provides theoretical relations

for the calculation of mass transfer coefficients, however in most cases (semi-)empirical correlations of various dimensionless groups are to be used [1-9]. If mass transfer is fully controlled by the conditions of the continuous phase, the accuracy of the calculated drying rates is 20-30% at the best [3].

Mass transfer in the dispersed phase depends on *process conditions* (e.g. mass transfer in the gas phase, temperature and humidity of the drying air) and *product properties*, such as:

- *sorption-isotherm* [10,11], which describes the equilibrium between the thermodynamic moisture activity and the moisture content of the material;

- *parameters describing the various mass transfer mechanisms*, such as molecular diffusion, capillary transport, etc. [12,13]. In this thesis we confine ourselves to the description of rigid systems with a uniform temperature, thus internal circulations and temperature gradients do not contribute to mass transfer;

- *shrinkage behaviour* [14-16]; three cases can be distinguished:
  maximum-shrinking, if the decrease of the body volume equals the volume of the removed moisture;
  partial-shrinking, if the decrease of the body volume is less than the volume of the removed moisture;
  non-shrinking, if the volume of the body remains constant during drying.

  In case of partial- and non-shrinking systems a porous solid will be formed during a drying process.

On the one hand, calculation models taking into account all mass transfer mechanisms with a maximum of physical relevance are generally not suited for practical use. On the other hand, easy to handle

calculation models with a too small physical basis often fail in predicting the drying behaviour with sufficient accuracy. Thus, in developing physical/mathematical models for the calculation of drying processes a good balance has to be found between the theoretical basis and the manageability of the calculation method.

Despite the occurrence of various mechanisms, quite often mass transfer is described with a single parameter, viz. the effective diffusion coefficient (D), in which many mechanisms are lumped together. This rather rigid physical simplification implies that in general the diffusion coefficient will be strongly dependent on moisture content and temperature; a decrease of several orders of magnitude during drying may occur, e.g. for water in aqueous carbohydrate solutions [17-22]. For the mathematical description of the drying processes two main problems remain:

first, from a mass balance over an infinite small shell volume the diffusion equation is obtained. For constant diffusivity this equation has been solved analytically for many initial and boundary conditions. However, especially for particles with the geometry of a hollow cylinder or sphere the algebraic solutions are rather complicated and relatively difficult to handle (see Chapter IV). For concentration dependent diffusion coefficients a numerical approach is required. The numerical calculations are complicated, require highly sophisticated programming skill and high speed computers.

second, product properties, such as the relationship between diffusion coefficient and moisture content are rather inaccurate; deviations of 50% or more, depending on the range of moisture content, are quite common; moreover, in most cases product properties are even unknown and must be obtained from rather laborious experiments.

4

In general, *mathematically exact calculation procedures may be very complicated and require product properties, which however, are not exact ,so there is a lot of room left for approximate calculation methods without substantial loss of overall accuracy.*

Approximate calculation procedures show the following advantages:
first, they offer a better insight; simple equations will contribute to a better understanding of drying kinetics;
second, they are relatively easy to handle, especially of interest for practical engineers and designers;
third, the simple equations can be used in the evaluation of relevant product properties from laboratory drying experiments;
fourth, the approximate methods can also be useful in building up algorithms for controlling drying processes.

1.2 Strategy for Developing Approximate Calculation Methods.

In Figure 1.1 a strategy for developing approximate calculation methods is schematically depicted. First of all a description of the processs in terms of physical phenomena is required. From this *physical model* a *mathematical model* can be derived. Usually the mathe-matical model consists of a partial differential equation with initial and boundary conditions. Next, we have to find the *exact solutions.* Sometimes these solutions can be found as algebraic expressions in literature, however in most cases one has to resort to a numerical approach. For *extreme situations* (e.g. short times, large times, low flux, high flux) quite often the exact solutions reduce to a simple form. Then the approximate solutions of the two extremes are connected by means of a simple correlation (*short-cut of extremes,* therefore the approximate methods are often referred to as *short-cut*

calculation methods). Finally, the approximate solutions are compared with the exact solutions. The result of this *verification* determines whether one has to make corrections or not.

It will be shown in this thesis that by tolerating small errors ($\leq$5%) tremendous simplifications of the calculation procedure can be achieved.

```
            ┌──────────────────────┐
    ┌──────▶│   PHYSICAL MODEL     │
    │       └──────────────────────┘
    │                  │
    │                  ▼
    │       ┌──────────────────────┐
    │       │  MATHEMATICAL MODEL  │
    │       └──────────────────────┘
    │                  │
    │                  ▼
    │       ┌──────────────────────┐
    │       │    EXACT SOLUTION    │
    │       └──────────────────────┘
    │                  │
    │                  ▼
    │       ┌──────────────────────┐
    │       │  EXTREME SOLUTIONS   │
    │       └──────────────────────┘
    │                  │
    │                  ▼
    │       ┌──────────────────────┐
    │       │ SHORT-CUT OF EXTREMES│
    │       └──────────────────────┘
    │                  │
    │                  ▼
    │       ┌──────────────────────┐
    │       │    VERIFICATION      │
    │       └──────────────────────┘
    │                  │
    └──── not O.K. ────┤
                       │
                       ▼
                     O.K.
```
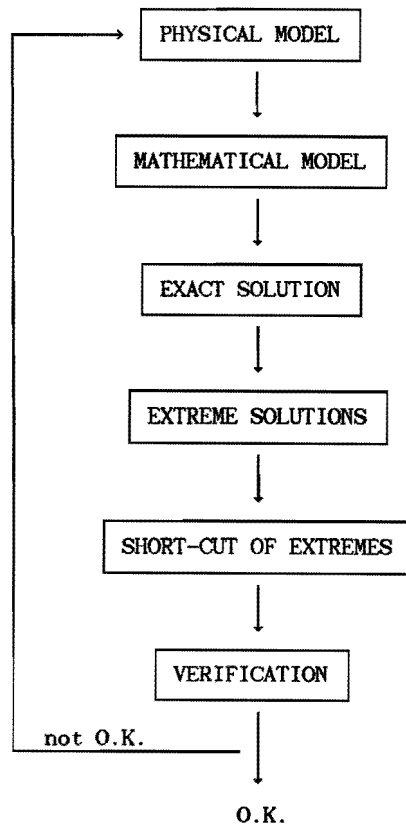
Figure 1.1 Strategy for developing short-cut calculation methods.

1.3 Short History

This research on approximate calculation methods for drying processes
is a continuation of the investigations carried out by Schoeber
[23,24], Luyben, Olieman, Bruin and Liou [25-30]. Similar research on
drying kinetics was later started by Yamamoto, Sano and Hoshika
[31,32].

Schoeber analyzed the numerical solutions of the diffusion equation
for many kinds of concentration dependence of the diffusion coeffi-
cient. From the numerical solutions he developed general approximate
methods for the calculation of mass transfer in diffusion processes.
Schoeber's concept is based on the combination of "short time solu-
tions" (Penetration Period) and "large time solutions" (Regular
Regime). It appears from his analysis that the Regular Regime solu-
tions can serve as a basis for the evaluation of diffusion coeffi-
cients from experimental drying curves.

Luyben measured the drying curves of a number of food materials and
compared them with calculated drying curves obtained from short-cut
calculations (based on Schoeber's approach) and "exact" numerical
calculations. Furthermore, based on Schoeber's equations, he developed
a method to derive diffusion coefficients from non-isothermal drying
curves of bodies with various geometries (slabs, cylinders and
spheres).

The concentration dependence of the diffusion coefficient can be
described in many ways: exponential, logaritmic, power law, polynom,
etc.. However, none of them will really describe in a satisfying way
the experimental values of the diffusion coefficient of various sys-
tems over the whole concentration range of interest, unless one re-
sorts to equations with many (more than two) fitting parameters.

Based on the work of Schoeber and Luyben a power law dependence of the
effective diffusion coefficient (D) with concentration was put forward

by Liou and Bruin:

$$D\rho_s^2 = b \left[\frac{\rho_m}{\rho_s}\right]^a \qquad (1.1)$$

in which, D is diffusion coefficient $[m^2/s]$, ρ_m and ρ_s are the concentrations of moisture and solid $[kg/m^3]$, a and b are fitting parameters.

Liou proposed a short-cut calculation method for drying rates, drying times and concentration profiles. His method is valid for non-shrinking and maximum-shrinking slabs, massive cylinders and massive spheres with a constant surface concentration.

Liou's approximate method for "power law diffusion" has been extended to hollow and massive systems with any degree of shrinkage and to systems with constant surface flux by Coumans and Thijssen [33,34]; this approach will be described systematically in this thesis.

1.4 Drying Stages.

The mathematical formulation of the external boundary condition of the diffusion equation depends on the drying stage. In this thesis three main stages are distinguished (see also Chapter IV):

Stage I, at the beginning of the drying process the surface moisture activity remains nearly constant. For slabs and non-shrinking cylinders and spheres this period is characterized by a nearly constant surface flux.

Stage II, both the boundary flux and the boundary concentration decrease considerably during this stage. The boundary condition now is more complex and requires good knowledge of the sorption-isotherm.

Stage III: the surface concentration, relative to its total change,
hardly changes anymore. Thus, by good approximation, there is a con-
stant surface concentration.

All three main stages can be subdivided into two substages:
Penetraton Period (for short times), which is characterised by a
centre concentration which has hardly changed.
Regular Regime (for large times), during which the centre concentra-
tion, compared to its initial value, significantly decreases; the most
striking feature of this drying stage is that _the drying behaviour has
become independent of the initial conditions._
It appears that every substage has its own approximate equations.

This thesis only deals with drying stages I and III. It is assumed
that drying stage II, which is rather hard to describe, has a minor
contribution to the total drying time (see Chapter VI); therefore
drying stage II has not been investigated. Approximate methods for the
calculation of the surface concentration as function of time (stage I)
and for the calculation of drying rates and drying times at any given
value of the averaged moisture concentration (stage III) have been
derived from the analytical and numerical solutions of the diffusion
equation.
The short-cut equations of drying stage I will be of special interest
e.g. for spray drying processes [21] in order to predict whether
droplets will agglomerate or not, or whether they will stick to the
wall of the dryer or not. Also the application of the method in
short-cut calculation methods for the prediction of aroma losses
during drying [35,36] is interesting. The equations of drying stage
III will be advantageous in predicting overall drying times, since for
high intensity drying this stage contributes dominantly to the total

drying time.

The described short-cut methods refer to mass transfer in dispersed phases, where diffusion plays an important role and even may become rate controlling; though this thesis emphasizes drying processes the methods described may also be applied to processes such as leaching, absorption, humidification and desorption.

1.5 Scope of this Thesis.

The contents of the chapters are briefly summarized below.

Chapter II: Based on a comparison of mass transfer in maximum- and non-shrinking systems, a generalized *mass transfer equation* is formulated for systems with any degree of shrinkage. Further some aspects of mass and heat transfer coefficients in the gas phase are considered.

Chapter III: Mass transfer in slabs, hollow and massive cylinders and spheres with any degree of shrinkage is described with a *generalized diffusion equation*. By transforming this equation into a dimensionless form, a similarity of solutions is obtained. Also a generalized representation of the total mass balance is presented.

Chapter IV: Approximate equations are derived from the analytical solutions of *non-shrinking systems with constant diffusivity*. It appears that this most simple drying situation yields approximate equations, which only need slight adaptations for shrinking systems with variable diffusion coefficients.

Chapter V: For power law diffusion in *systems with any degree of shrinkage* approximate equations are derived from the numerical solutions.

Chapter VI: An experimental set-up for the continuous registration of the weight of a drying slab as function of time is described. Several drying experiments have been performed with thin layers of aqueous maltodextrin solutions. From the socalled _drying curves_ (=sample weight versus time) relevant physical information is derived by means of the approximate equations of Chapter V. Finally, drying curves are predicted and compared with the experimental ones.

CHAPTER II

MASS AND HEAT TRANSFER IN DRYING PROCESSES

2.1 Introduction.

Mass transfer in drying bodies is often described by means of an effective diffusion coefficient. In literature one comes across many definitions of the diffusion coefficient and the mass transfer equations can take on many forms. Sometimes the definitions used are somewhat obscure.

The aim of this chapter is to define in an unambiguous way the basic equations for mass transfer in well-defined binary systems. Unfortunately, in most cases drying systems are thermodynamically ill-defined. Further, extra complications are caused by shrinkage due to the loss of moisture during drying. Therefore a comparison between shrinking and non-shrinking systems is given, leading to a generalized definition of the mass transfer equation for systems irrespective of their shrinkage behaviour.

The drying process is induced by the conditions of the external gas phase, especially the temperature, the humidity and the mass- and heat-transfer coefficients. The last part of this chapter deals with some aspects of these mass- and heat-transfer coefficients relevant for drying processes.

2.2 Mass Transfer in Ideal One-Phase Systems.

In one-phase systems, like gas mixtures and liquid solutions, two mechanisms for mass transfer can be distinguished:

- molecular diffusion caused by a concentration gradient;

- convection caused by a pressure gradient (forced convection) or a vertical density gradient (free convection); bulk flow may also be induced by a concentration gradient.

It is important to realize that the contribution of *each* mechanism depends on the definition of the coordinate system with respect to which mass fluxes are defined. In a coordinate system, fixed with respect to the observer, the mass flux n_i of a component i with concentration ρ_i and velocity v_i is given by:

$$n_i = \rho_i v_i \tag{2.1}$$

The mass flux n_i is built up of a convective flux and a diffusion flux j_i, which is defined with respect to a certain reference velocity v_{ref}. Equation 2.1 can also be written as:

$$n_i = \rho_i v_{ref} + \rho_i(v_i - v_{ref}) \tag{2.2}$$

or

$$n_i = \rho_i v_{ref} + j_i \tag{2.3}$$

The reference velocity v_{ref} can be defined as:

i)   the mass average velocity v:

$$v = \frac{\sum\limits_i \rho_i v_i}{\sum\limits_i \rho_i} = \frac{\sum\limits_i n_i}{\rho} \tag{2.4}$$

where ρ is the total mass concentration of the mixture.

ii) the volume average velocity $v^{\square}$:

$$v^{\square} = \frac{\sum_i \frac{\rho_i}{d_i} v_i}{\sum_i \frac{\rho_i}{d_i}} = \sum_i \frac{n_i}{d_i} \tag{2.5}$$

where d_i is the partial density of component i,

ρ_i/d_i is the volume fraction of component i in the mixture and

n_i/d_i is the volume flux of i.

iii) the velocity of another component in the mixture, for instance of component b, thus $v_{ref} = v_b$.

iv) molar average velocity v^o:

$$v^o = \frac{\sum_i c_i v_i}{\sum_i c_i} = \frac{\sum_i N_i}{c} \tag{2.6}$$

where c_i is the molar concentration of component i,

c is the total molar concentration of the mixture and

N_i is the molar flux of component i.

Most frequently the mass average velocity is chosen as a reference for the diffusion flux. Thus for a binary mixture with components a and b we get for the convective flux of a:

$$\rho_a v = \rho_a \frac{n_a + n_b}{\rho} = (n_a + n_b)\omega_a \tag{2.7}$$

where ω_a is the mass fraction of component a on total basis.

The diffusion flux j_a is described according to Fick's law with a

diffusion coefficient D_a:

$$j_a = -D_a \rho \frac{\partial \omega_a}{\partial r} \qquad (2.8)$$

From equations 2.3, 2.7 and 2.8 the basic equation for mass transfer
in binary solutions follows:

$$n_a = (n_a + n_b)\omega_a - D_a \rho \frac{\partial \omega_a}{\partial r} \qquad (2.9)$$

In fact equation 2.9 defines the diffusion coefficient D_a of component
a in a binary mixture. It can simply be proved that $D_a = D_b = D$.
Taking another reference velocity will change the separate
contributions of convection and molecular diffusion to the total mass
flux. In Table 2.1 a survey is given of expressions for the mass flux.
It should be realised that in all these equations the diffusion
coefficient D is defined according to equation 2.9. Further, all these
equations are equivalent, because they all describe the same mass
flux. However, in some special cases a sensible choice will lead to a
simplification of the flux expression, namely:

i)   no net mass flux (*equimass*)   : $n_a + n_b = 0$ ⟶ choose I

ii) no net volume flux (*equivolumetric*) : $\frac{n_a}{d_a} + \frac{n_b}{d_b} = 0$ ⟶ choose II

iii) Stefan diffusion   : $n_b = 0$ ⟶ choose I,II
                                                               III or IV

iv) no net molar flux (*equimolar*)   : $N_a + N_b = 0$ ⟶ choose IV

Strictly, the equations of Table 2.1 only apply to binary one-phase
systems, however most drying systems are multi-component systems and
consist of more than two phases.

Table 2.1 Survey of expressions for the massflux of
           component a in a binary mixture.

reference velocity	total mass flux	=	convective flux	+	diffusive flux
I mass average	n_a	=	$(n_a + n_b)\omega_a$	$-$	$D\rho\, \dfrac{\partial \omega_a}{\partial r}$
II volume average	n_a	=	$\left[\dfrac{n_a}{d_a} + \dfrac{n_b}{d_b}\right]\rho_a$	$-$	$D\, \dfrac{\partial \rho_a}{\partial r}$
III velocity of b	n_a	=	$n_b\, \dfrac{\omega_a}{1-\omega_a}$	$-$	$\dfrac{D\rho}{1-\omega_a}\, \dfrac{\partial \omega_a}{\partial r}$
IV molar average	N_a	=	$(N_a + N_b)x_a$	$-$	$Dc\, \dfrac{\partial x_a}{\partial r}$

Help equations:

1. $\rho_a + \rho_b = \rho$ 2. $\omega_a = \dfrac{\rho_a}{\rho}$ 3. $\omega_a + \omega_b = 1$

4. $c_a + c_b = c$ 5. $x_a = \dfrac{c_a}{c}$ 6. $x_a + x_b = 1$

7. $\omega_a = \dfrac{\rho_a}{\rho} = \dfrac{\rho_a}{\rho_a + \rho_b} = \dfrac{\rho_a/\rho_b}{1 + \rho_a/\rho_b}$

2.3 Mass Transfer in Real Systems.

In drying processes three types of systems can be distinguished:
maximum-shrinking, partial-shrinking and non-shrinking systems.
Henceforth it is assumed that shrinkage, if present, is isotropic
(e.g. the shape of a shrinking body does not change) and that partial
densities are constant.

2.3.1 Maximum-Shrinking Systems.

Shrinking is maximum if the volume decrease of the drying material

equals the volume of the removed moisture (Examples: sugar solutions,

milk, coffee extract, fruit juices). It is true that these systems are

seldom binary, however, with respect to the drying process they may be

considered as such with components moisture(m) and dissolved

solids(s). In these systems the volume balance reads:

$$\frac{\rho_m}{d_m} + \frac{\rho_s}{d_s} = 1 \qquad (2.10)$$

where ρ_m/d_m and ρ_s/d_s are the volume fractions of moisture and

dissolved solids respectively. Mass transfer of moisture and solids

occurs by means of convection and molecular diffusion, so the

equations of Table 2.1 may be applied. The basic mass transfer

equation now reads:

$$n_m = (n_m + n_s)\omega_m - D\rho \frac{\partial \omega_m}{\partial r} \qquad (2.11)$$

Because no pores are formed during drying, there is no net volume flux

in maximum shrinking systems, thus also:

$$n_m = - D \frac{\partial \rho_m}{\partial r} \qquad (2.12)$$

An expression for the moisture diffusion flux j_m^s with respect to the

solids velocity v_s is found as follows:

$$n_m = \rho_m v_s + j_m^s \qquad (2.13)$$

Also

$$n_s = \rho_s v_s \tag{2.14}$$

Eliminating n_m and n_s from equations 2.11, 2.13 and 2.14 gives:

$$j_m^s = - \frac{D\rho}{1-\omega_m} \frac{\partial \omega_m}{\partial r} \tag{2.15}$$

With the help equations of Table 2.1 this expression can be transformed into:

$$j_m^s = - D\rho_s \frac{\partial(\rho_m/\rho_s)}{\partial r} \tag{2.16}$$

It should be noticed, that ρ_m/ρ_s is the so-called solids based moisture concentration (kg m/kg s).

2.3.2 Non-Shrinking Systems.

Non-shrinking systems are characterized by a constant volume during drying. This means that the volume of the moisture, which has been removed from the system, will be replaced by an equal volume of gas. (Examples: air-drying of ceramics and sand.)

During the drying process of such systems a capillary porous material is built up, consisting of:

- three components viz. moisture (m), solid (s) and air (a),
- several phases, viz. a solid matrix (S) with pores containing liquid moisture (L) and/or moisture vapour (G) and/or air (G).

Mass transfer of moisture in capillary porous materials may occur by several mechanisms [12,13], such as capillary liquid flow, molecular diffusion, evaporation-condensation, surface diffusion, etc.. During a particular stage of the drying process one of these mechanisms may

dominate, but in general several mechanisms will be present simultaneously. A fundamental description of mass transfer based on all occurring mechanisms will lead to rather complicated physical/ mathematical models.

In a rigorous but more practical approach the non-shrinking material is considered as a pseudo one-phase system with three components viz. moisture(m), solid(s) and air(a). The volume fraction of the gaseous components (air/vapour) is called the porosity ϵ. Assuming that a neglible part of the moisture is present as vapour the volume balance reads:

$$\frac{\rho_m}{d_m} + \frac{\rho_s}{d_s} = 1-\epsilon \tag{2.17}$$

Similar to a binary system the diffusion coefficient of this ternary system is defined as:

$$n_m = (n_m+n_s+n_a)\omega_m - D\rho \frac{\partial \omega_m}{\partial r} \tag{2.18}$$

Because a certain volume of liquid (moisture) is replaced by an equal volume of gas (air) the averaged moisture flux will be about 1400 times larger than the averaged air flux, therefore:

$$n_m \approx (n_m+n_s)\omega_m - D\rho \frac{\partial \omega_m}{\partial r} \tag{2.19}$$

In non-shrinking systems a rigid non-moving solid matrix exists $(n_s=0)$, so that:

$$n_m = - \frac{D\rho}{1-\omega_m} \frac{\partial \omega_m}{\partial r} \tag{2.20}$$

and from equation 2.13:

$$n_m = j_m^s \tag{2.21}$$

Taking into account that the solid concentration is constant $(\rho_s = \rho_{so})$ and that

$$\omega_m = \frac{\rho_m}{\rho} = \frac{\rho_m}{\rho_m + \rho_s + \rho_a} \approx \frac{\rho_m}{\rho_m + \rho_s} \tag{2.22}$$

equation 2.20 can be transformed into:

$$n_m = j_m^s = -D \frac{\partial \rho_m}{\partial r} = -D\rho_s \frac{\partial(\rho_m/\rho_s)}{\partial r} \tag{2.23}$$

From the above it can be stated that a non-shrinking system can also be looked upon as a pseudo binary system (m+s). However, it is not meaningful to speak now in terms of equivolumetric mass transfer or not, because mass transfer of moisture may occur both as vapour and liquid. Further, the parameter D should be considered now as an effective diffusion coefficient, in which the contributions of several mass transfer mechanisms are lumped together.

2.3.3 Systems with Any Degree of Shrinkage.

Characteristics of maximum-shrinking and non-shrinking systems are summarized once more in Table 2.2. From this table it can be seen that the same mass transfer equations apply for two extremes in shrinking behaviour, so it is obvious to apply these equations also for intermediate shrinking behaviour. Thus for all systems, regardless

Table 2.2 Comparison of mass transfer in maximum-shrinking
and non-shrinking systems.

MAXIMUM-SHRINKING SYSTEM	NON-SHRINKING SYSTEM
mass transfer in one phase	mass transfer in more phases
pseudo binary system (m+s)	pseudo ternary (m+s+gas) or pseudo binary (m+s) system
migrating components in solution	migrating components may occur in several aggregate states
two mechanisms of mass transfer	several mechanisms of mass transfer
volume balance: $$\frac{\rho_m}{d_m} + \frac{\rho_s}{d_s} = 1$$	volume balance: $$\frac{\rho_m}{d_m} + \frac{\rho_s}{d_s} = 1-\epsilon$$
equivolumetric mass transfer: $$\frac{n_m}{d_m} + \frac{n_s}{d_s} = 0$$	non-moving solid matrix: $$n_s = 0 \quad \text{and} \quad \rho_s = \rho_{s0} = \text{constant}$$
practical and thermodynamical-ly meaningful definition of the diffusion coefficient:	practical but thermodynamically meaningless definition of the diffusion coefficient:

$$n_m = (n_m + n_s)\omega_m - D\rho_s \frac{\partial \omega_m}{\partial r}$$

equivolumetric $n_s = 0$ and $\rho_s =$ constant

$$n_m = - D \frac{\partial \rho_m}{\partial r} \quad \text{and} \quad j_{mi}^s = - D\rho_s \frac{\partial (\rho_m/\rho_s)}{\partial r}$$
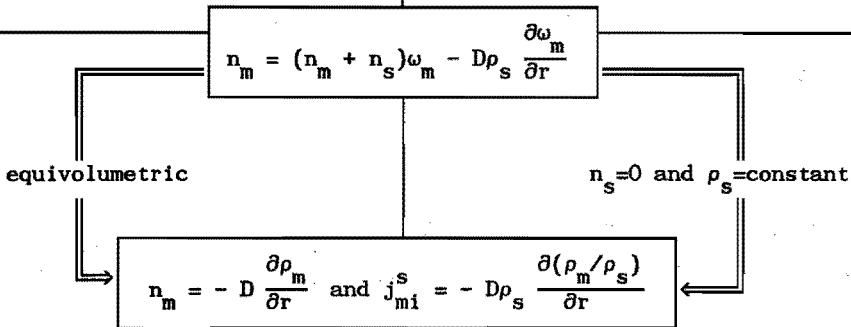
their degree of shrinkage, equation I (see Table 2.1) is taken as the generalized basic equation for mass transfer:

$$n_m = (n_m + n_s)\omega_m - D\rho \frac{\partial \omega_m}{\partial r} \tag{2.24}$$

Because equations 2.13 and 2.14 are general, it follows that equation 2.15 gives a general relation for the diffusion flux with respect to the solids velocity; applying equation 2.22 then yields:

$$j_m^s = - D\rho_s \frac{\partial(\rho_m/\rho_s)}{\partial r} \tag{2.25}$$

The generalized volume balance reads:

$$\frac{\rho_m}{d_m} + \frac{\rho_s}{d_s} = 1-\epsilon \tag{2.26}$$

where the porosity ϵ not only depends on moisture concentration but also on the degree of shrinkage. The relationship among porosity, moisture concentration and degree of shrinkage will be worked out in Chapter III.

Irrespective of the shrinkage behaviour, it appears that the basic mass transfer equation 2.24 can also be transformed into:

$$n_m = -D \frac{\partial \rho_m}{\partial r} \tag{2.27}$$

This result seems to be trivial, however it is not, because it can not be seen beforehand that equations 2.24, 2.25 and 2.27 are also consistent for systems irrespective their shrinkage behaviour.

2.4 Simultaneous Heat and Mass Transfer.

For a description of the external mass transfer of a drying body one has to deal correctly with the simultaneously occurring heat transfer from the gas phase towards the body. A sophisticated approach for this problem can be found in literature [8,9]. However, in this section simple basic equations for mass and heat transfer in the gas phase will be given.

2.4.1 Heat Flux and Heat Transfer Coefficient.

In most convective dryers heat transfer takes place to bodies submerged in a relatively extended gas phase, mostly air. It is assumed that the resistance for heat transfer is concentrated in a thin film at the interface i (Figure 2.1). In this film, with thickness δ_H, the temperature of the gas phase increases from θ_i' at the interface to θ_∞' in the bulk.
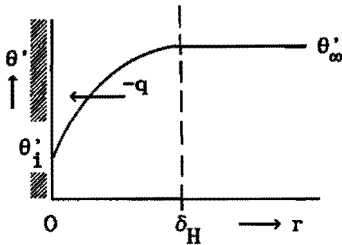
Figure 2.1 Schematic representation of film for heat transfer.

Consider now steady-state conditions for mass and heat transfer. The heat flux q in the film consists of a convective heat flux caused by the moisture flux and a conductive heat flux due to the temperature gradient:

$$q = n_m c_{pv}(\theta' - \theta_i') - \lambda \cdot \frac{\partial \theta'}{\partial r} \qquad (2.28)$$

where c_{pv} is the heat capacity of the vapour; the diffusive
contribution is written by analogy with the Fourier law of heat
conduction, however, the quantity λ' is now the so called "turbulent
coefficient of thermal conductivity" or "Eddy Conductivity" [1]. It is
important to realize that λ' is not a physical property of the gas
phase, but depends on position, direction and the nature of the
turbulent flow in the film.

Because of steady-state conditions equation 2.28 can now be integrated
between the limits r=0 (interface) and $r=\delta_H$ (bulk). In case of no mass
flux (n_m=0) integration yields:

$$q = \frac{1}{\int\limits_0^{\delta_H} \frac{\partial r}{\lambda'}} (\theta_i' - \theta_\infty') \qquad (2.29)$$

The heat transfer coefficient α' is defined according to:

$$\frac{1}{\alpha'} = \int\limits_0^{\delta_H} \frac{\partial r}{\lambda'} \qquad (2.30)$$

and thus equation 2.29 now becomes:

$$q = \alpha'(\theta_i' - \theta_\infty') \qquad (2.31)$$

For an adiabatic drying process ($n_m \neq 0$) it is assumed that all the heat
reaching the interface is used for evaporation of the moisture, thus:

$$q + n_m L_i = 0 \qquad (2.32)$$

where L_i is the enthalpy of evaporation at θ_i'.

Elimination of n_m from equations 2.28 and 2.32 and next integration

yields:

$$q = -\alpha' \frac{L_i}{c_{pv,f}} \ln\left[1 + \frac{c_{pv,f}}{L_i} (\theta'_\infty - \theta'_i)\right] \qquad (2.33)$$

where $c_{pv,f}$ is the heat capacity of the vapour at average film conditions.

The effective heat transfer coefficient (α'_{eff}) is defined as:

$$q = \alpha'_{eff}(\theta'_i - \theta'_\infty) \qquad (2.34)$$

Thus:

$$\frac{\alpha'_{eff}}{\alpha'} = \frac{\ln\left[1 + \frac{c_{pv,f}}{L_i} (\theta'_\infty - \theta'_i)\right]}{\frac{c_{pv,f}}{L_i} (\theta'_\infty - \theta'_i)} \qquad (2.35)$$

In many practical drying situations $\frac{c_{pv,f}}{L_i} (\theta'_\infty - \theta'_i) \ll 1$ and a first approximation of equation 2.35 is given by:

$$\frac{\alpha'_{eff}}{\alpha'} = 1 - \frac{1}{2} \frac{c_{pv,f}}{L_i} (\theta'_\infty - \theta'_i) \qquad (2.36)$$

Quite often it even holds that $\alpha'_{eff} \approx \alpha'$. It can be concluded now that *in many practical drying situations the influence of mass transfer on the heat transfer coefficient α' will be neglible.*
Values of α' are calculated from (semi-) empirical correlations for heat transfer [1-9], which take in general the following form:

$$Nu = c_1 + c_2 Re^n Pr^m \qquad (2.37)$$

where Nu is Nusselt number, Re is Reynolds number, Pr is Prandtl
number, c_1, c_2, n, m are (semi-)empirical constants. In Table 2.3 the
definitions of Nu, Re and Pr are summarized.

2.4.2 Mass Flux and Mass Transfer Coefficient.

Consider steady-state mass transfer from the surface of a drying
material to an unsaturated drying gas. It is generally assumed, that
the resistance for mass transfer is concentrated in a thin film close
to the interface (Figure 2.2).
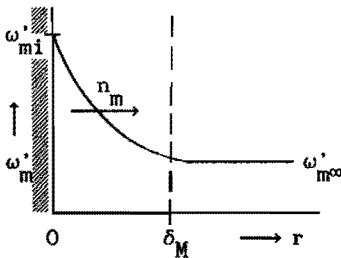
Figure 2.2 Schematic representation
of film for mass transfer.

The gas phase may be seen as a pseudo binary one-phase system with
components moisture(m) and air(a).
In a way similar to the heat transfer coefficient(§ 2.4.1), the mass
transfer coefficient k' in the gas phase is defined by:

$$\frac{1}{k^{\cdot}} = \int_0^{\delta_M} \frac{dr}{D^{\cdot}} \tag{2.38}$$

With shrinking systems no air is transferred across the interface.
With non-shrinking or partial-shrinking systems the air flux through
the interface will be negligible with respect to the moisture flux
(§ 2.3.2). So, the mass transfer of moisture in the film can be
described as a Stefan diffusion process:

$$n_m = \frac{D'\rho'}{1-\omega'_m} \frac{\partial \omega'_m}{\partial r} \qquad (2.39)$$

By integrating this equation a problem arises. In most practical cases the moisture concentration will be very low, so that ρ' is hardly affected by the concentration. However, because of simultaneous heat transfer a temperature gradient in the film exists and ρ' will be a function of space r. Finding the space dependence of ρ' is a rather complicated problem. One can get around this difficulty by putting a constant value ρ'_f, which is defined as the total concentration at the average film conditions θ'_f and ω'_f, where:

$$\theta'_f = \frac{\theta'_i + \theta'_\infty}{2} \qquad \text{and} \qquad \omega'_f = \frac{\omega'_i + \omega'_\infty}{2} \qquad (2.40)$$

Integration of equation 2.39 now yields the expression for the mass flux in the film:

$$n_m = k'\rho'_f \ln\left[\frac{1-\omega'_{m,\infty}}{1-\omega'_{m,i}}\right] \qquad (2.41)$$

The effective mass transfer coefficient k'_{eff} is defined as:

$$n_m = k'_{eff}\rho'_f(\omega'_{mi} - \omega'_{m\infty}) \qquad (2.42)$$

From equations 2.41 and 2.42 follows:

$$\frac{k'_{eff}}{k'} = \frac{\ln\left[\frac{1-\omega'_{m\infty}}{1-\omega'_{mi}}\right]}{\omega'_{mi} - \omega'_{m\infty}} \qquad (2.43)$$

At not too high temperatures of the interface (e.g. $\theta_i' \lesssim 50\ ^oC$) the moisture concentrations in the film will be very low ($\omega_{mi}' \ll 1$ and surely $\omega_{m\infty}' \ll 1$) and a first approximation of equation 2.43 is:

$$\frac{k_{eff}'}{k'} \approx \frac{1}{1-\omega_{mi}'} \tag{2.44}$$

and in many practical drying situations even: $k_{eff}' \approx k'$.

The mass transfer coefficient k' is found from (semi-)empirical correlations, which can be obtained by analogy with the heat transfer correlations (Table 2.2). In general, the correlations for steady-state mass transfer to bodies, submerged in an extensive fluidum take on the following form (see also equation 2.37):

$$Sh = c_1 + c_2 Re^n Sc^m \tag{2.45}$$

where Sh is the Sherwood number for the gas phase and Sc is the Schmidt number.

Table 2.3   Analogy between Heat and Mass Transfer.

heat transfer			mass transfer		
number	symbol	definition	number	symbol	definition
Nusselt	Nu	$\dfrac{\alpha' l}{\lambda'}$	Sherwood	Sh	$\dfrac{k' l}{D'}$
Reynolds	Re	$\dfrac{v' l}{v'}$	Reynolds	Re	$\dfrac{v' l}{v'}$
Prandtl	Pr	$\dfrac{v'}{a'}$	Schmidt	Sc	$\dfrac{v'}{D'}$

CHAPTER III

GENERALIZED FORMULATION OF DIFFUSION EQUATION AND MASS BALANCE

3.1 Physical Model.

The physical model used in this thesis is based on the concept of a
concentration dependent diffusion coefficient, which accounts for the
fact that not all of the moisture is bound equally strong or through
the same physical mechanisms. Considered is the drying of shrinking
and non-shrinking bodies with the following standard geometries:
the infinite slab, the infinite (hollow) cylinder and the (hollow)
sphere.

Postulates underlying the physical model are as follows:

1.   The particle has a uniform temperature, which does not change
     with time (isothermal drying).

2.   The particle consists of two or three components:
     - solid component (e.g. milk solids);
     - moisture component (e.g. water);
     - gas component (e.g. air), replacing the removed moisture in
       case of not completely shrinking systems.

3.   Mass transfer in the particle, however, is regarded as a pseudo
     binary diffusion process (moisture and solid), for which,
     irrespective of the degree of shrinkage, the mass transfer

equations of §2.2.3 may be applied.

4. The moisture diffusion coefficient depends on the moisture
    content; for practical calculations a power-law relationship is
    proposed. The temperature dependence of the diffusion coefficient
    can be described by means of an Arrhenius type relation.

5. The volume reduction of shrinking systems is:
    - linear proportional to the moisture loss;
    - isotropic (no deformation of the body);
    - homogeneous (the local porosity in the moisture free solid is
      independent of the space coordinates).

6. The partial quantities (e.g. densities) of the constituting
    components are independent of the changing composition.

7. The moisture flux towards the gas phase, enclosed in hollow
    bodies, is assumed to be zero.

8. The size of the enclosure, in case of hollow bodies, remains
    constant.

9. Diffusion can be described by using only one space coordinate.

10. Drying starts with a body of homogeneous composition, not
    considering the hollow core if any.

11. The external boundary condition is determined by the equilibrium
    sorption properties of the material being dried and the
    conditions of the gas medium carrying off the moisture. Two
    special cases will be considered:
    - constant surface water activity (e.g. in case of non-shrinking
      bodies this means a constant surface flux);
    - constant surface water concentration (e.g. surface of the
      drying body close to equilibrium with the external gas medium).

3.2 Mathematical Model.

The diffusion equation describing moisture transfer follows from a mass balance over an infinite small shell volume:

Partial differential equation:

$$\frac{\partial \rho_m}{\partial t} = \frac{1}{r^v} \frac{\partial}{\partial r}(r^v n_m) \qquad\qquad (3.1)$$

Initial condition:

$$t=0 \qquad R_1 < r < R_2(0) \qquad \rho_m = \rho_{m0} \qquad (3.2)$$

Boundary conditions:

$$t>0 \qquad r = R_1 \qquad \frac{\partial(\rho_m/\rho_s)}{\partial r} = 0 \qquad (3.3)$$

$$r = R_2(t) \qquad \rho_m = \rho_{mi}(t) \qquad (3.4)$$

or

$$-D\rho_s \frac{\partial(\rho_m/\rho_s)}{\partial r} = j_{mi}^s(t) \qquad (3.5)$$

---

in which ρ_m is the volume based concentration of the moisture (kg/m^3); t is time (s); r is the space coordinate (m); R_1 is the fixed internal radius of a hollow cylinder or sphere (see Figure 3.1); in case of a one sided drying slab $R_1=0$; $R_2(t)$ is the (dynamic) external radius of the (shrinking) body at time t; n_m is the moisture flux at space r (kg/m^2s) with respect to stationary space coordinates; j_{mi}^s is the moisture flux through the external interface (kg/m^2s); v is the *geometry parameter*, with

$v = 0$ infinite slab

$v = 1$ infinite massive or hollow cylinder

$v = 2$ massive or hollow sphere
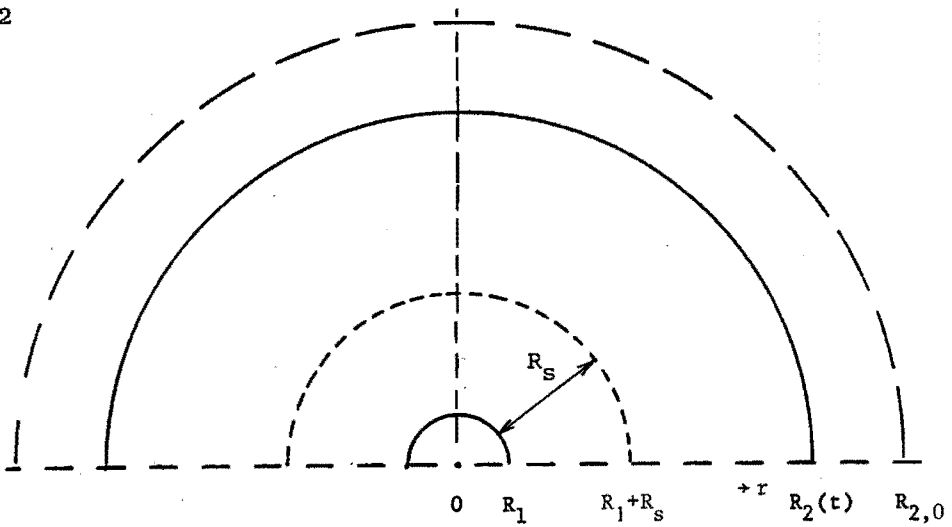
Figure 3.1 Illustration of the boundary planes for (non-)shrinking hollow cylinders and spheres.

3.3 Dimensionless Diffusion Equation.

The mathematical transformation of the diffusion equation (eqns. 3.1-3.5) into a dimensionless form is described in Appendix A. Similar transformations for maximum- and non-shrinking systems have been given by Schoeber [23], Liou [28] and Van de Lijn [21]. In this thesis their work is generalized to massive and hollow systems with any degree of shrinkage. The transformation of the diffusion equation results in:

Generalized partial differential equation:

$$\frac{\partial m}{\partial \tau} = \frac{\partial}{\partial \phi}(D_r X^2 \frac{\partial m}{\partial \phi}) \qquad (3.6)$$

Initial condition:

$$\tau = 0 \qquad 0 \leq \phi \leq 1 \qquad m = 1 \qquad (3.7)$$

Boundary conditions:

$$\tau > 0 \qquad \phi = 0 \qquad X \frac{\partial m}{\partial \phi} = 0 \qquad (3.8)$$

$$\phi = 1 \qquad m = m_i \qquad (3.9)$$

or

$$-D_r X_i \frac{\partial m}{\partial \phi} = F \qquad (3.10)$$

The various (dimensionless) parameters and the shrinkage model used are explained in the following sections.

3.3.1 Mass Concentration.

The solids based moisture concentration u is defined as kg moisture per kg dry solid (kg m/kg ds), so that:

$$u = \frac{\rho_m}{\rho_s} \tag{3.11}$$

The dimensionless concentration m is defined as:

$$m = \frac{u - u_\#}{u_0 - u_\#} = \frac{v - v_\#}{v_0 - v_\#} \qquad \text{with } 0 \leq m \leq 1 \tag{3.12}$$

in which v is the ratio of the volume fractions of moisture (ρ_m/d_m) and solid (ρ_s/d_s), expressed by:

$$v = \frac{d_s}{d_m} \frac{\rho_m}{\rho_s} = \frac{d_s}{d_m} u \tag{3.13}$$

In this expression d_s and d_m are the partial densities of solid and moisture respectively. It is assumed that the partial densities are independent of composition and are equal to the densities of the pure components ($d_m = d_{mp}$, $d_s = d_{sp}$). The initial value of v is denoted as v_0, the averaged value as $\bar{v}$ and the equilibrium value as $v_\ast$; $v_\#$ is some arbitrary reference value, e.g. the value where the diffusion coefficient is practically zero, or the equilibrium value $v_\ast$.

3.3.2 Space Coordinate.

The dimensionless solids based space coordinate ϕ is defined as:

$$\phi = \frac{\int_{R_1}^{r} \rho_s r^\upsilon dr}{\int_{R_1}^{R_2} \rho_s r^\upsilon dr} \qquad \text{with } 0 \leq \phi \leq 1 \qquad (3.14)$$

This space coordinate is based on a ratio of amounts of dry solids. Introduction of this space coordinate turns a dynamic external boundary $(r=R_{2,t})$ into a fixed one $(\phi=1)$.

3.3.3 Diffusion Coefficient.

The dimensionless diffusion coefficient D_r is defined as:

$$D_r = \frac{D \rho_s^2}{D_0 \rho_{s0}^2} \qquad (3.15)$$

in which D is the actual diffusion coefficient (m^2/s); D_0 represents the value of the diffusion coefficient at ρ_{m0}.

3.3.4 Time.

The dimensionless time τ is defined as:

$$\tau = \frac{D_0 \rho_{s0}^2 \, t}{(d_{s,ap} R_s)^2} \qquad (3.16)$$

where the solid radius R_s is the thickness of a one sided drying slab
or the thickness of the shell of a hollow body if all the water has
been removed ($\bar{v}=0$); $d_{s,ap}$ is the apparent density of the moisture free
(porous) solid; it will be obvious that $d_{s,ap}$ will depend on the
degree of shrinkage and the initial moisture content. In general it is
true that :

$$\rho_{s0} \leq d_{s,ap} \leq d_{sp}$$

and
$$R_{s,p} \leq R_s \leq R_{2,0} - R_1 \tag{3.17}$$

3.3.5 Hollowness Factor.

The hollowness factor λ of the drying body is defined as:

$$\lambda = \frac{R_1}{R_1 + R_s} \quad \text{with } 0 \leq \lambda \leq 1 \tag{3.18}$$

By this definition the hollowness factor λ remains constant during
drying. For massive bodies $\lambda=0$; if $\lambda \to 1$ the shell thickness of a hollow
body is extremely thin with respect to its external radius, so in case
of λ-values approaching 1 the hollow geometry tends to be similar to
the slab geometry. For this reason the solids radius R_s of hollow
systems is based on the dry shell thickness and not on the dry body
radius, as is done by Schoeber [23].

3.3.6 Flux Parameter.

The dimensionless flux parameter F is defined as:

$$F = \frac{j_{mi}^{s} \, d_{s,ap} \, R_{s}}{D_{0}\rho_{s0}^{2}(u_{0}-u_{\#})}$$

(3.19)

During drying the flux parameter F will only change if j_{mi}^{s} changes, because all other quantities in equation 3.19 are constants.

3.3.7 X-parameter.

The definition of the X-parameter is given by:

$$X = (v+1)\frac{1-\lambda}{1-\lambda^{v+1}} \left[\lambda^{v+1} + (1-\lambda^{v+1})d_{s,ap} \int_{0}^{\phi} \frac{d\phi}{\rho_{s}}\right]^{\frac{v}{v+1}}$$

(3.20)

and X_{i} follows by putting $\phi{=}1$ in the above equation. The physical meaning of X_{i} will be explained in § 3.4.

The X-parameter still contains the volume based concentration ρ_{s}. The relation between ρ_{s} and ρ_{m} depends on the porosity of the material and therefore ρ_{s} can only be expressed in terms of the dimensionless concentration m if the shrinkage behaviour is known (see § 3.3.8).

3.3.8 Shrinkage Model.

Quite often the volume V of a material is a linear function of the average moisture content [44], which is expressed by:

$$V = V_{s}(1+\sigma\bar{v})$$

(3.21)

where the solids volume V_s is the moisture free volume of the material; $\bar{v}$ is the ratio of the averaged volume fractions of moisture and solid (eqn. 3.13); σ is the *shrinkage coefficient*, which is actually defined by equation 3.21.

The solids mass balance reads:

$$\bar{\rho}_s V = d_{s,ap} V_s \tag{3.22}$$

so from equations 3.21 and 3.22 follows:

$$\frac{d_{s,ap}}{\bar{\rho}_s} = 1 + \sigma \bar{v} \tag{3.23}$$

For non-shrinking systems $\bar{\rho}_s = \rho_{so} = d_{s,ap}$, so $\sigma = 0$.

For maximum-shrinking systems the volume balance reads:

$$\frac{\bar{\rho}_m}{d_m} + \frac{\bar{\rho}_s}{d_s} = 1 \tag{3.24}$$

or

$$\frac{d_s}{\bar{\rho}_s} = 1 + \bar{v} \tag{3.25}$$

Because now $d_s = d_{sp} = d_{s,ap}$ it follows that $\sigma = 1$.

In general, for drying bodies with constant partial quantities the shrinkage coefficient will obey to $0 \leq \sigma \leq 1$.

Assuming that shrinkage occurs isotropic and homogeneous and that σ is independent of moisture content, equation 3.23 will also be valid for local concentrations. Therefore:

$$\frac{d_{s,ap}}{\rho_s} = 1 + \sigma v \tag{3.26}$$

and the expression for the X-parameter now becomes:

$$X = (v+1)\frac{1-\lambda}{1-\lambda^{v+1}} \left[\lambda^{v+1} + (1-\lambda^{v+1}) \int_0^\phi (1+\sigma v)d\phi\right]^{\frac{v}{v+1}} \tag{3.27}$$

where v can be expressed in terms of the dimensionless concentration m by (eqn. 3.12):

$$v = v_\# + (v_0 - v_\#)m \tag{3.28}$$

The X_i-parameter follows from equation 3.27 with $\phi=1$:

$$X_1 = X_{1,\sigma=0} \left[1 + (1-\lambda^{v+1})\sigma\bar{v}\right]^{\frac{v}{v+1}} \tag{3.29}$$

where:

$$X_{1,\sigma=0} = (v+1)\frac{1-\lambda}{1-\lambda^{v+1}} \tag{3.30}$$

3.3.9 Generalized Biot Number.

j_{mi}^s in equation 3.19 must also obey the mass transfer equation 2.41 in the gas phase:

$$j_{mi}^s = k'\rho_f' \ln\left[\frac{1-\omega_{m\infty}'}{1-\omega_{mi}'}\right] \tag{3.31}$$

The *moisture activity* a_m for ideal gas mixtures is defined as:

$$a_m = \frac{P_m}{P_{m,sat}} = \frac{\rho'_m}{\rho'_{m,sat}} \qquad (3.32)$$

where P_m is the partial pressure (N/m^2) of the moisture in the gas

phase, $P_{m,sat}$ is the saturation pressure of the moisture at the given

temperatures; ρ'_m and $\rho'_{m,sat}$ are moisture concentrations (kg/m^3) in the

gas phase.

The mass transfer coefficient (k"), based on a difference in moisture

activities, is defined by:

$$j^s_{mi} = k''(a_{mi} - a_{m\infty}) \qquad (3.33)$$

From equations 3.31 and 3.33 it can be derived that for constant

k'-values the value of k" will remain constant only if the temperature

remains constant.

Substitution of expression 3.33 into equation 3.14 yields:

$$F = Bi \cdot m_i \qquad (3.34)$$

where Bi is the generalized Biot number, defined as:

$$Bi = \frac{\gamma \, k'' \, d_{s,ap} R_s}{D_0 \rho^2_{s0}} \qquad (3.35)$$

in which γ follows from the equilibrium relation a_m versus u (*sorption isotherm*; see Figure 4.1):

$$\gamma = \frac{a_{mi} - a_{m\infty}}{u_i - u_*} \qquad (3.36)$$

Substitution of equation 3.34 into the external boundary condition

3.10 yields the most general formulation of the external boundary condition. In chapter IV it will be elucidated that this condition sometimes may be formulated as a constant surface flux or as a constant surface concentration.

3.4 Mass Balance and Drying Time.

The moisture balance over the drying body during a time interval dt reads:

$$j_{mi}^s \ A \ dt = -\bar{\rho}_s V \ d(\bar{\rho}_m/\bar{\rho}_s) \tag{3.37}$$

where A is the mass exchanging area and V is the (shell-)volume of the drying body.

The averaged drying efficiency E is defined as the fraction of moisture removed:

$$E = \frac{v_0 - \bar{v}}{v_0 - v_\#} = \frac{u_0 - \bar{u}}{u_0 - u_\#} = 1 - \bar{m} \tag{3.38}$$

Putting the balance in a dimensionless form one finds:

$$FX_i d\tau = dE \tag{3.39}$$

where

$$X_i = \frac{A \ d_{s,ap} R_s}{\bar{\rho}_s V} = \frac{A \ R_s}{V_s} \tag{3.40}$$

It can be proven that X_i according to equation 3.40 equals X_i

according to equation 3.29. However, equation 3.40 offers a better insight in the physical meaning of X_i. *One can visualize X_i as the ratio of the solids volumina of a slab and the actual body, both with the same external area A and the same solids radius R_s.* Thus for slabs it simply follows that $X_i=1$, which is in agreement with equation 3.29. Further, during a drying process X_i wil only change if the surface area A changes, because R_s and V_s will remain constant. *In this view X_i may be looked upon as a dimensionless surface area.*
Integration of equation 3.39 gives the basic equation for the calculation of the drying time:

$$\tau = \int_0^E \frac{dE}{FX_i} \qquad (3.41)$$

It is obvious that the drying time can be calculated if both F and X_i are known as functions of E.
The relationship between X_i and E is given by equations 3.29, and 3.38. These equations can be rearranged to:

$$X_i = X_{i0} \; (1-sE)^{\frac{v}{v+1}} \qquad (3.42)$$

in which

$$X_{i0} = X_{i,\sigma=0} \; \left[1+(1-\lambda^{v+1})\sigma v_0\right]^{\frac{v}{v+1}} \qquad (3.43)$$

and

$$s = \frac{(1-\lambda^{v+1})\sigma(v_0-v_\#)}{1+(1-\lambda^{v+1})\sigma v_0} \qquad (3.44)$$

The parameter s is a *modified shrinkage coefficient*, which indicates to what extent the shrinking properties of the material will influence the drying behaviour, e.g. a material with a low initial water content v_0 will hardly shrink any more even if σ has a high value.

The relationship between F and E is far more complicated to be found and the following chapters of this thesis are dealing with this problem:

Chapter IV: non-shrinking systems ($\sigma=0$) with a concentration independent diffusion coefficient ($D_r=1$).

Chapter V: (non-)shrinking systems ($0 \leq \sigma \leq 1$) with a power law dependence of the diffusion coefficient ($D_r=m^a$).

3.5 Summary of Generalized Diffusion Equation, Mass Balance and Definitions of Dimensionless Parameters.

Generalized partial differential equation:

$$\frac{\partial m}{\partial \tau} = \frac{\partial}{\partial \phi}(D_r X^2 \frac{\partial m}{\partial \phi})$$

Initial condition:

$\tau = 0 \qquad 0 \leq \phi \leq 1 \qquad m = 1$

Boundary conditions:

$\tau > 0 \qquad \phi = 0 \qquad X \frac{\partial m}{\partial \phi} = 0$

$\qquad\qquad\qquad \phi = 1 \qquad m = m_i$

$\qquad\qquad\qquad\qquad$ or

$$-D_r X_i \frac{\partial m}{\partial \phi} = F$$

Mass balance:

$$FX_i d\tau = dE \qquad \longrightarrow \qquad \tau = \int_0^E \frac{dE}{FX_i}$$

$$X_i = X_{i0}(1-sE)^{\frac{v}{v+1}}$$

$$X_{i0} = X_{i,\sigma=0}\left[1+(1-\lambda^{v+1})\sigma v_0\right]^{\frac{v}{v+1}}$$

$$X_{i,\sigma=0} = (v+1)\frac{1-\lambda}{1-\lambda^{v+1}}$$

$$s = \frac{(1-\lambda^{v+1})\sigma(v_0-v_{\#})}{1+(1-\lambda^{v+1})\sigma v_0}$$

Summary of definitions:

concentration: $u = \dfrac{\rho_m}{\rho_s}$	diffusion coefficient : $D_r = \dfrac{D\rho_s^2}{D_0\rho_{s0}^2}$
concentration: $v = \dfrac{d_s}{d_m}\dfrac{\rho_m}{\rho_s} = \dfrac{d_s}{d_m}u$	time : $\tau = \dfrac{D_0\rho_{s0}^2\, t}{(d_{s,ap}R_s)^2}$
concentration: $m = \dfrac{u-u_{\#}}{u_0-u_{\#}} = \dfrac{v-v_{\#}}{v_0-v_{\#}}$	averaged efficiency : $E = \dfrac{v_0-\bar{v}}{v_0-v_{\#}} = 1-\bar{m}$
space coordinate : $\phi = \dfrac{\int_{R_1}^r \rho_s r^v dr}{\int_{R_1}^{R_2} \rho_s r^v dr}$	flux parameter : $F = \dfrac{j_{mi}^s\, d_{s,ap}\, R_s}{D_0\rho_{s0}^2(u_0-u_{\#})}$
hollowness factor : $\lambda = \dfrac{R_1}{R_1+R_s}$	Biot number: $Bi = \dfrac{\gamma\, k''\, d_{s,ap} R_s}{D_0\rho_{s0}^2}$

$$X = (v+1)\frac{1-\lambda}{1-\lambda^{v+1}}\left[\lambda^{v+1} + (1-\lambda^{v+1})\oint_0^\phi(1+\sigma v)d\phi\right]^{\frac{v}{v+1}}$$

CHAPTER IV

NON-SHRINKING SYSTEMS WITH CONCENTRATION INDEPENDENT DIFFUSION

COEFFICIENT

4.1 Diffusion Equation in Linear y-Coordinates.

For isothermal drying of non-shrinking bodies with concentration

independent diffusion coefficient analytical solutions of the

diffusion equation can be obtained. In order to find these solutions

we depart from the dimensional diffusion equation (§3.2), which in a

form adapted for this case reads:

Partial differential equation:

$$\frac{\partial \rho_m}{\partial t} = \frac{1}{r^\nu} \frac{\partial}{\partial r} \left(r^\nu D \frac{\partial \rho_m}{\partial r} \right) \tag{4.1}$$

Initial condition:

$$t = 0 \qquad R_1 < r < R_2 \qquad\qquad \rho_m = \rho_{m0} \tag{4.2}$$

Boundary conditions:

$$t > 0 \qquad r = R_1 \qquad\qquad \frac{\partial \rho_m}{\partial r} = 0 \tag{4.3}$$

$$r = R_2 \qquad\qquad \rho_m = \rho_{mi} \tag{4.4}$$

or

$$-D \frac{\partial \rho_m}{\partial r} = j_{mi}^s \tag{4.5}$$

Table 4.1 Summary of parameters for non-shrinking system.

concentration:	$m = \dfrac{\rho_m - \rho_{m*}}{\rho_{m0} - \rho_{m*}}$	(4.6)
space :	$\phi = \dfrac{r^{\nu+1} - R_1^{\nu+1}}{R_2^{\nu+1} - R_1^{\nu+1}}$	(4.7)
diffusion coefficient :	$D_r = \dfrac{D}{D_0}$	(4.8)
time :	$\tau = \dfrac{D_0 t}{(R_2 - R_1)^2}$	(4.9)
hollowness factor :	$\lambda = \dfrac{R_1}{R_2}$	(4.10)
flux parameter :	$F = \dfrac{j_{mi}^s (R_2 - R_1)}{D_0 (\rho_{m0} - \rho_{m*})}$	(4.11)
Biot number :	$Bi = \dfrac{\tau}{\rho_{s0}} \dfrac{k''(R_2 - R_1)}{D_0}$	(4.12)
local efficiency :	$E' = \dfrac{\rho_{m0} - \rho_m}{\rho_{m0} - \rho_{m*}} = 1 - m$	(4.13)
average efficiency :	$E = \dfrac{\rho_{m0} - \bar{\rho}_m}{\rho_{m0} - \rho_{m*}} = 1 - \bar{m}$	(4.14)
$X = X_{i,\sigma=0} \left[\lambda^{\nu+1} + (1 - \lambda^{\nu+1}) \phi \right]^{\frac{\nu+1}{\nu}}$		(4.15)
$X_i = \dfrac{A(R_2 - R_1)}{V} = X_{i,\sigma=0} = (\nu+1) \dfrac{1 - \lambda}{1 - \lambda^{\nu+1}}$		(4.16)

Non-shrinking systems are characterized by $\sigma=0$ and $\rho_s=\rho_{s0}=d_{s,ap}$. Choosing the equilibrium concentration as reference value ($m_\#=m_*$), the dimensionless parameters as defined in Chapter III now become as given in Table 4.1.

In the literature no solutions are found in terms of a volume based space coordinate (ϕ), therefore a dimensionless linear space coordinate (y) is introduced:

$$y = \frac{r - R_1}{R_2 - R_1} \tag{4.17}$$

Substitution of the dimensionless parameters into the equations 4.1-4.5 gives, in case of a constant diffusion coefficient ($D=D_0$, so $D_r=1$), the following diffusion equation in linear y-coordinates:

Partial differential equation:

$$\frac{\partial m}{\partial \tau} = \frac{1}{[\lambda+(1-\lambda)y]^\nu} \frac{\partial}{\partial y} \left([\lambda+(1-\lambda)y]^\nu \frac{\partial m}{\partial y}\right) \tag{4.18}$$

Initial condition:

$$\tau = 0 \qquad 0 < y < 1 \qquad\qquad m = 1 \tag{4.19}$$

Boundary conditions:

$$\tau > 0 \qquad\qquad y = 0 \qquad\qquad \frac{\partial m}{\partial y} = 0 \tag{4.20}$$

$$y = 1 \qquad\qquad m = m_i \tag{4.21}$$

or

$$-\frac{\partial m}{\partial y} = F \tag{4.22}$$

From the analytical solutions of the above differential equation (implicit) expressions for the drying time τ as a function of the average efficiency E can be derived. In the short-cut approach, as

will be described in this chapter, (explicit) expressions for τ versus E are obtained from the integration of the mass balance:

$$\tau = \frac{1}{X_{i,\sigma=0}} \int_0^E \frac{dE}{F}$$ (4.23)

The integration requires the relationship between fluxparameter F and average efficiency E. Finding approximate equations for this relationship, which appears to depend on the drying stage, is the main theme of this chapter.

4.2 Drying Stages.

Let us assume an adiabatic drying process with constant external conditions, which means constant temperature θ'_∞, constant humidity $\omega'_{m\infty}$, and constant mass transfer coefficient k'. Further, assume that the initial concentration u_0 of the material is such, that the corresponding equilibrium moisture activity a_m approaches 1 (see Figure 4.1). Thus, after a relatively short time the material will take on the wet bulb temperature. For a drying system one can safely assume that at the interface the thermodynamic equilibrium relation a_m versus u (sorption-isotherm) holds. Thus the local values at the interface (u_i, a_{mi}) can be obtained from Figure 4.1.

The moisture flux j^s_{mi} through the interface, expressed in terms of gas phase conditions (§2.3.2), reads:

$$j^s_{mi} = k'\rho'_f \ln\left[\frac{1-\omega'_{m\infty}}{1-\omega'_{mi}}\right]$$ (4.24)

As long as the surface moisture activity a_{mi} remains nearly constant
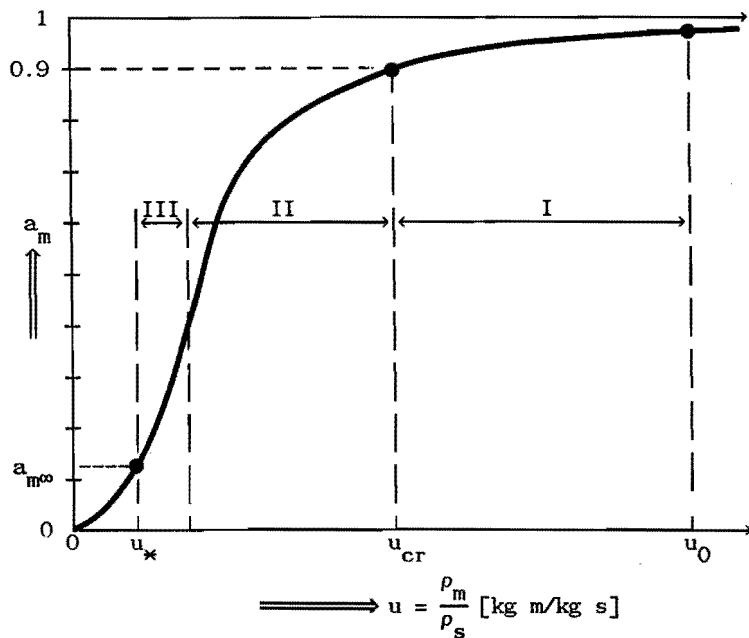
Figure 4.1

Schematic representation of a sorption-isotherm and some characteristic quantities (for explanation see text).

Main Drying Stages:

I : nearly constant surface moisture activity

(constant boundary flux for non-shrinking systems)

II : decreasing surface moisture activity

III : nearly constant surface moisture concentration

(constant boundary concentration)

(e.g. $a_{mi} \gtrsim 0.9$), then ω'_{mi} will remain nearly constant (see eqn. 3.32) and therefore the boundary flux j^s_{mi} will remain nearly constant as well.

This first drying stage (I), often referred to as the "constant flux period" or "constant activity period", is fully controlled by external conditions: the drying material behaves almost like pure moisture. For the boundary condition of the diffusion equation at y=1 (eqn. 4.22) now holds:

$F = F_{ca} \approx$ constant

The end of the constant activity period is arbitrarily defined at $a_{mi}=0.9$ .At this moment the surface moisture concentration has reached the so called critical value u_{cr}. From now on the surface moisture activity starts to decrease significantly and drying stage II has started. It will be obvious from equation 4.24 that the boundary flux will decrease. Consequently, the temperature of the drying material gradually increases towards the dry-bulb temperature. The boundary condition of the diffusion equation at y=1 is now given by equation 4.22, with:

$F = Bi \cdot m_i$

For a non-shrinking system the Biot number is given by equation 4.12; the value of γ follows from the sorption isotherm. If, in the concentration interval of interest, the sorption-isotherm may be approximated by a linear relationship ($\gamma \approx$ constant) and k" does not change too much despite of an increasing gas film temperature, then the Biot number will remain nearly constant during drying. However, in most practical drying situations this will not be the case. Arbitrarily, drying stage II ends and drying stage III starts ,when the surface concentration reaches a nearly constant value (e.g. $m_i \le 0.1$). During this final drying stage, often referred to as

"constant boundary concentration period" or *"zero boundary concentration period"*, the relative changes in the surface concentration u_i with respect to the maximum attainable change $(u_o - u_*)$ remain small. The boundary condition for the diffusion equation is now best given by equation 4.21, with: $m_i \approx 0$.

During this final drying stage the temperature of the material gradually increases until, in case of complete equilibrium, the dry-bulb temperature has been reached.

Each of the three main stages can be split up into two substages, namely:
- *Penetration Period*, during which the centre concentration changes hardly from the initial value (e.g. $m_{centre} \geq 0.9$).
- *Regular Regime*, during which the centre concentration changes significantly from its initial value (e.g. $m_{centre} \leq 0.9$).

Not all six possible drying stages can occur during a drying process. The occurrence of drying stages depends on the initial conditions (especially the starting flux) and the physical properties of the material (especially the sorption-isotherm). In Figure 4.2 two examples are given to illustrate the subsequent occurrence of stages during a drying process.

This thesis only deals with the drying stages I (*nearly* constant surface activity) and III (*nearly* constant surface concentration); drying stage II (decreasing surface activity) was not investigated (see §1.4).

As a first physical approximation a constant surface activity for stage I and a constant surface concentration for stage III are assumed in the remaining part of this thesis.

high initial flux ($F_{ca}=4$)   low initial flux ($F_{ca}=1$)
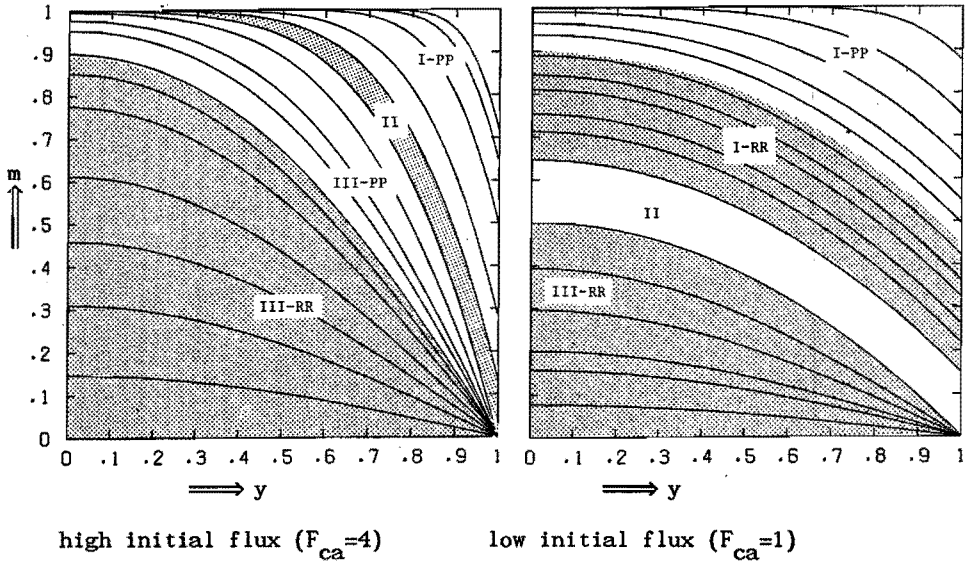
Figure 4.2   Two examples of the subsequent occurrence of drying stages for a non-shrinking slab with a constant diffusion coefficient (PP=Penetration Period; RR=Regular Regime).

4.3   Drying Stage with Constant Surface Flux.

The end of this drying stage is defined as the moment, where the local drying efficiency at the interface has reached the critical value $E^{\cdot}_{i,cr}$: the corresponding average critical efficiency is denoted E_{cr}. The drying time follows from the integrated mass balance:

$$\tau = \frac{E}{F_{ca}X_{i,\sigma=0}} \tag{4.25}$$

The duration of the constant activity period τ_{ca} follows from equation 4.25, if E_{cr} is known. Values of E_{cr} decrease with increasing values of the constant flux parameter F_{ca}. The relationship between E_{cr} and

F_{ca}, the so-called "critical-point curve", depends on the critical surface concentration $E'_{i,cr}$. The value of $E'_{i,cr}$ is derived from the sorption-isotherm; next the critical-point curve is known from the relationship among E, E'_i and F_{ca}; for this the diffusion equation has to be solved.

4.3.1 Analytical Solutions (F_{ca} = constant).

The solutions for the massive systems and hollow cylinders can be found in literature [37-39]; the diffusion equation of the hollow sphere was solved by Bosch [40]. Here the solutions are given in two different ways: one obtained by solving the diffusion equation via separation of variables and the other obtained via Laplace transformation. In Appendix B the solutions for massive and hollow systems, obtained by separation of variables, are given. In this main text only the solutions for massive systems will be presented.

Slab (v=0)

Via separation of variables:

$$\frac{E'}{F_{ca}} = \tau + \frac{1}{2}y^2 - \frac{1}{6} - 2 \sum_{1}^{\infty} \frac{\cos(\mu_k y)}{\cos(\mu_k)} \frac{\exp(-\mu_k^2 \tau)}{\mu_k^2} \tag{4.26}$$

in which μ_k are the positive roots of the characteristic equation :
$\sin(\mu_k) = 0$, thus $\mu_k = k\pi$ and $\cos(\mu_k) = (-1)^k$.

Via Laplace transformation:

$$\frac{E'}{F_{ca}} = 2 \frac{\sqrt{\tau}}{\sqrt{\pi}} \sum_{0}^{\infty} \left[\exp(\frac{-(2k+1-y)^2}{4\tau}) - \frac{2k+1-y}{2\sqrt{\tau}} \sqrt{\pi} \ \mathrm{erfc}(\frac{2k+1-y}{2\sqrt{\tau}}) + \right.$$
$$\left. \exp(\frac{-(2k+1+y)^2}{4\tau}) - \frac{2k+1+y}{2\sqrt{\tau}} \sqrt{\pi} \ \mathrm{erfc}(\frac{2k+1+y}{2\sqrt{\tau}}) \right] \tag{4.27}$$

Massive cylinder (v=1)

Via separation of variables:

$$\frac{E'}{F_{ca}} = 2\tau + \frac{1}{2}y^2 - \frac{1}{4} - 2 \sum_{1}^{\infty} \frac{J_0(\mu_k y)}{J_0(\mu_k)} \frac{\exp(-\mu_k^2 \tau)}{\mu_k^2} \tag{4.28}$$

in which μ_k are the positive roots of the characteristic equation :
$J_1(\mu_k) = 0$; J_o and J_1 are Bessel functions [41] of the first kind of order 0 respectively order 1.

Via Laplace transformation:

$$\frac{E'}{F_{ca}} = 2 \frac{\sqrt{\tau}}{\sqrt{y}} \text{ierfc}(\frac{1-y}{2\sqrt{\tau}}) + \frac{1+3y}{2y} \frac{\tau}{\sqrt{y}} \text{i}^2\text{erfc}(\frac{1-y}{2\sqrt{\tau}}) +$$

$$\frac{9+33y^2+6y}{16y} \frac{\tau\sqrt{\tau}}{\sqrt{y}} \text{i}^3\text{erfc}(\frac{1-y}{2\sqrt{\tau}}) + \ldots\ldots \tag{4.29}$$

Massive sphere (v=2)

Via separation of variables :

$$\frac{E'}{F_{ca}} = 3\tau + \frac{1}{2}y^2 - \frac{3}{10} - \frac{2}{y} \sum_{1}^{\infty} \frac{\sin(\mu_k y)}{\sin(\mu_k)} \frac{\exp(-\mu_k^2 \tau)}{\mu_k^2} \tag{4.30}$$

in which μ_k are the positive roots of the characteristic equation :
$\tan(\mu_k) = \mu_k$.

Via Laplace transformation:

$$\frac{E'}{F_{ca}} \approx \frac{1}{y} \left[\exp[-(1-y)+\tau] \text{ erfc}(\frac{1-y}{2\sqrt{\tau}} -\sqrt{\tau}) - \text{erfc}(\frac{1-y}{2\sqrt{\tau}}) \right] \tag{4.31}$$

This latter solution is an approximation. The exact solution can not be found, because of an unsolved back transformation from the Laplace

domain [40]. However, the given approximation appears to be quite close to the exact solution, obtained via separation of variables (eqn. 4.30).

4.3.2 Penetration Period (F_{ca} = constant).

At sufficiently small τ values the concentration profiles are not yet penetrated into the centre of the system, in other words : the centre concentration has hardly changed from its initial value. During this period, which is called "*Penetration Period with constant boundary flux*", the concentration profiles are independent of the hollowness factor λ.

The solutions, obtained via Laplace transformation, reduce for low τ values to the first term of the series. Nevertheless, a fairly complicated expression remains, which can be further simplified by developing the exponential- and error functions in infinite series [41], which in their turn reduce to a few dominant terms for small τ values. The following expression appears to be a very good approximation for the surface efficiency (maximum deviations about 2% for $\tau \leq 0.15$):

$$\frac{E_i'}{F_{ca}} = \frac{2}{\sqrt{\pi}}\sqrt{\tau} + \frac{v}{2}(1-\lambda)\tau + \frac{v(v+2)}{6\sqrt{\pi}}(1-\lambda)^2\tau\sqrt{\tau} + \frac{v(v+2)}{16}(1-\lambda)^3\tau^2 \qquad (4.32)$$

For extremely small τ values, equation 4.32 reduces to:

$$\frac{E_i'}{F_{ca}} = \frac{2}{\sqrt{\pi}}\sqrt{\tau} \qquad\qquad (4.33)$$

Thus, for this extreme situation E_i'/F_{ca} only depends on τ and is independent of the geometry parameter v and the hollowness factor λ;

in this respect all massive and hollow systems behave like a slab. Elimination of τ from equation 4.33 by means of the mass balance (eqn. 4.25) gives :

$$\frac{F_{ca}}{E_i^{'}} = \frac{\pi}{4} X_{i,\sigma=0} \frac{E_i^{'}}{E}$$

(4.34)

We now define a G-*parameter*:

$$G = \frac{\frac{F}{E_i^{'}} \frac{E}{E_i^{'}}}{X_i}$$

(4.35)

From equations 4.34, 4.35 and 4.36 follows the initial value G_0:

$$G_0 = \lim_{\tau \to 0} G = \lim_{E \to 0} G = \frac{\pi}{4}$$

(4.36)

It can be concluded that the G_0-parameter is independent of geometry and hollowness, in other words: the G_0 parameter may be looked upon as a quantity expressing that all hollow and massive geometries behave like a slab geometry at $\tau \to 0$.

For small τ-values, elimination of τ from equation 4.32 and the mass balance (eqn. 4.25), yields a rather complicated expression. A better approach is based on finding a correlation of the exact calculated values of $F_{ca}/E_i^{'}$ versus $E_i^{'}/E$, which appears to be a nearly straight line :

$$\frac{F_{ca}}{E_i^{'}} = G_0 X_{i,\sigma=0} \left[\frac{E_i^{'}}{E} - \alpha\right]$$

(4.37)

in which for the correlation parameter α the following relations can be obtained by fitting:

For a slab : $\alpha = 0$ (4.38a)

For a cylinder: $\alpha = 0.60-0.12\lambda-0.31\lambda^2-0.17\lambda^3$ (4.38b)

For a sphere : $\alpha = 0.76-0.08\lambda+0.04\lambda^2-0.72\lambda^3$ (4.38c)

Note that equation 4.37 can also be expressed as:

$$G = G_0(1-\alpha \frac{E}{E_i^\cdot})$$ (4.39)

and α can also be found by putting G versus $E/E_i^\cdot$.

4.3.3 Regular Regime (F_{ca} = constant).

At sufficiently high τ values, in case of low drying drying rates, the solutions obtained via separation of variables degenerate to a very simple form, because all terms in the series are negligible small compared with τ. During this drying stage concentration profiles are parabolic and decrease linearly with time (see Figure 4.2). Irrespective of the values of the constant surface flux and the initial moisture content, eventually the concentration profiles will take on the parabolic shape. This drying stage is called "Regular Regime with constant boundary flux".

From equations 4.26, 4.28 and 4.30 the following expression for the surface efficiency can be derived:

$$\frac{E_i^\cdot}{F_{ca}} = (v+1)\tau + \frac{1}{v+3}$$ (4.40)

Elimination of τ by using the mass balance (eqn. 4.25) gives:

$$F_{ca} = (v+3)(E_i'-E) \qquad (4.41)$$

Defining the mass transfer coefficient k_d for the dispersed phase as follows:

$$j_{mi}^s = k_d(\bar{\rho}_m - \rho_{mi}) \quad . \qquad (4.42)$$

or in a dimensionless form:

$$F = \frac{k_d(R_2-R_1)}{D_0} (\bar{m}-m_i) \qquad (4.43)$$

and defining the Sherwood number for the dispersed phase according to:

$$Sh_d = \frac{2k_d(R_2-R_1)}{\bar{D}} \qquad (4.44)$$

gives :

$$F = \frac{1}{2}Sh_d\bar{D}_r(\bar{m}-m_i) \qquad (4.45)$$

where $\bar{D}_r$ is an average reduced diffusion coefficient, defined as:

$$\bar{D}_r = \frac{\bar{D}}{D_0} \equiv \frac{\int_{m_i}^{\bar{m}} D_r\,dm}{\bar{m}-m_i} \qquad (4.46)$$

For concentration independent diffusion coefficient $\bar{D}_r = D_r = 1$ equation 4.45 can be written as:

$$F = \frac{1}{2}Sh_d(E_i' - E) \tag{4.47}$$

For _massive geometries_ the following simple expression for Sh_d can be derived from equations 4.41 and 4.47:

$$Sh_d = 6 + 2v \tag{4.48}$$

In a similar way the following expressions for Sh_d can be obtained in case of _hollow cylinders_:

$$Sh_d = 8 \frac{(1+\lambda^2)(1-\lambda)^3}{(1-4\lambda^2) + [3-4\ln(\lambda)]\lambda^4} \tag{4.49}$$

and for _hollow spheres_:

$$Sh_d = 10 \frac{(1+\lambda+\lambda^2)^2}{1+3\lambda+6\lambda^2+5\lambda^3} \tag{4.50}$$

Thus, _during the Regular Regime with constant boundary flux Sh_d takes on constant values_ (eqns. 4.48, 4.49 and 4.50).
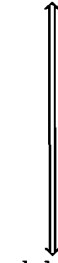
In Table 4.2 values of Sh_d are summarized. For a hollow geometry the values lay between those of the massive geometry ($\lambda=0$) and the slab geometry ($\lambda \to 1$).

It appears that equations 4.48–4.50 can be combined into one single handy relation:

$$Sh_d = 6 + 2v \left[\frac{X_{i,\sigma=0}^{-1}}{v} \right]^{2.15-0.18v} \tag{4.51}$$

Only the exponent in this equation is a correlation parameter, obtained by fitting of the exact values. Deviations between approximate and exact values are less than 0.3% (see Table 4.2).

Tabel 4.2: Values of Sh_d during Regular Regime with constant boundary flux $(D_r=1, \sigma=0)$.

	cylinder($v=1$)		sphere ($v=2$)		
λ	exact (eqn.4.49)	approx. (eqn.4.51)	exact (eqn.4.50)	approx. (eqn.4.51)	
0	8	8	10	10	massive
0.05	7.638	7.642	9.504	9.480	
0.1	7.341	7.347	9.026	8.999	
0.2	6.898	6.890	8.179	8.165	
0.3	6.594	6.591	7.503	7.504	
0.4	6.383	6.377	6.993	7.002	
0.5	6.236	6.230	6.622	6.633	
0.6	6.136	6.130	6.360	6.372	
0.7	6.069	6.066	6.185	6.195	
0.8	6.028	6.026	6.075	6.083	
0.9	6.006	6.006	6.017	6.021	
1	6	6	6	6	slab ($v=0$)

4.3.4 Transition from Penetration Period to Regular Regime (F_{ca} = constant).

At high values of F_{ca}/E_i' the Regular Regime correlation (eqn. 4.47) gives too low values of the drying time; at low values of F_{ca}/E_i' the Penetration Period correlation (eqn. 4.37) predicts too high values of the drying time. The transition (T) is chosen nearby the value of F_{ca}/E_i' where the difference between the drying times, obtained from the two correlations, is minimal. Based on the exact solutions of the differential equation, it appears that the transition criterium can be formulated as:

$$\left[\frac{F_{ca}}{E_i'}\right]_T = 1.5-\lambda+\lambda^2 \tag{4.52}$$

For values of F_{ca}/E_i' larger than this criterium the correlation for the Penetration Period should be used, whereas at lower values the

correlation for the Regular Regime should be applied. Thus, the two drying periods are short-cut in a simple way: stepping over from the one correlation to the other at a specific value of F_{ca}/E_i'. The maximum error in the predicted drying time occurs at this transition point. By allowing maximum errors of about 4% the transition criterium could be formulated indepent of the geometry parameter v.

Because initially $E_i'=0$ and thus $F_{ca}/E_i'\to\infty$, every drying process with a constant boundary flux will show a Penetration Period. However, at sufficiently high drying fluxes the surface efficiency will reach the critical value $E_{i,cr}'$ before the concentration profiles are penetrated into the centre of the material; from the transition criterium follows that this will happen if:

$$F_{ca} \geq (1.5-\lambda+\lambda^2)E_{i,cr}' \qquad\qquad (4.53)$$

In these cases no Regular Regime with constant boundary flux will succeed the Penetration Period (see Figure 4.2).

4.3.5 Algorithm for Short-Cut Calculation (F_{ca} = constant).

An algorithm for calculating τ and E from given values of v, λ, F_{ca} and $E_i^{\cdot}$ could take on the following form:

begin {short-cut algorithm, D_r=1, σ=0, F=F_{ca}}

read(v,λ,F_{ca},$E_i^{\cdot}$)

if $\dfrac{F_{ca}}{E_i^{\cdot}} \geq 1.5-\lambda+\lambda^2$

   then {Penetration Period}

      calculate α from equations 4.38a–4.38c

      calculate E from equation 4.37

   else {Regular Regime}

      calculate Sh_d from equation 4.51

      calculate E from equation 4.47

calculate τ from equation 4.25

write(τ,E)

end.

Comparing this short-cut calculation of τ and E with the exact calculation method ,reveals that the *maximum errors* in τ and E occur near the transition point and are *less then 4%*!!

4.4 Drying Stage with Constant Surface Concentration.

Assume a sufficiently high initial flux, so that the moisture concentration profiles hardly have penetrated into the drying material at reaching the condition of nearly constant surface concentration (stage III). Consequently, the moisture distribution in the material still will be nearly uniform and the drying time of the preceding

stages I and II will be negligible with respect to the total drying time of the material. During drying stage III the drying flux will decrease continuously and in case of an *isothermal* process the drying time should be calculated using equation 4.23 . The relationship between the flux F and the efficiency E has to be obtained from the (analytical) solution of the diffusion equation. For the situation as described above, the diffusion equation 4.18 is solved with a uniform initial concentration and a zero boundary concentration.

4.4.1 Analytical Solutions ($m_i = 0$).

The analytical solutions for massive and hollow systems with zero boundary concentration can be found in literature [37-39] and are summarized in Appendix B. In this main text only the solutions for massive systems are presented.

Slab (ν=0)

$$E' = 1-2 \sum_{1}^{\infty} \frac{\cos(\mu_k y)}{\sin(\mu_k)} \frac{\exp(-\mu_k^2 \tau)}{\mu_k} \tag{4.54}$$

in which μ_k are the positive roots of the characteristic equation $\cos(\mu_k)=0$; thus $\mu_k=(k-\frac{1}{2})\pi$ and $\sin(\mu_k)=(-1)^{k+1}$.

Massive Cylinder (ν=1)

$$E' = 1-2 \sum_{1}^{\infty} \frac{J_0(\mu_k y)}{J_1(\mu_k)} \frac{\exp(-\mu_k^2 \tau)}{\mu_k} \tag{4.55}$$

in which J_0 and J_1 are Bessel functions [41] of the first kind of

64

order 0 respectively order 1; μ_k are the positive roots of $J_0(\mu_k) = 0$.
A quite well approximation of the first six roots is given by
$\mu_k = 2.4048 + (k-1)\pi$ with deviations $\leq 0.5\%$.

Massive Sphere ($v=2$)

$$E' = 1 + \frac{2}{y} \sum_1^\infty \frac{\sin(\mu_k y)}{\cos(\mu_k)} \frac{\exp(-\mu_k^2 \tau)}{\mu_k} \qquad (4.56)$$

in which μ_k are the positive roots of $\sin(\mu_k)=0$; thus $\mu_k = k\pi$
and $\cos(\mu_k) = (-1)^k$.

From the above solutions the following expressions for the flux and
the efficiency can be derived :

$$F = -\left(\frac{\partial m}{\partial y}\right)_{y=1} = \left(\frac{\partial E'}{\partial y}\right)_{y=1} = 2 \sum_1^\infty \exp(-\mu_k^2 \tau) \qquad (4.57)$$

and

$$1-E = \int_\tau^\infty FX_{i,\sigma=0} d\tau = 2(v+1) \sum_1^\infty \frac{\exp(-\mu_k^2 \tau)}{\mu_k^2} \qquad (4.58)$$

4.4.2 Penetration Period ($m_i = 0$).

At small τ-values concentration profiles have not yet penetrated into
the centre of the material and a slab may be looked upon as an
infinite body. Moreover, cylinders and spheres behave like a slab in
case of extremely small τ-values ($\tau \to 0$). For these situations quite a
number of terms of the series solutions (eqns. 4.54–4.56) is required.
A simple short-time solution can be obtained from the analytical

solution of the diffusion equation for infinite slabs $(-\infty < y \leq 1)$ with a homogeneous initial concentration and a zero boundary concentration [37]:

$$E' = 1 - erf\left(\frac{1-y}{2\sqrt{\tau}}\right) \tag{4.59}$$

For the flux follows:

$$F = \left(\frac{\partial E'}{\partial y}\right)_{y=1} = \frac{1}{\sqrt{(\pi\tau)}} \tag{4.60}$$

and for the drying efficiency:

$$E = \int_0^\tau FX_{i,\sigma=0} d\tau = 2X_{i,\sigma=0}\frac{\sqrt{\tau}}{\sqrt{\pi}} \tag{4.61}$$

Elimination of τ from equations 4.60 and 4.61 gives the relation wanted between F and E:

$$F = \frac{2}{\pi} X_{i,\sigma=0}\frac{1}{E} \tag{4.62}$$

This equation is valid during the entire Penetration Period of slabs, but for cylinders and spheres, as already mentioned, only for extreme small τ-values $(\tau \to 0)$.

Applying the definition of the G-parameter (eqn. 4.35) now gives (realise that $m_i=0$, thus $E_i'=1$):

$$G_0 = \frac{2}{\pi} \tag{4.63}$$

and it appears that also in this situation G_0 is *independent of geometry and hollowness*.

The entire Penetration Period for all hollow and massive geometries can be described very well with the correlation:

$$F = G_0 X_{i,\sigma=0} \left[\frac{1}{E} - \beta \right] \qquad (4.64)$$

in which for the correlation parameter β the following relations can be obtained by fitting:

For a slab   : $\beta = 0$ (4.65a)

For a cylinder: $\beta = 0.71 - 0.13\lambda - 0.58\lambda^2$ (4.65b)

For a sphere   : $\beta = 0.88 - 0.08\lambda - 0.08\lambda^2 - 0.72\lambda^3$ (4.65c)

In terms of the G-parameter equation 4.64 reads:

$$G = G_0(1 - \beta E) \qquad (4.66)$$

It can be concluded now, that *penetration processes with both constant boundary flux and constant boundary concentration can be described in a similar way.*

4.4.3 Regular Regime ($m_i = 0$).

At sufficiently high τ-values the analytical solutions of §4.4.1 can be approximated quite well by the first term of the series. *The concentration profiles take on the shape of a cosine, Bessel or damped sine function and decrease exponential with time.* This shape no longer changes (similarity of concentration profiles) and the drying behaviour has become independent of the initial conditions; sooner or later, *every* drying process will arrive at this drying stage, which is called: *"Regular Regime with constant boundary concentration".*

The Regular Regime solution for the flux reads:

$$F = 2\exp(-\mu_1^2\tau) \tag{4.67}$$

and for the efficiency:

$$1-E = 2(\nu+1)\frac{\exp(-\mu_1^2\tau)}{\mu_1^2} \tag{4.68}$$

Elimination of τ from those two equations gives a simple expression for the relation between F and E :

$$F = \frac{\mu_1^2}{\nu+1}(1-E) \tag{4.69}$$

Analog to equation 4.47 the flux versus efficiency can also be expressed as (remember $m_i=0$, so $E_i'=1$):

$$F = \frac{1}{2}Sh_d(1-E) \tag{4.70}$$

From equations 4.69 and 4.70 it follows for _massive geometries_:

$$Sh_d = \frac{2\mu_1^2}{\nu+1} \tag{4.71}$$

In a similar way, for both _massive and hollow geometries_, one finds:

$$Sh_d = \frac{2\mu_1^2}{X_{i,\sigma=0}} \tag{4.72}$$

in which μ_1 follows from the characteristic equations as given in the

Appendix C.

Apparently, during the Regular Regime with constant boundary concentration Sh_d takes on a constant value. Furthermore, it can be concluded that the Regular Regimes with constant boundary flux and constant boundary concentration can be described in a similar way.

In Table 4.3 values of Sh_d are summarized. As expected, the values for a hollow geometry lay between those of the massive geometry and the slab. *Note that at $\lambda=0.6$–0.7 a minimum value of Sh_d occurs!* The exact Sh_d values of Table 4.3 can be correlated quite well by the following polynoms of λ:

$$\text{For a slab} \quad : Sh_d = \frac{\pi^2}{2} = 4.935 \tag{4.73a}$$

$$\text{For a cylinder} : Sh_d = 5.75 - 4.36\lambda + 6.34\lambda^2 - 2.82\lambda^3 \tag{4.73b}$$

$$\text{For a sphere} \quad : Sh_d = 6.58 - 7.14\lambda + 8.78\lambda^2 - 3.29\lambda^3 \tag{4.73c}$$

The maximum deviations between the exact and approximated values of Sh_d amount 0.7% for cylinders and 0.4% for spheres.

Tabel 4.3: Values of Sh_d during Regular Regime with constant boundary concentration ($D_r=1$, $\sigma=0$, $m_i=0$).

λ	cylinder ($v=1$)		sphere ($v=2$)		
	exact (eqn.4.72)	approx. (eqn.4.73)	exact (eqn.4.72)	approx. (eqn.4.73)	
0	5.783	5.750	6.580	6.580	massive
0.1	5.339	5.375	5.953	5.951	↑
0.2	5.087	5.109	5.462	5.477	
0.3	4.943	4.936	5.127	5.139	
0.4	4.864	4.840	4.918	4.918	
0.5	4.828	4.803	4.802	4.794	
0.6	4.819	4.807	4.752	4.746	
0.7	4.830	4.837	4.752	4.756	
0.8	4.856	4.876	4.787	4.803	
0.9	4.891	4.906	4.850	4.867	↓
1	4.935	4.910	4.935	4.930	slab ($v=0$)

4.4.4 Transition from Penetration Period to Regular Regime ($m_i = 0$).

Again it appears that both extremes can be connected most simply by just stepping over from the approximation of the one extreme to that of the other. Further, it has practical advantages now to formulate the transition criterium in terms of efficiencies, in other words: the Penetration Period ends and the Regular Regime starts at some specified value of the efficiency ($E=E_T$). From the exact calculated values of F versus E the following transition criterium is found:

$$E_T = 0.5+0.05v(5-v)(1-\lambda) \tag{4.74}$$

4.4.5 Algorithm for Short-Cut Calculation ($m_i = 0$).

Expressions for the drying time can now be found from equations 4.23, 4.64 and 4.70:

Penetration Period ($E \leq E_T$):

For a slab $: \tau = \dfrac{E^2}{2G_0}$ (4.75)

For a cylinder $: \tau = \dfrac{-\beta E-\ln(1-\beta E)}{G_0(X_{i,\sigma=0})^2\beta^2}$ (4.76)
and a sphere

Regular Regime ($E > E_T$):

For all $: \tau = \tau_T + \dfrac{2}{Sh_d X_{i,\sigma=0}} \ln\left[\dfrac{1-E_T}{1-E}\right]$ (4.77)
geometries

where τ_T is the drying time at the end of the Penetration Period, when transition takes place.

Assuming that the drying times of stage I and II are negligible with respect to the total drying time, the following algorithm could be used for the calculation of the drying flux F and the drying time τ at any given value of the drying efficiency E.

begin {short-cut algorithm, $D_r=1$, $\sigma=0$, $m_i=0$, isothermal}

    read (v,λ,E)

    calculate β from equations 4.65a–4.65c

    calculate E_T from equation 4.74

    if $E \leq E_T$

        then   {Penetration Period}

                calculate F from equation 4.64

                calculate τ from equations 4.75 or 4.76

        else   {Regular Regime}

                calculate τ_T from equations 4.75 or 4.76

                calculate Sh_d from equations 4.73

                calculate F from equations 4.70

                calculate τ from equations 4.77

write (F,τ)

end.

Comparison of this short-cut calculation with the exact calculation shows that maximum errors in the flux and in the drying time occur at the transition point. It should be noticed that at the transition point the flux calculated with the penetration correlation yields a too high value, whereas the regular regime correlation gives a too low value. In any case, the relative deviation between both approximate fluxes and the the exact flux is within 5% .

The maximum errors in the approximated drying times are only 3% .

4.5 Adiabatic Drying Process.

During the constant activity period of an adiabatic drying process the drying system takes on the *wet-bulb-temperature* T_{wb}. After this *isothermal* period the temperature of the system will increase. As was pointed out in literature [23,26,33] heat transfer from a gas phase *to* a body is very slow with respect to heat diffusivity *in* the body. This means that the temperature distribution in the body will remain nearly uniform, so the averaged temperature $\bar{\theta}$ of the body nearly equals the surface temperatures θ_i; and because equilibrium is assumed at the interface: $\theta \approx \bar{\theta} \approx \theta_i = \theta_i'$, where θ_i' is the interface temperature in the gas phase.

Because in general the (latent) heat of evaporation (L) of the moisture is many times larger than the heat capacity of the body, a negligible part of the total heat flux is left to accumulate in the body. From this it follows that by good approximation the heat transfer process may be considered as a *quasi steady-state adiabatic evaporation process*, for which the following thermal energy balance holds:

$$\alpha(\theta_\infty' - \theta_i) \approx j_{mi}^S \, L_i \qquad (4.78)$$

Note that this equation represents the wet bulb equation in its elementary form.

In case of an enclosed gas phase, hollow systems will blow up with increasing temperature; however, this complication will not be considered here and the internal and external radii (R_1 and R_2) are assumed to remain constant.

The diffusion coefficient D_0 depends on the temperature and so changes during the drying process. The mass balance over the drying system now reads:

$$FX_{i,\sigma=0} \frac{D_0}{(R_2-R_1)^2} \, dt = dE \tag{4.79}$$

and the dimensional drying time t:

$$t = \frac{(R_2-R_1)^2}{X_{i,\sigma=0}} \int_0^E \frac{dE}{FD_0} \tag{4.80}$$

Assuming a constant value of the hollowness factor λ, which is certainly true for massive bodies, the *relationship F versus E* (§4.4) *is independent of temperature*. In order to keep a maximum attainable value 1 for the efficiency E, the equilibrium moisture content ρ_{m*} in the definitions of the fluxparameter F and the efficiency E should be taken from the sorption isotherm at dry bulb temperature. The temperature dependence of the diffusion coefficient D_0 can often be expressed by an Arrhenius type relation:

$$D_0(T) = D_0(T_1) \, \exp\left[- \frac{A_D}{R}(\frac{1}{T_1} - \frac{1}{T})\right] \tag{4.81}$$

in which T is the absolute temperature of the body (^oK),
A_D is the activation energy for diffusion [Joule/mol^oK] and
R is the gas constant.
From the definition of the flux parameter (eqn.4.11) and the thermal energy balance (eqn.4.78) the following relation for FD_0 can be derived:

$$\frac{FD_0}{(FD_0)_{ca}} = \frac{j_{mi}^s}{(j_{mi}^s)_{ca}} = \frac{\alpha}{\alpha_{ca}} \frac{L_{ca}}{L_i} \frac{\theta_\infty' - \theta}{\theta_\infty' - \theta_{ca}} \tag{4.82}$$

in which the subscript "ca" indicates the value of the parameters at

the condition of constant surface activity (thus θ_{ca} is the wet bulb temperature); parameters without this subscript have actual values. If the difference between the dry- and wet-bulb temperature is not too high, the heat transfer coefficient α and the evaporation enthalpy L will not change too much and equation 4.82 simplifies to:

$$\frac{FD_0}{(FD_0)_{ca}} \approx \frac{\theta'_\infty - \theta}{\theta'_\infty - \theta_{ca}} = \frac{T'_\infty - T}{T'_\infty - T_{ca}} \tag{4.83}$$

Assuming again very short stages I and II the drying curves F versus E, as given by equations 4.64 and 4.70, have to be used and the drying time can be calculated from equation 4.80; however, now the integration has to be carried out numerically (e.g. trapezium rule). The relationship FD_0 versus E can be found by the following procedure:

- choose a value for T (remember: $T_{ca} \leq T \leq T'_\infty$)
- calculate FD_0 from equation 4.82 or 4.83
- calculate D_0 from equation 4.81
- calculate F from the values of FD_0 and D_0
- calculate E from the temperature independent relationship
  F versus E (eqns.4.64 and 4.70)

The above procedure yields at any given temperature T the values of E, F and D. If one desires to integrate with equal steps of E, the temperature T must be found by iteration from equation 4.83.

CHAPTER V

POWER LAW DIFFUSION IN SYSTEMS WITH ANY DEGREE OF SHRINKAGE

5.1 Concentration Dependence of Diffusion Coefficient.

It is assumed that the moisture diffusion coefficient depends on the moisture concentration according to a power law relation (see also chapter I):

$$D\rho_s^2 = b\left[\frac{\rho_m}{\rho_s} - \frac{\rho_{m\#}}{\rho_{s\#}}\right]^a = b(u-u_\#)^a \tag{5.1}$$

$\rho_{m\#}$ is the moisture concentration where the diffusion coefficient becomes practically zero; this thesis only deals with systems in which the diffusion coefficient approaches to zero at the equilibrium moisture content, so that $u_\# \approx u_*$.

a and b are fitting parameters, which can be found by linear regression of $\ln(D\rho_s^2)$ versus $\ln(u-u_\#)$. In chapter VI it will be pointed out how these fitting parameters can be derived from a drying experiment.

The diffusion coefficient D_0 at the initial concentration u_0 is given by:

$$D_0\rho_{s0}^2 = b(u_0-u_\#)^a \tag{5.2}$$

Applying the definitions of the reduced diffusion coefficient D_r and the concentration m (§3.3) yields:

$$D_r = m^a \tag{5.3}$$

It will be clear that for *non-shrinking* systems, a concentration independent diffusion coefficient ($D_r=1$, so a=0) is a special case of power law diffusion. However, it should be noticed that for *shrinking* systems a=0 does *not* correspond with a constant diffusion coefficient.

5.2 Numerical Solution of the Diffusion Equation.

The power relation for D_r has to be substituted in the generalized diffusion equation with ϕ-coordinates (§3.3) or in the diffusion equation with linear coordinates (§4.1).

In general, the diffusion equation, both in ϕ-coordinates and linear coordinates, requires a numerical approach to be solved. It is beyond the scope of this thesis to deal extensively with the numerical approach. Only some important aspects, which may cause serious problems, are treated in Appendix D.

In general the solution of the diffusion equation (§3.3) can be written as:

$$m = m(\phi, \tau, \upsilon, \lambda, a, \sigma v_0, \sigma v_\#, \text{drying stage}) \tag{5.4}$$

and the averaged concentration is given by:

$$\bar{m} = \bar{m}(\tau, \upsilon, \lambda, a, \sigma v_0, \sigma v_\#, \text{drying stage}) \tag{5.5}$$

The drying time is calculated by integration of the mass balance (§3.4); the required relationship F versus E is now obtained from the numerical computer output and will be a function of the following form:

$$F = F(E, v, \lambda, a, \sigma v_0, \sigma v_\#, \text{drying stage}) \tag{5.6}$$

For didactical reasons the drying stage with constant surface concentration will be discussed first.

5.3 Drying Stage with Constant Surface Concentration ($m_i = 0$).

For this drying stage Liou [28,29] proposed short-cut correlations for F versus E, which are valid for slabs, massive cylinders and massive spheres. The Regular Regime is described with Sherwood numbers, whereas the Penetration Period of non-shrinking systems is described with Taylor series expansions for the G-parameter. In this section the method, used by Liou, is simplified and extended to hollow bodies, irrespective of their degree of shrinkage.

5.3.1 Non-Shrinking Systems ($D_r = m^a, \sigma = 0, m_i = 0$).

Penetration Period

It appears that during this period G versus E can be approximated quite well by a linear relationship. During the Penetration Period the expressions for the drying flux and drying time are similar to those of constant diffusion coefficient, however, the parameters G_0 and β now depend on the exponent a:

$$F = G_0 \, X_{i,\sigma=0} \, (\frac{1}{E} - \beta) \tag{5.7}$$

For a slab: $\qquad \tau = \dfrac{E^2}{2G_0}$ $\qquad\qquad\qquad\qquad$ (5.8)

For a cylinder
and a sphere : $\qquad \tau = \dfrac{-\beta E - \ln(1-\beta E)}{G_0(X_{i,\sigma=0})^2\beta^2}$ $\qquad\qquad$ (5.9)

in which:

$$G_0 = \frac{2}{\pi}\left[\frac{1.42}{a+1.42}\right]^{1.98} \qquad \text{for } 0\leq a<\infty \qquad\qquad (5.10)$$

and

$$\beta = \beta_{a=0}\,(1.25)^a \qquad\qquad \text{for } 0\leq a<2 \qquad\qquad (5.11)$$

The expressions for $\beta_{a=0}$ are given by equations 4.65.

Regular Regime $(D_r= m^a, \; \sigma = 0, \; m_i = 0)$

During this drying period mass transfer is best described by means of a Sherwood number according to equations 4.45 and 4.47. For power law diffusion and a zero boundary concentration the flux equation now becomes:

$$F = \frac{1}{2}\frac{Sh_d}{a+1}\,(1-E)^{a+1} \qquad\qquad\qquad (5.12)$$

Schoeber [23] observed that in case of power law diffusion $(D_r=m^a)$ during the Regular Regime the Sherwood numbers (Sh_d) have constant values. Liou [28,29] reports that those constant values depend pseudo linearly on $\frac{a}{a+2}$. (However, both Schoeber and Liou did not recognize that constant values of Sh_d will *not* occur in case of a *non zero* boundary concentration!)

Both observations are quite important, because they enable the development of very accurate correlations for the Regular Regime, being the drying stage that contributes predominantly to the drying time. A similar behaviour may be expected for hollow systems. Indeed, from the numerical computer output the following correlations for Sh_d can be derived:

$$Sh_d = Sh_{d,a \to \infty} - \Delta Sh_d \cdot \frac{2}{a+2} \qquad (5.13)$$

in which:

$$\Delta Sh_d = Sh_{d,a \to \infty} - Sh_{d,a=0} \qquad (5.14)$$

$$Sh_{d,a \to \infty} = 7.391 + (3.516v - 0.034)\left[\frac{X_{i,\sigma=0}}{v} - 1\right]^{1.535 - 0.075v} \qquad (5.15)$$

$Sh_{d,a=0}$ is given by λ-polynoms according to equations 4.73. However, a more elegant correlation for ΔSh_d, based on normalized X_i-values, reads:

$$\Delta Sh_d = 2.456 + (2.720v - 0.087)\left[\frac{X_{i,\sigma=0}}{v} - 1\right]^{1.04} \qquad (5.16)$$

Note: only the exponents in equations 5.15 and 5.16 follow from a regression analysis.

The accuracy of the above correlation is within ± 1% .

The Regular Regime expressions for the drying time (isothermal) follow from the integration of the mass balance with the aid of equation 5.12:

$$\text{For } \alpha=0 \quad : \quad \tau = \tau_T + \frac{2}{Sh_{d,}X_{i,\sigma=0}} \ln\left[\frac{1-E_T}{1-E}\right] \qquad (5.17)$$
(eqn. 4.77)

$$\text{For } \alpha\neq0: \quad \tau = \tau_T + \frac{2}{Sh_d X_{i,\sigma=0}} \frac{a+1}{a}\left[\frac{1}{(1-E)^a} - \frac{1}{(1-E_T)^a}\right] \qquad (5.18)$$

<u>Transition</u> $(D_r = m^\alpha, \; \sigma = 0, \; m_i = 0)$

The Liou approach needs a quite severe criterium to be sure of Regular Regime behaviour, namely:

$$E \geq \frac{2}{a+2} \qquad (5.19)$$

So, in case of a concentration independent diffusion coefficient (a=0) the criterium becomes E=1, and the whole drying process is considered as a penetration process. However, the more simple approach described in this thesis takes better advantage of the Regular Regime properties, as given in Chapter IV.

From the numerical calculated solutions the following transition criterium has been derived:

$$E_T = \frac{1+0.1\nu(5-\nu)(1-\lambda)}{a+2} \qquad (5.20)$$

<u>5.3.2 Systems with any Degree of Shrinkage</u> $(D_r = m^a, \; 0 \leq \sigma \leq 1, \; m_i = 0)$

At the same value of the drying efficiency E, the flux parameter F of the shrinking system $(\sigma>0)$ is related to the flux parameter $F_{\sigma=0}$ of the non-shrinking system by means of the shrinkage factor H, introduced by Liou [28,29]:

$$H = \frac{F}{F_{\sigma=0}} \qquad (5.21)$$

Finding F versus E has been reduced now to finding expressions for the shrinkage factor H.

For a _slab_ geometry ($v=0$) the solutions of the generalized diffusion equation (§3.4) are independent of the shrinkage behaviour, because in all cases $X_\phi = X_i = X_{i,\sigma=0} = 1$. So the solutions of non-shrinking slabs, expressed in dimensionless quantities, are identical with those of shrinking slabs. The shrinkage properties of the material now emerge from the definitions of the dimensionless parameters and the diffusion relation (eqn. 5.1).

Conclusion: the shrinkage factor of slabs is 1, irrespective of the drying stage.

For _cylinders_ and _spheres_ correlations of the shrinkage factor were derived according to Liou's method: first find the initial value ($\tau \rightarrow 0$), then look for an approximate solution for large times and eventually connect both extreme situations by means of a Taylor series expansion.

Penetration with extremely short times ($D_r = m^a$, $0 \leq \sigma \leq 1$, $m_i = 0$)
The flux parameter of the shrinking system (eqn. 3.14) is related to the flux parameter of a (fictive) non-shrinking system (eqn. 4.11) with exactly the same initial conditions and the same product properties. From the definitions of the flux parameters (eqns. 3.14 and 4.11) follows:

$$\lim_{\tau \rightarrow 0} H = H_0 = \frac{d_{s,ap} R_s}{\rho_{s0}(R_{2,0} - R_1)} \tag{5.22}$$

Equation 5.22 can also be written as:

$$H_0 = \frac{A_0 R_s}{V_s} \cdot \frac{d_{s,ap} V_s}{\rho_{s0} V_0} \cdot \frac{V_0}{A_0 (R_{2.0} - R_1)} \qquad (5.23)$$

where A_0 and V_0 are the initial values of the surface area and the (shell-)volume of the system.

From the solid mass balance $d_{s,ap} V_s = \rho_{s0} V_0$ and from the definitions of X_i (eqns. 3.40 and 4.16) follows:

$$H_0 = \frac{X_{i,0}}{X_{i,\sigma=0}} \qquad (5.24)$$

Substituting the expression for $X_{i,0}$ (eqn. 3.43) gives:

$$H_0 = \left[1 + (1 - \lambda^{\upsilon+1}) \sigma v_0 \right]^{\frac{\upsilon}{\upsilon+1}} \qquad (5.25)$$

This expression confirms that for a slab ($\upsilon=0$ or $\lambda\to1$) the shrinkage factor $H_0=1$.

Note:

Applying the definition of the G-parameter (eqn. 4.35) to a shrinking system with zero boundary concentration yields:

$$G_0 = \lim_{\tau\to0} \frac{FE}{X_i} = \lim_{\tau\to0} \frac{H F_{\sigma=0} E}{X_i} = \lim_{\tau\to0} \frac{H_0 F_{\sigma=0} E}{X_{i,0}} \qquad (5.26)$$

with the aid of equation 5.24:

$$G_0 = \lim_{\tau\to0} \frac{F_{\sigma=0} E}{X_{i,\sigma=0}} \qquad (5.27)$$

Conclusion: the G_0-correlation for non-shrinking systems (eqn. 5.10)
is valid for shrinking systems as well.

Regular Regime $(D_r = m^a, \ 0 \leq \sigma \leq 1, \ m_i = 0)$

A relation for the initial shrinkage factor H_0 could be found by an algebraic analysis. However, the Regular Regime correlations for the shrinkage factor has to be deduced from the numerical computer output. The Sherwoord numbers for shrinking systems, which do not take on constant values during the Regular Regime, are described by Schoeber [23] in the following way:

$$Sh_d = Sh_{d,\sigma=0} + \Delta Sh_d \qquad (5.28)$$

and the shrinkage factor simply follows:

$$H = 1 + \frac{\Delta Sh_d}{Sh_{d,\sigma=0}} \qquad (5.29)$$

For strongly concentration dependent diffusion coefficients $(a \to \infty)$ the concentration profile is rectangular $(m=\bar{m})$ and $\Delta Sh_{d, a \to \infty}$ can be calculated analytically by comparing the flux expressions:

$$F = -D_r X_i \left(\frac{\partial m}{\partial \phi}\right)_{\phi=1} \qquad (5.30)$$

$$F_{\sigma=0} = -D_r X_{i,\sigma=0} \left(\frac{\partial m}{\partial \phi}\right)_{\phi=1} \qquad (5.31)$$

from which follows:

$$H_{a \to \infty} = \frac{X_i}{X_{i,\sigma=0}} \qquad (5.32)$$

and from equations 5.29 and 5.32 with $Sh_{d,\sigma=0} = Sh_{d,a\to\infty}$:

$$\Delta Sh_{d,a\to\infty} = Sh_{d,a\to\infty} \left[\frac{X_i}{X_{i,\sigma=0}} - 1\right] \qquad (5.33)$$

Schoeber [23] observed that ΔSh_d is hardly influenced by the kind of concentration dependence of the diffusion coefficient, so $\Delta Sh_d \approx \Delta Sh_{d,a\to\infty}$ and from equations 5.29 and 5.33 now follows with $Sh_{d,\sigma=0} = Sh_{d,a}$:

$$H = 1 + \frac{Sh_{d,a\to\infty}}{Sh_{d,a}} \left[\frac{X_i}{X_{i,\sigma=0}} - 1\right] \qquad (5.34)$$

Substitution of the expressions for X_i (eqn. 3.42) and H_0 (eqn. 5.25) finally yields for the shrinkage factor:

$$H = 1 + \frac{Sh_{d,a\to\infty}}{Sh_{d,a}} \left[H_0(1-sE)^{\frac{\upsilon}{\upsilon+1}} - 1\right] \qquad (5.35)$$

The Sherwood numbers in this equation are to be calculated with equations 5.13–5.16.

From equation 5.35 it can be seen that the shrinkage factor H decreases as the drying efficiency E increases. If the averaged moisture content $\bar{v} = v_{\ast} = 0$, the shrinkage factor reaches the minimum value 1. Thus, at decreasing moisture concentrations the shrinking abilities of the material become less and *at very low moisture concentrations the shrinking system even behaves like a non-shrinking system.*

Transition Period $(D_r = m^a, \ 0 \leq \sigma \leq 1, \ m_i = 0)$

According to the criterium, used in Liou's approach [28,29], the Regular Regime correlation 5.35 may be used if $E \geq E_Q$, with:

$$E_Q = \frac{a}{a+2} \tag{5.36}$$

For the transition region $(0 < E < E_Q)$ the shrinkage factor H is approximated by an appropiate Taylor series expansion, starting in $(E=0, H=H_0)$ and merging into the Regular Regime correlation at $E=E_Q$. To obtain a smooth transition at $E=E_Q$, equal zero and first derivatives of the Regular Regime correlation and the Taylor function at $E=E_Q$ are imposed:

$H=H_Q$ (equal zero derivatives) and

$H^{(1)}=H_Q^{(1)}$ (equal first derivatives).

The following Taylor series expansion appears to be a satisfying approximation of the transition region:

$$H = H_0 + \frac{H_0^{(2)}}{2} E^2 + \frac{H_0^{(3)}}{6} E^3 \tag{5.37}$$

where $H_0^{(2)}$ and $H_0^{(3)}$ result from the above two conditions at $E=E_Q$:

$$H_0^{(2)} = \frac{6}{E_Q^2} \left[H_Q - H_0 - \frac{E_Q}{3} H_Q^{(1)} \right] \tag{5.38}$$

$$H_0^{(3)} = \frac{2}{E_Q^2} \left[H_Q^{(1)} - E_Q H_0^{(2)} \right] \tag{5.39}$$

<u>Drying times</u> $(D_r = m^a, \ 0 \leq \sigma \leq 1, \ m_i = 0)$

The drying time follows from the integration of the mass balance:

$$\tau = \int_0^E \frac{dE}{FX_i} = \int_0^E \frac{dE}{HF_{\sigma=0}X_i} \tag{5.40}$$

where, $F_{\sigma=0}$ is given by equation 5.7 for $0 \leq E \leq E_T$ and

by equation 5.12 for $E > E_T$

H is given by equations 5.37 for $0 \leq E \leq E_Q$ and

by equation 5.35 for $E > E_Q$

X_i is given by equation 3.42

In general this integration has to be carried out by means of numerical methods (e.g. trapezium rule).

5.4   Drying Stage with Constant Surface Activity.

5.4.1 Non-Shrinking Systems $(D_r = m^a, \ \sigma = 0, \ F_{ca} \approx \text{constant})$

During the period with constant surface moisture activity $(a_{mi} \approx \text{constant})$ the drying flux of a non-shrinking system will remain nearly constant: $F = F_{ca} \approx \text{constant}$ (see chapter IV).

The contents of §4.3 also apply to systems with concentration dependent diffusion coefficients. However, the relationship among F_{ca}, E and E_i' has to be derived now from the numerical computer output. A straight forward use of the G-parameter (eqn. 4.35) and of correlations according to equation 4.37 now fails, because the parameter E/E_i' no longer is a continuously increasing quantity in all drying situations, e.g. at high fluxes E/E_i' versus τ may show a maximum!

A different but succesful approach for power law diffusion departs

from a transformation of the generalized diffusion equation with $\tilde{m} = m^{a+1}$ (see also Appendix D):

Generalized partial differential equation:

$$\frac{\partial \tilde{m}}{\partial \tau} = (\tilde{m})^{\frac{a}{a+1}} \frac{\partial}{\partial \phi}(X^2 \frac{\partial \tilde{m}}{\partial \phi}) \qquad (5.41)$$

Initial condition:

$$\tau = 0 \qquad 0 \leq \phi < 1 \qquad \tilde{m} = 1 \qquad (5.42)$$

Boundary conditions:

$$\tau > 0 \qquad \phi = 0 \qquad X \frac{\partial \tilde{m}}{\partial \phi} = 0 \qquad (5.43)$$

$$\phi = 1 \qquad -X_i \frac{\partial \tilde{m}}{\partial \phi} = \tilde{F} \qquad (5.44)$$

---

where $\tilde{F} = F(a+1)$.

The solution of this transformed diffusion equation can be written as:

$$\tilde{m} = \tilde{m} (\phi, \tau, \nu, \lambda, \frac{a+1}{a}, \tilde{F}, \sigma v_0, \sigma v_\#) \qquad (5.45)$$

For high a-values a limit solution is approached, because $\frac{a}{a+1} \rightarrow 1$. In addition to $\tilde{m}$ and $\tilde{F}$ some more helpful parameters are defined below.

Table 5.1 Definitions of some parameters.

$\tilde{m} = m^{a+1}$	$\tilde{F} = F(a+1)$
$\tilde{E} = 1-(\overline{m})^{a+1}$	$\tilde{E}_i^{\cdot} = 1-(m_i)^{a+1}$
$\epsilon = \dfrac{\tilde{E}}{\tilde{E}_i^{\cdot}} = \dfrac{1-(\overline{m})^{a+1}}{1-(m_i)^{a+1}}$	$\tilde{G} = \dfrac{\dfrac{\tilde{F}}{\tilde{E}_i^{\cdot}} \dfrac{\tilde{E}}{\tilde{E}_i^{\cdot}}}{X_i}$

Regular Regime $(D_r = m^{\alpha}, \ \sigma = 0, \ F_{ca} \approx constant)$

From equations 4.45 and 4.46 now follows:

$$F_{ca} = \frac{1}{2} \cdot \frac{Sh_{d,ca}}{a+1} \left[(\bar{m})^{a+1} - (m_i)^{a+1} \right] \tag{5.46}$$

and expressed in the parameters of Table 5.1:

$$\tilde{F}_{ca} = \frac{1}{2} Sh_{d,ca} (\tilde{E}_i' - \tilde{E}) \tag{5.47}$$

This latter expression for the flux parameter is analogous to equation 4.47 for concentration independent diffusion coefficient. However, *in case of power law diffusion with $a \neq 0$ no constant value for the Sherwood number is obtained*: after passing through a minimum value (Figure 5.1) the Sherwood number is gradually increasing until an end value at $E_i'=1$ is reached. Schoeber [23] observed that this end value is nearly independent of the flux parameter F_{ca}. For massive geometries Liou [28,29] found a pseudo linear relationship by plotting the numerically computed values of $Sh_{d,ca}$ at $E_i'=1$ against values of $\frac{a}{a+2}$; it appears now that this linearity also holds for hollow geometries. The correlation for $Sh_{d,E_i'=1}$ then reads:

$$Sh_{d,E_i'=1} = Sh_{d,a=0} + (Sh_{d,a\to\infty} - Sh_{d,a=0}) \frac{a}{a+2} \tag{5.48}$$

in which $Sh_{d,a=0}$ is given by equation 4.51:

$$Sh_{d,a=0} = 6+2v \left[\frac{X_{i,\sigma=0}^{-1}}{v} \right]^{2.15-0.18v} \tag{4.51}$$

and

$$Sh_{d,a\to\infty} = 10.443+5.935\upsilon \left[\frac{X_{i,\sigma=0}}{\upsilon}^{-1}\right]^{1.25-0.03\upsilon} \qquad (5.49)$$

Note that also in equation 5.49 only the exponent is a correlation parameter.

For Regular Regime behaviour with $E_i' \lesssim 1$ the Sherwood number of the constant activity period $Sh_{d,ca}$ is approximated quite well with the correlation:

$$Sh_{d,ca} = Sh_{d,a=0} + \left[Sh_{d,E_i'=1} - Sh_{d,a=0}\right] E_i' \qquad (5.50)$$

From equations 5.50 and 5.48 finally follows:

$$Sh_{d,ca} = Sh_{d,a=0} + \left[Sh_{d,a\to\infty} - Sh_{d,a=0}\right] \frac{a}{a+2} E_i' \qquad (5.51)$$

<u>Penetration Period</u> $(D_r = m^a, \ \sigma = 0, \ F_{ca} \approx constant)$

Approximations for this drying stage are based on Taylor series expansions of $\tilde{G}$ versus ϵ according to:

$$\tilde{G} = \tilde{G}_0 \left[1 + \tilde{\alpha}\epsilon + \tilde{\gamma}\epsilon^3\right] \qquad (5.52)$$

from which follows:

$$\frac{\tilde{F}_{ca}}{\tilde{E}_i'} = \tilde{G}_0 X_i \left[\frac{1}{\epsilon} + \tilde{\alpha} + \tilde{\gamma}\epsilon^2\right] \qquad (5.53)$$

in which *the initial value* $\tilde{G}_0$ *appears to be independent of the power* a. The solution can be derived analytically (Appendix E):

$$\tilde{G}_0 = \frac{\pi}{4} \qquad (5.54)$$

From the numerical calculations the initial slope of $\tilde{G}$ versus ϵ proved to be pseudo linear with aF_{ca} and the following correlation for $\tilde{\alpha}$ can be derived:

$$\tilde{\alpha} = \frac{0.5\ aF_{ca} - v(1-\lambda)}{X_{i,\sigma=0}} \qquad (5.55)$$

A correlation for $\tilde{\gamma}$ is based on the end point $(\epsilon=\epsilon_e, \tilde{G}=\tilde{G}_e)$ of the Penetration Period:

$$\tilde{\gamma} = \frac{\tilde{G}_e/\tilde{G}_0 - 1 - \tilde{\alpha}\ \epsilon_e}{\epsilon_e^3} \qquad (5.56)$$

With respect to the end of the Penetration Period two situations are to be considered:

1) *the Penetration Period ends where the Regular Regime starts.*
Similarly to a concentration independent diffusion coefficient the following transition criterium should be used:

$$\frac{\tilde{F}_{ca}}{\tilde{E}_i^{\cdot}} = 1.5 \qquad (5.57)$$

Elimination of $\tilde{F}_{ca}$ from the Regular Regime approximation (eqn. 5.47) and the transition criterium (eqn. 5.57) gives:

$$\epsilon_e = 1 - \frac{3.0}{Sh_{d,ca}} \qquad (5.58)$$

and from the definition of $\tilde{G}$ (Table 5.1):

$$\tilde{G}_e = \frac{1.5}{X_{i,e}}\ \epsilon_e \qquad (5.59)$$

Note, that in the approach of this chapter the transition criterium can be formulated independently of the geometry parameter v *and* the hollowness factor λ (compare with eqn. 4.52).

2) *the Penetration Period ends if* $E'_i = E'_{i,cr}$

If $\widetilde{F}_{ca} \geq 1.5 \; \widetilde{E}'_{i,cr}$ then the transition criterium (eqn. 5.57) indicates, that *there will not be a Regular Regime (with a constant boundary flux) succeeding the Penetration Period.* In this case the drying stage with a constant boundary flux ends with a concentration profile, which has not yet penetrated into the centre of the material. The end value ϵ_e will be higher as $\widetilde{F}_{ca}$ is choosen higher. The *critical point curve* $\widetilde{F}_{ca}$ versus ϵ_e with $\widetilde{E}'_{i,cr} = E'_{i,cr} = 1$ shows great similarity to the *penetration curve* (eqn. 5.7) of a drying process with a zero boundary concentration. However, a much better approximation is found if F_{ca} versus E_e is considered instead of $\widetilde{F}_{ca}$ versus ϵ_e:

$$F_{ca} = G_{0,ca} X_i \left(\frac{1}{E_e} - \alpha \right) \tag{5.60}$$

For a=0 this equation must be identical with the penetration curve of a drying proces with constant boundary flux and $E'_i = 1$ (eqn. 4.37) From the numerical computer output the following correlations for $G_{0,ca}$ and α are derived:

$$G_{0,ca} = \frac{\pi}{4} \left[\frac{1.45}{a+1.45} \right]^{1.89} \qquad \text{for } 0 \leq a < \infty \tag{5.61}$$

$$\alpha = \alpha_{a=0} + \Delta\alpha \qquad \text{for } 0 \leq a < 4 \tag{5.62}$$

where $\alpha_{a=0}$ is given by equations 4.38; for $a \neq 0$ a correction $\Delta\alpha$, which is pseudo linear with a, has to be added:

For a slab   : $\Delta\alpha = (0.11)a$ (5.63a)

For a cylinder: $\Delta\alpha = (0.22-0.05\lambda-0.20\lambda^2+0.14\lambda^3)a$ (5.63b)

For a sphere : $\Delta\alpha = (0.24+0.03\lambda-0.19\lambda^2+0.03\lambda^3)a$ (5.63c)

5.4.2 Systems with Any Degree of Shrinkage

$(D_r = m_-^a, \; 0 \leq \sigma \leq 1, \; a_{mi} \approx$ constant$)$.

For shrinking cylinders and spheres the *drying flux will not remain constant* during the period with constant surface water activity, because the mass transfer coefficient in the gas phase depends on the dynamic outer radius $R_{2,t}$ of the shrinking body. In general the following relation holds:

$$j_{wi,t}^s (R_{2,t})^q = \text{constant} = j_{wi,0}^s (R_{2,0})^q \qquad (5.64)$$

where,

q=0   in case of a slab ($v=0$);

q=1   if the Sherwood number for the gasphase (Sh) is constant;
         for instance, Sh=2 for a droplet in a spray drier.

q=1-n   if Sh depends on the Reynolds number according to Sh $\sim R_e^{\,n}$
         (eqn. 2.45)

The flux parameter of the constant activity period (F_{ca}) can be related to its initial value $(F_{ca,0})$ from equation 5.64 as follows:

$$\frac{F_{ca}}{F_{ca,0}} = \frac{j_{wi,t}^s}{j_{wi,0}^s} = \left[\frac{R_{2,0}}{R_{2,t}}\right]^q = \left[\frac{A_0}{A_t}\right]^{\frac{q}{v}} = \left[\frac{X_{i,0}}{X_i}\right]^{\frac{q}{v}} \qquad (5.65)$$

and applying the expression for X_i (eqn. 3.42):

$$F_{ca} = \frac{F_{ca,0}}{(1-sE)^{\frac{q}{\nu+1}}}$$

(5.66)

Equation 5.66 now becomes the boundary condition of the diffusion equation at $\phi = 1$.

Integration of the mass balance (eqn. 3.41) by using the expressions for X_i (eqn. 3.42) and F_{ca} (eqn. 5.66) gives:

$$\tau = \frac{(\nu+1)\left[1-(1-sE)^{\frac{q+1}{\nu+1}}\right]}{(q+1)\ sF_{ca,0}X_{i,0}}$$

(5.67)

The relationship among $F_{ca,0}$, E and E_i' has to be derived from the numerical solutions; however, this was not investigated.

CHAPTER VI

EVALUATION OF EXPERIMENTAL DRYING CURVES

6.1 Introduction.

To investigate the practical aspects of power law diffusion, drying

experiments were carried out using aqueous maltodextrin solutions. In

a vacuum drying apparatus samples with a slab geometry were dried

isothermally; the weight of the sample as function of time was

registrated automatically by means of a micro-computer.

A slab geometry has some very important advantages over other

geometries, viz.:

- the data reduction of the experimental drying curves is very simple,

  because the relative simple correlations derived for non-shrinking

  systems, may be applied irrespective of the degree of shrinkage;

- the exchange surface area is independent of the shrinkage behaviour

  and thus remains constant during an experiment;

- samples can be prepared easily and reproducably;

- isothermal drying conditions can be created relatively easily.

This chapter deals first with some theoretical aspects with respect to

the data reduction of slab drying experiments, viz. the calculation of

concentration dependent diffusion coefficients according to Schoeber's

method [23] and the description and prediction of drying curves. Next

the drying apparatus and the experimental procedure are described.

Finally the results of the drying experiments are evaluated.

Some relevant properties of maltodextrin are summarized in Appendix F.

6.2   Theoretical Aspects.

6.2.1   Determination of Diffusion Coefficients.

Schoeber [23] describes a method to derive diffusion coefficients from experimental Regular Regime (with $m_i=0$) drying curves. By analyzing several concentration dependences of the diffusion coefficient he correlated Sh_d with $dlnF/dln(1-E)$. He observed that a power law dependence showed a good "average" behaviour: irrespective of the concentration dependence of the diffusion coefficient, Sh_d-values deviate less than 15% from the Sh_d-values belonging to the power law dependence. Schoeber's method and its practical application are described below.

In Chapter IV the following expression (eqns. 4.45 and 4.46) for the flux parameter F was introduced:

$$F = \frac{1}{2} Sh_d D_r (\bar{m} - m_i) \tag{6.1}$$

in which,

$$D_r(\bar{m} - m_i) = \int_{m_i}^{\bar{m}} D_r dm \tag{6.2}$$

From equations 6.1 and 6.2 with $m_i=0$ follows:

$$\int_0^{\bar{m}} D_r \, dm = \frac{2F}{Sh_d} \tag{6.3}$$

Differentiation of this equation yields:

$$D_r = \frac{d(2F/Sh_d)}{d\bar{m}} \qquad \text{at } m=\bar{m} \tag{6.4}$$

and the equation for the calculation of the diffusion coefficient follows by applying the definitions of D_r, F and $\bar{m}$ (see §3.5):

$$D = \frac{1}{(\bar{\rho}_s)^2} \frac{2}{Sh_d} \frac{d(j_{mi}^s d_s R_s)}{d\bar{u}} \qquad \text{at } u=\bar{u} \tag{6.5}$$

The value of Sh_d is found from the Regular Regime correlation between Sh_d and $d\ln F/d\ln(1-E)$. Assuming a power law concentration dependence of the diffusion coefficient, it follows from equations 5.13–5.16 for a slab geometry:

$$Sh_d = 4.935 + 2.456 \frac{a}{a+2} \tag{6.6}$$

where a is found from:

$$\frac{d\ln F}{d\ln(1-E)} = a+1 \tag{6.7}$$

Equation 6.5 can also be expressed in terms of the efficiency E as follows below.

From the mass balance over the slab follows ($d_s R_s = \rho_{s0} R_0$):

$$j_{mi}^s d_s R_s = d_s^2 R_s^2 (u_0 - u_*) \frac{dE}{dt} \tag{6.8}$$

In case of perfect shrinkage behaviour $(\sigma=1)$ the relation between $\bar{\rho}_s$ and E is given by:

$$\frac{\bar{\rho}_s}{\rho_{s0}} = \frac{1+v_0}{1+v_0(1-E)}$$

(6.9)

and from equations 6.5, 6.8 and 6.9 follows:

$$D = \frac{2R_0^2}{Sh_d} \left[\frac{1+v_0(1-E)}{1+v_0}\right]^2 \frac{d(\frac{dE}{dt})}{d(1-E)}$$

(6.10)

The mass balance can also be written as:

$$F = \frac{R_0^2}{D_0} \frac{dE}{dt}$$

(6.11)

so equation 6.7 becomes:

$$\frac{d\ln(\frac{dE}{dt})}{d\ln(1-E)} = a+1$$

(6.12)

Slight modification of Schoeber's method

If power law diffusion is assumed, then:

$$F = \frac{1}{2} \frac{Sh_d}{a+1} (1-E)^{a+1}$$

(6.13)

From equations 6.11 and 6.13 follows:

$$\frac{dE}{dt} = \frac{1}{2} \frac{Sh_d}{a+1} \frac{D_0}{R_0^2} (1-E)^{a+1}$$

(6.14)

and from equations 6.10 and 6.14 can be derived, that the diffusion
coefficient can also be calculated by using:

$$D = D_0 \left[\frac{1+v_0(1-E)}{1+v_0}\right]^2 (1-E)^a \qquad (6.15)$$

in which a and D_0 are found by linear regression over small intervals
of $\ln(dE/dt)$ versus $\ln(1-E)$:

$$\ln\left(\frac{dE}{dt}\right) = \ln\left[\frac{1}{2}\frac{Sh_d}{a+1}\frac{D_0}{R_0^2}\right] + (a+1)\ln(1-E) \qquad (6.16)$$

6.2.2 Description of Isothermal Drying Curves.

During drying of slabs with a high initial flux three drying stages
can be distinguished:

- a relatively short period with a nearly constant surface moisture
  activity and thus a nearly constant drying flux;

- a Penetration Period with a nearly constant surface concentration
  ($m_i \approx 0$), followed by

- a Regular Regime ($m_i \approx 0$)

In case of power law diffusion the isothermal drying of a material can
be described fully by only two parameters, accounting for the
concentration dependence of the diffusion coefficient, either a and b
or a and D_0.

These parameters can be derived from the Regular Regime drying curve
by means of linear regression of $\ln(dE/dt)$ versus $\ln(1-E)$ according to
equation 6.16, however, now regression should be performed over all
data points of the Regular Regime.

For high initial drying fluxes the Penetration Period should be

evaluated by using the expression (see Chapter V):

$$t = \frac{1}{2} \frac{R_0^2}{G_0 D_0} E^2 \qquad\qquad (6.17)$$

in which,

$$G_0 = \frac{2}{\pi} \left[\frac{1.42}{a+1.42} \right]^{1.98} \qquad\qquad (6.18)$$

and from equation 5.1:

$$D_0 = \frac{b(u_0 - u_*)^a}{\rho_{s0}^2} \qquad\qquad (6.19)$$

Data reduction by linear regression of t versus E^2 gives a value for the slope $R_0^2/(2G_0 D_0)$. Finding a and b from the slope, in combination with equations 6.18 and 6.19, requires at least two experiments at different initial concentrations u_0.

6.3   Experimental.

6.3.1 Description of Drying Apparatus.

As we have seen in §6.2 the data reduction of the experiments requires the first and second derivatives of the drying curves. Therefore the measurement of the weight should be as free of noise as possible and many data points of weight versus time should be acquired. For this reason the drying is performed under vacuum conditions (no noisy drag forces caused by a streaming gas) and the experimental set-up is fully automated by means of a micro-computer.

The drying apparatus (Figure 6.1) consists of two horizontal cylindrical chambers, one on top of the other. The chambers are connected with each other by means of a tube and are accessible at the front. The diameter and the depth of each chamber are 50 cm. The sample holder in the lower chamber is connected to an electronic precision balance (resolution 1 mg) in the upper chamber.

The temperature of the sample is kept constant by an electrically heated radiation wire, placed about 10 cm above the sample holder. The temperature of the sample layer is measured with a thermocouple (type T, Cu/CuNi). The power supplied to the radiation wire is regulated by a temperature controller.

To dilute the evaporated moisture ($\rho'_{m\infty} \approx 0$) clean and dry air ($R_4$) is blown as evenly as possible over the sample. In order to avoid uneven drying of the slab a sieve plate is placed between the sample and the air stream. The distance between sieve plate and sample is about 1 cm. This space may be considered as a diffusional resistance. The moisture diffusion coefficient in the gas phase is inversely proportional to the absolute pressure [1]. The initial rate of drying depends on the slab temperature, absolute pressure in the chambers and the distance between sample holder and sieve plate. The absolute pressure in chambers is kept constant by means of a pressure transmitter and a pressure controller, which activates the servo motor of a needle valve (R_2). The sample holder is made of PTFE, which hardly takes up any moisture. Moreover, PTFE is a good heat insulator, which favours a uniform temperature distribution in the slab. The sample holder has a cylindrical shape with diameter 6 cm and depth 2.5 mm.

For data-acquisition the digital weight balance, the temperature controller, the pressure controller and several thermocouples are connected to a microcomputer. During a drying experiment the following
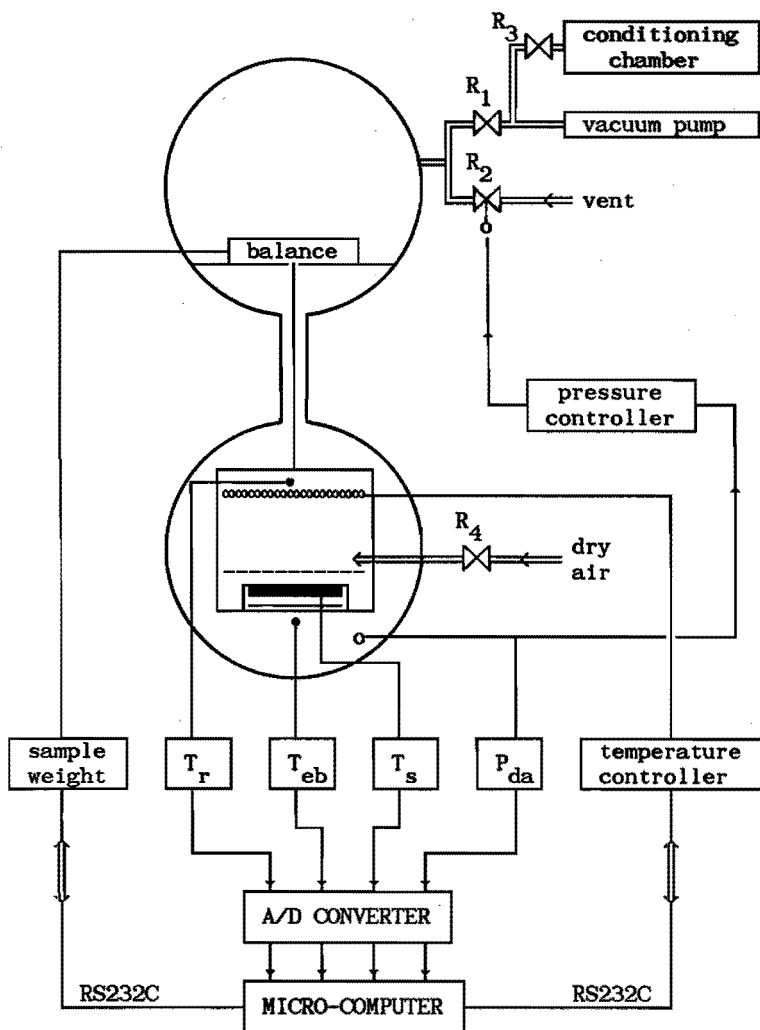
Figure 6.1   Vacuum drying apparatus

■■■■ = sample;   --- = sieve plate;

∞∞∞∞ = radiation source; T_s = sample temperature;

T_{eb}= temperature external bottom sample holder;

T_r = temperature of radiation source;

P_{da}= pressure in drying apparatus.

physical quantities are automatically recorded:

- the sample weight;

- the temperature of the slab;

- the temperature in the neighbourhood of the radiation wire; this
  temperature is a rough indication for the activity of the radiation
  source;

- the temperature of the external bottom of the sample holder (to
  ascertain a uniform temperature in the sample);

- the absolute pressure in the chambers (to ascertain constant
  external drying conditions).

6.3.2 Experimental Procedure.

Sample preparation.

To avoid internal circulations inside the slab, a gel of the aqueous
maltodextrin solutions is prepared by adding a small amount of
agar-agar (1 wt% on water basis). A sample layer is obtained by
injecting the warm solution (50 ^{o}C) into the sample holder via a cover
with two holes in it (Figure 6.2).

sample injection

cover
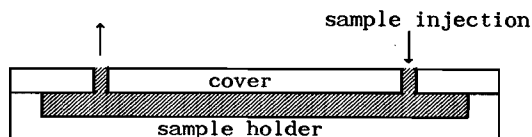
sample holder

Figure 6.2 Preparation of a gelled layer.

After gelation at a lower temperature (e.g. 0°C), the cover is shifted
away and a perfectly smooth slab is obtained. Immediately the sample
holder is closed with a stainless steel cover plate provided with a
"O" ring.

Sample conditioning.

It takes about three minutes to reach the desired pressure (about 12000 N/m^2) in the drying chamber. To obtain a well-defined starting point it must be avoided, that during this period the sample starts drying. Therefore the sample, with a cover over it, is first placed in a separate conditioning chamber (Figure 6.3).
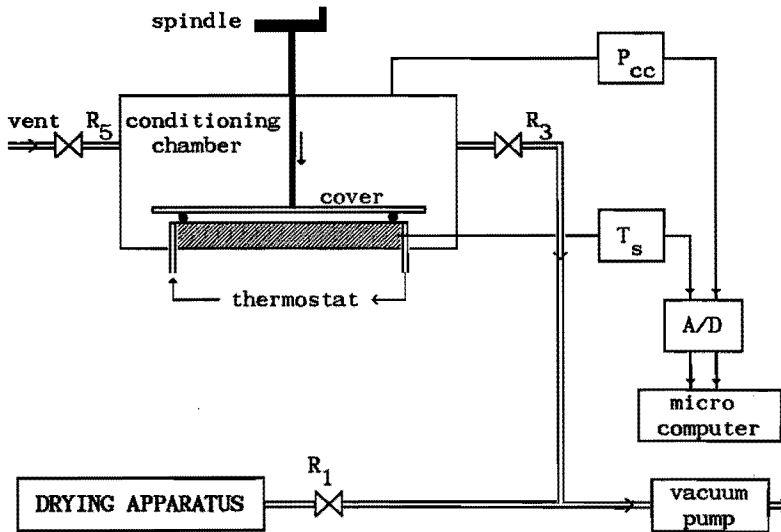
Figure 6.3   Conditioning chamber

     ▨ = double-walled heat exchanger, in which sample

       holder is placed;

     P_{cc}= chamber pressure; T_s = sample temperature.

At reaching the desired pressure (P_{cc}) and temperature (T_s) of the sample the cover plate with "O"-ring is pressed firmly to the sample holder by means of a spindle and then the chamber is brought to atmospheric pressure again.

Start of drying experiment.

Because of the underpressure in the small space between cover plate and sample surface, the sample holder will "stick" to the cover plate. In this condition the sample holder is placed in the drying chamber, whereby the cover plate is resting on two bars (Figure 6.4).
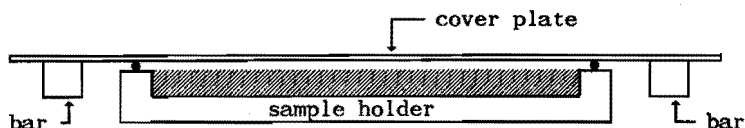
Figure 6.4 Position of sample holder just before the start of a drying experiment (▨ = sample layer)

The drying chamber is closed and the pressure is brought to the desired value. A short time before the end pressure is reached, the sample holder releases from the cover plate and falls on the digital electronic weight balance. The sudden change of the balance signal is registrated by the micro-computer and interpretated as the start of the experiment; at the same time the balance is zeroed and a motor is activated to pull away the cover plate.

During drying experiment.

About 1000 times during an experiment the computer samples the following data: time, signal of the weight balance, signals of thermocouples (sample, external bottom of sample holder, radiation source) and signal of pressure transmitter.

End of drying experiment.

The experiments are aborted if the drying efficiency is at least 0.95. The duration of an experiment varies from several hours to one day.

Representation of results.

From the momentary, initial and final weight of the sample the drying efficiency E can be calculated quite simply. For the evaluation of the drying experiment (§6.2) also dE/dt is required. To obtain sufficiently accurate values for dE/dt the increase of the efficiency during a time interval should be large enough. Therefore a selection of about 100 time intervals from all collected data has been made; during the selected time intervals the increase of the effiency is about 0.007-0.01.

In Table 6.1 a summary of the conditions used in the various drying experiments is given. The pertinent experimental data (efficiency E versus time t) can be found in Appendix G.

Table 6.1 Drying experiments of gelled maltodextrin/water layers (R_0=2.50 mm, d_s=1610 kg/m^3)

exp. number	%wt of solid	temp. (^{o}C)	pressure (N/m^2)	initial weight of layer (g)	ρ_{s0} (kg/m^3)	u_0 (kg/kg)
5	29.4	41.4	12500	7.66	331	2.40
6	29.4	32.8	12450	7.84	331	2.40
7	29.4	26.4	12400	7.92	331	2.40
8	17.1	35.8	12400	7.51	183	4.85
9	17.1	26.7	12200	7.65	183	4.85

6.4 Results and Discussion.

From calculations, based on temperatures of the sample layer and of the external bottom of the sample holder, it could be confirmed that sample temperatures were uniform within ± 0.2 ^{o}C. It appeared, that the temperature change of a sample during a whole experiment was of

the same magnitude. The pressure in the drying chamber was constant within ± 100 N/m^2.

6.4.1 Merging of drying curves.

The relationship D versus u is a physical property of the material and so it has to be independent of the initial drying conditions. Therefore it follows from equation 6.5 that curves $j_{mi}^{s} d_s R_s$ versus $\bar{u}$ for e.g. different initial moisture concentrations must merge in the Regular Regime.

This conclusion has been verified experimentally by Schoeber [23] for aqueous glucose solutions and by Luyben et.al. [25-27] for a number of materials. From our investigation it appears, that also for aqueous maltodextrin solutions, at low concentrations the two drying curves coincide (Figure 6.5); from this merging part of the drying curves the initial conditions can not be reconstructed. Actually, Figure 6.5 gives the experimental proof for the occurrence of Regular Regimes.

6.4.2 Diffusion coefficients.

Diffusion coefficients can be calculated from the experimental data in two ways: according to equation 6.10 and according to equation 6.15. Both methods have been used and they both require the relation of dE/dt versus (1-E). To reduce noise and irregularities the first derivative dE/dt is smoothed by recalculating each data point as an average of its original value and four surrounding data points, two before and two after the original point; all points are weighted equally.
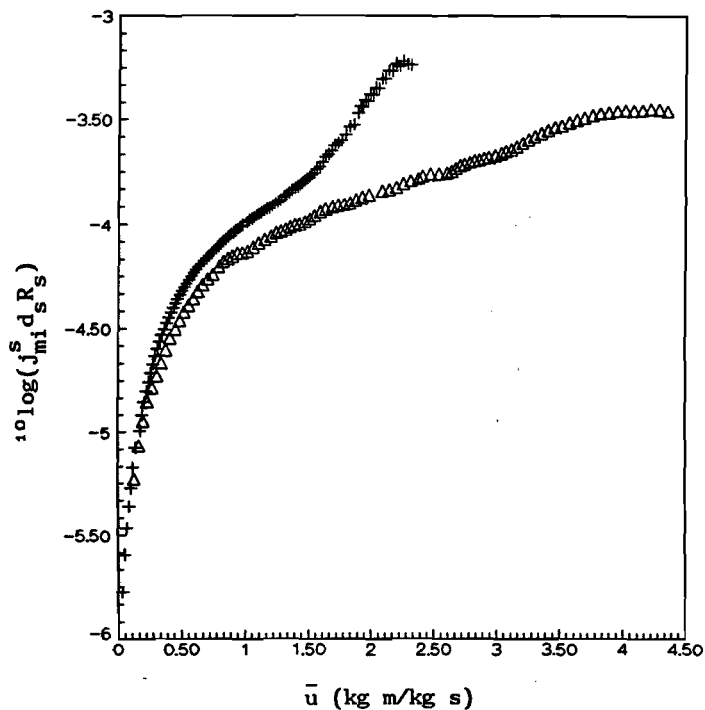
Figure 6.5

Merging of drying curves
with different initial
conditions.

+ experiment 7
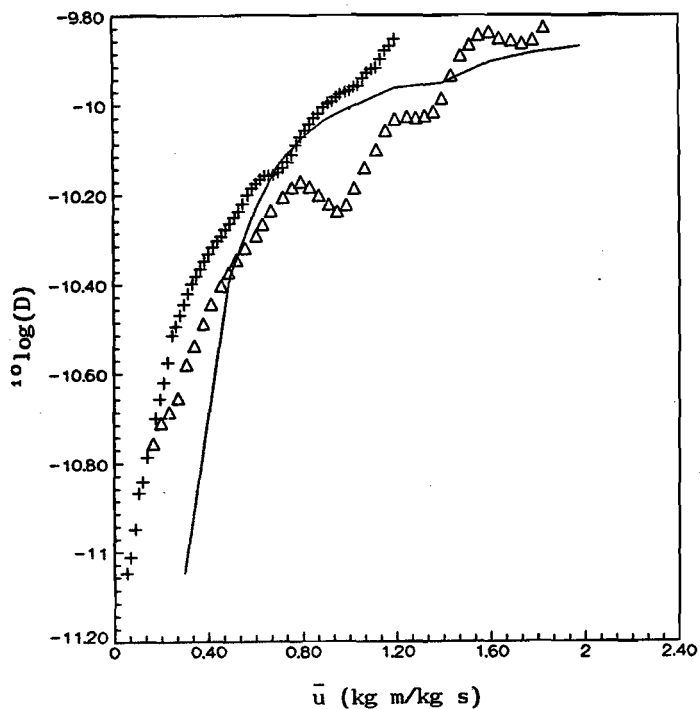
Δ experiment 9

Figure 6.6

Diffusion coefficient of
water in aqueous malto-
dextrin solution at 27 °C

+ experiment 7

Δ experiment 9

— Furuta et.al.

At each data point the second derivative in equation 6.10 and the a and D_0 values in equations 6.12 and 6.16 are determined via linear regression of 9 data points, 4 points before and 4 points after the central data point; all points are weighted equally.

It appears that diffusion coefficients calculated according to equation 6.10 do not deviate significantly from those calculated with equation 6.15. Diffusion coefficients, derived from experiments 7 and 9 with the modified Schoeber's method (eqn. 6.15) are represented in Figure 6.6. The oscillations, especially in experiment 9, due to experimental noise and irregularities, are not fully eliminated by smoothing and regression techniques. The *random errors*, caused by these oscillations, are about ±10 % .

Systematic deviations are found between diffusion coefficients, which have been derived from experiments with different initial moisture contents. For example, in a large concentration range diffusion coefficients from experiment 7 (u_0=2.40 kg m/kg s) are about 25% higher than those from experiment 9 (u_0=4.85 kg m/kg s). Because experiment 9 starts at a higher initial moisture concentration, higher efficiencies are obtained at the same actual moisture concentration than in experiment 7; from this it is concluded that experiment 9 is more "regular" and will give more reliable diffusion coefficients than experiment 7.

At lower concentrations the two drying curves coincide and nearly the same diffusion coefficients are found. Deriving diffusion coefficients from *one* drying curve, as proposed by Schoeber [23], appears to be doubtful. *Deriving diffusion coefficients from the merging parts of several drying curves with different initial moisture concentrations, as done by Luyben et.al.[25], appears to be a better approach.* Diffusion coefficients at low concentrations will be more reliable, if

they are derived from experiments with low initial moisture concentrations. For example: at u=0.1 (kg m/kg s) a drying efficiency of 0.975 is required if u_0=4 and 0.9 is required if u_0=1; in the first case relative errors in 1-E, due to experimental inaccuracies, will be larger than in the second case.

Furuta et.al. [22] obtained diffusion coefficients of water in maltodextrin solutions from many desorption experiments. By applying low driving forces their concentration profiles were rather flat and the total change of the concentration during each single experiment was rather small. Therefore the diffusion coefficient could be assumed constant within those small concentration intervals. Their results (see Figure 6.6) are in fairly good agreement with ours, except for low concentrations (u<0.3 kg m/kg s), where large deviations exist.

6.4.3 Description of experimental drying curves.

A single drying experiment can be described quite well by means of the short-cut equations for power law diffusion (see Chapter V). This will be shown from experiment 9 as a typical example. In Figure 6.7 some characteristic relations, derived from this experiment, are represented.

From a first examination of the Regular Regime drying curve it was estimated that a≈0. Therefore Regular Regime behaviour was assumed for E≥0.5. Linear regression of $\ln(dE/dt)$ versus $\ln(1-E)$, including all data points in this range, gives a better value for a and thus a better estimate for the pertinent concentration range; after two or three iterations a = 0.075 and D_0 = $1.00 \cdot 10^{-9}$ m^2/s were found. Taking these values of a and D_0, the drying history can be reconstructed as follows.
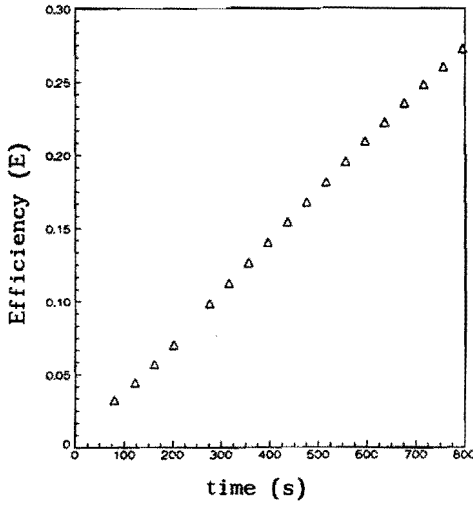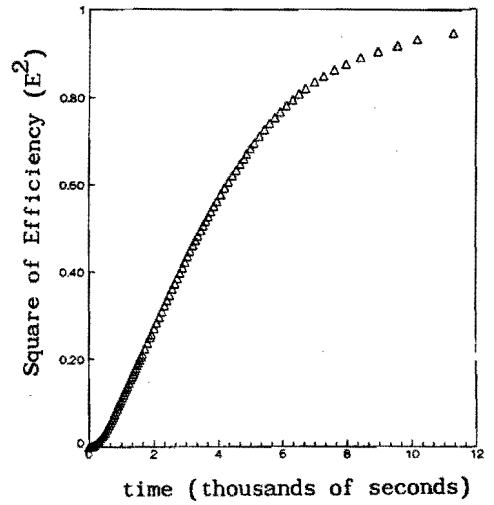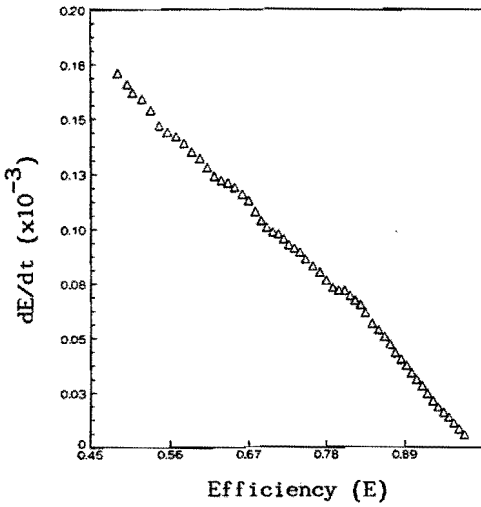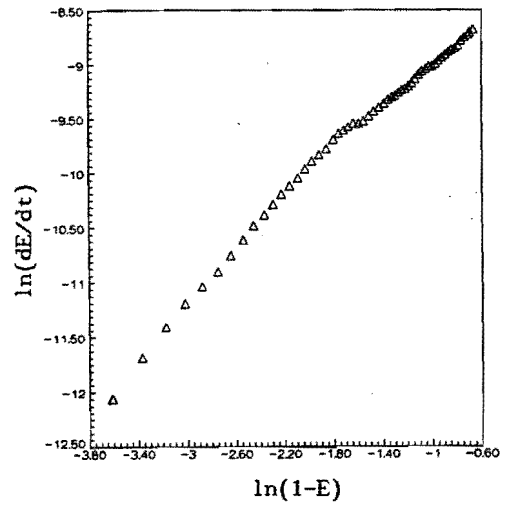
Figure 6.7 Experiment 9 (see text)

(a) E versus t   (b) E^2 versus t

(c) dE/dt versus E   (d) ln(dE/dt) versus ln(1−E)

Constant flux period

The imposed initial drying flux $dE/dt = 3.50 \cdot 10^{-4}$ s^{-1} is obtained by linear regression of E versus t in the arbitrarily chosen range $0 \leq E \leq 0.2$. Now the initial value of the flux parameter $F_{ca} = 2.187$ follows from equation 6.11. The critical moisture concentration $u_{cr} = 0.362$ kg m/kg s follows from the sorption-isotherm of maltodextrin/water (see Appendix F), assuming that the critical moisture activity $a_{mi} = 0.9$. From the definition of the efficiency follows for the critical surface efficiency $E'_{i,cr} = 0.925$. From equation 5.53 follows after iteration, that at the end of this period the average efficiency $E_{ca} = 0.273$.

Now the duration of the constant flux period can be calculated from the mass balance $\tau_{ca} = E_{ca}/F_{ca} = 0.125$. Applying the definition of τ finally gives $t_{ca} = 779$ seconds.

Penetration Period $(m_i = 0)$

In case of the extreme situation that $E'_{i,cr} = 1$, it follows from equation 5.60 that $E_{ca} = 0.325$ and $t_{ca} = 928$ seconds. With respect to the total drying time the difference between 928 s and 779 s is small and therefore it is assumed now, that the transition period, in which the surface efficiency increases from the critical value $(E'_i = E'_{i,cr})$ to the equilibrium value $(E'_i = 1$ or $m_i = 0)$ is reached within a neglible time interval. This means that it is assumed, that the critical point curve $(F_{ca}$ versus E_{ca} with $m_{i,cr} = 0)$ nearly coincides with the penetration curve (F versus E with $m_i = 0$).

Because in this experiment the constant flux period contributes substantially to the total drying time, the Penetration Period should be calculated with:

$$t = t_{ca} + \frac{R_0^2}{2G_0 D_0} (E^2 - E_{ca}^2) \qquad\qquad (6.20)$$

in which,

$E_{ca} = 0.273$, $t_{ca} = 779$ seconds and $G_0 = 0.575$ (from eqn. 6.18).

Transition

The transition from the Penetration Period to the Regular Regime

occurs at $E_T = 0.482$ (from eqn. 5.20).

Regular Regime

For $E > E_T$ the Regular Regime expression (from eqn. 5.18) reads:

$$t = t_T + \frac{2R_0^2}{Sh_d D_0} \frac{a+1}{a} \left[\frac{1}{(1-E)^a} - \frac{1}{(1-E_T)^a} \right] \qquad\qquad (6.21)$$

in which $Sh_d = 5.024$ (from eqn. 6.6) and $t_T = 1634$ s (from eqn. 6.20).
A comparison of measured and calculated drying times shows, that
maximum deviations are about 10% (see Appendix G-9).
This result, which is typical for all drying experiments, proofs that
the whole drying history can be reconstructed from experimental data
of the Regular Regime.

Note

Though the initial value of the flux parameter is not very high in
this case, it still ensures the occurrence of a Penetration Period
with zero surface concentration ($m_i = 0$); higher initial values for F_{ca}
can be achieved by higher temperatures, lower pressures in the drying
chamber, thicker slabs and lower initial moisture contents (for
obtaining lower values for D_0); it should be noticed, however, that

thicker slabs and lower D_0-values will increase the duration of a drying experiment.

6.4.4 Prediction of experimental drying curves.

In case of power law diffusion data reduction of all drying curves, irrespective of the initial concentration, should give one a-value and one b-value. However, it appears from our experiments, that power law diffusion does not apply strictly to solutions of maltodextrin/water (see also §6.4.6). Therefore a *semi-empirical approach* for the prediction of drying curves is proposed here. It appears that from drying curves at higher initial moisture contents the drying curves at lower initial moisture contents can be predicted. This will be illustrated by predicting drying experiment 7 (u_0= 2.40 kg m/kg s) from drying experiment 9 (u_0= 4.85 kg m/kg s).

The prediction method is based on the former observation, that the Regular Regime drying curves contain all necessary information. The values of a and D_0 for the prediction of experiment 7 are derived from the Regular Regime of experiment 9. Assuming a = 0.075 (so, E_T= 0.482) the concentration range of the Regular Regime of experiment 7 is: $0{\leq}u{\leq}1.16$ kg m/kg s. Linear regression of ln(dE/dt) versus ln(1-E) with all data points from experiment 9 in this range gives a better a-value and thus a better estimate of the relevant concentration range; linear regression is repeated, etc.. After only two iterations: a = 0.292 and D_0= $5.03{\cdot}10^{-10}$ m^2/s. Similarly to the method, as described in §6.4.3, the drying times of experiment 7 are calculated. The maximum deviation between measured and calculated drying times appears to be 20% (see Appendix G-7).

The temperature dependence of drying curves, as stated by Schoeber
[23,24], can be expressed with an Arrhenius-type relation:

$$\left[\frac{dE}{dt}\right]_T = \left[\frac{dE}{dt}\right]_{T_1} \exp\left[-\frac{A_F}{R}\left(\frac{1}{T} - \frac{1}{T_1}\right)\right] \tag{6.22}$$

in which   R = 8.314 (J/mol ^{O}K);

T = absolute temperature (^{O}K);

A_F = activation energy of the flux (Joule/mol).

The activation energy A_F, which depends on the moisture concentration,
can be derived from at least two drying experiments with the same
initial concentration, but with different temperatures.
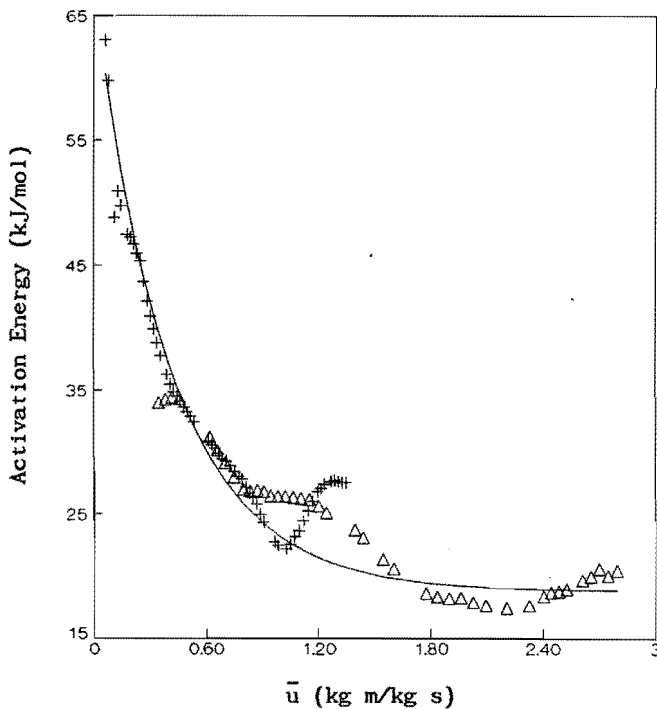
Figure 6.8

Activation energy of

drying flux.

+ from experiments 6 & 7

Δ from experiments 8 & 9

— equation 6.23

In Figure 6.8 the activation energies, derived from the Regular
Regimes of two different sets of drying experiments (6+7 and 8+9) are
represented. The concentration dependence of the activation energy A_F
can be described very well by the following correlation, as proposed
by Luyben [25]:

$$A_F = A \exp(-B\ u) + C \qquad\qquad (6.23)$$

in which for maltodextrin/water the following values of the fitting
parameters are found: $A = 48$ kJ/mol; $B = -2.40$ kg/kg, $C = 18.8$ kJ/mol.

Isothermal drying curves at *different temperatures* and *different
initial concentrations* can be predicted from experiment 9 as follows:
first, the Regular Regime of experiment 9 is translated to the desired
temperature by using equations 6.22 and 6.23.
second, the parameter a and D_0 at this temperature are obtained by
linear regression of $\ln(dE/dt)$ versus $\ln(1-E)$ in the concentration
range of interest. Because a is not known beforehand, some iterations
(mostly two) are required, to find the correct concentration range and
the corresponding values of a and D_0.
third, the drying curve at the desired temperature level and desired
initial concentration can be calculated similar to the method as
described in §6.4.3.

The above procedure has been applied to predict the drying curves of
experiments 5,6,(7) and 8 from the Regular Regime drying curve of
experiment 9; the agreement of predicted and measured drying times is
fairly good. Deviations between measured and calculated drying times
vary from a few percent to 30% (see Appendix G).

6.4.5 Prediction of Non-Isothermal Drying Curves.

At the desired initial moisture concentration, the Regular Regime curves are predicted at several temperature levels. Then by linear regression the best fitting a-value for *all* temperature levels is determined. Next the best fitting D_0 value at each temperature level is determined. The temperature dependence of D_0 is expressed with an Arrhenius type equation.

One single value of a is required to obtain temperature independent F versus E equations, so that the procedure analog to section 4.5 may be applied. The prediction of non-isothermal drying curves has not (yet) been verified experimentally in this study.

6.4.6 Deviations from Power Law Diffusion.

The exponent a can also be derived from drying experiments at different initial concentrations via:

- correlating values of D_0 with u_0 according to equation 6.19;
- evaluation of values of G_0D_0, found by linear regression of E^2 versus t with data from the Penetration Period (see Figure 6.7), by means of equations 6.17-19.

In both cases negative a-values are obtained (Table 6.2), which strongly deviate from the foregoing observed values. This inconsistency of results means, that the power law relation:

$$D\rho_s^2 = b(u-u_*)^a \qquad (6.24)$$

in fact does not apply to the whole concentration range of the system maltodextrin/water. At higher moisture concentrations the diffusion coefficient D is nearly independent of the concentration, whereas ρ_s^2 will increase and thus $D\rho_s^2$ *will increase* at a decreasing moisture concentration. At lower concentrations D will decrease more strongly

than the factor ρ_s^2 increases and thus $D\rho_s^2$ will *decrease*. Putting $D\rho_s^2$ versus ρ_m/ρ_s will show a <u>maximum</u>, and such a dependence can not be expressed by a power law relation.

One may wonder now why the description and prediction of drying curves, based on the power law concept, gives such satisfying results. The answer to this question might be, that drying behaviour is fully controlled by the lower concentrations at the interface, whereas the concentration dependence of the diffusion coefficient at the higher concentrations in the drying material is of minor importance then. In the range of rate controlling concentrations apparently a power law dependence of the diffusion coefficient may be assumed. Because power law diffusion evidently does not apply to the whole concentration range it has to be concluded that the parameters a and D_0 should be considered as fitting parameters, e.g. D_0 is a fictive value of the diffusion coefficient at the intial concentration.

Table 6.2 a-values calculated from drying experiments at different initial moisture concentrations.

exp	u_0 (kg/kg)	G_0D_0 from PP (m^2/s)	a	D_0 from RR (m^2/s)	a
7	2.40	$2.37 \cdot 10^{-10}$	-0.61	$5.03 \cdot 10^{-10}$	-0.71
9	4.85	$5.04 \cdot 10^{-10}$		$1.00 \cdot 10^{-9}$	

6.4.7 Conclusions.

Diffusion coefficients should be derived from the merging parts of several drying curves with different initial moisture concentrations. The whole drying history of a sample can be reconstructed from experimental data of the Regular Regime only.

Drying curves at lower initial moisture concentrations can be predicted from the Regular Regime data of drying curves at higher initial moisture concentrations.

Power law diffusion does not apply strictly to maltodextrin/water solutions. Though drying curves can be described and predicted fairly well by means of the equations of the short-cut method, the model parameters a and D_0 should be considered as fitting parameters with a limited physical meaning.

APPENDIX A

Transformation of Diffusion Equation.

The diffusion equation for moisture transfer in bodies of standard geometries reads (§3.2):

Partial differential equation:

$$\frac{\partial \rho_m}{\partial t} = -\frac{1}{r^v} \frac{\partial}{\partial r}(r^v n_m) \tag{A.1}$$

Initial condition:

$$t = 0 \qquad R_1 < r < R_2(0) \qquad \rho_m = \rho_{m0} \tag{A.2}$$

Boundary conditions:

$$t > 0 \qquad r = R_1 \qquad \frac{\partial(\rho_m/\rho_s)}{\partial r} = 0 \tag{A.3}$$

$$r = R_2(t) \qquad \rho_m = \rho_{mi}(t) \tag{A.4}$$

or

$$-D\rho_s \frac{\partial(\rho_m/\rho_s)}{\partial r} = j_{mi}^s(t) \tag{A.5}$$

By analogy with equation (A.1) the partial differential equation for mass transfer of the dissolved solids (s) is given by:

$$\frac{\partial \rho_s}{\partial t} = -\frac{1}{r^v} \frac{\partial}{\partial r}(r^v n_s) \tag{A.6}$$

Transforming the concentration.

For the transformation of the diffusion equation A.1, expressed in the volume based moisture concentration ρ_m (kg/m^3), into a form with the concentration u (kg m/kg s), the following two equations will be helpful:

$$\frac{\partial u}{\partial t} = \frac{\partial(\rho_m/\rho_s)}{\partial t} = \frac{1}{\rho_s}\frac{\partial\rho_m}{\partial t} - \frac{\rho_m}{\rho_s^2}\frac{\partial\rho_s}{\partial t} \tag{A.7}$$

and from equations 2.13, 2.25 and $u=\rho_m/\rho_s$:

$$n_m = \rho_m v_s + j_m^s = un_s - D\rho_s\frac{\partial u}{\partial r} \tag{A.8}$$

Dividing equation A.1 by ρ_s and multiplying equation A.6 by ρ_m/ρ_s^2 gives:

$$\frac{1}{\rho_s}\frac{\partial\rho_m}{\partial t} = -\frac{1}{\rho_s r^v}\frac{\partial}{\partial r}(r^v n_m) \tag{A.9}$$

$$\frac{\rho_m}{\rho_s^2}\frac{\partial\rho_s}{\partial t} = -\frac{1}{\rho_s r^v}\frac{\rho_m}{\rho_s}\frac{\partial}{\partial r}(r^v n_s) \tag{A.10}$$

Subtracting equations A.9 and A.10, making use of equation A.7 and eliminating n_m by means of equation A.8 results in:

$$\frac{\partial u}{\partial t} = \frac{1}{\rho_s r^v}\left[\frac{\partial}{\partial r}(\rho_s r^v D\frac{\partial u}{\partial r}) - r^v n_s\frac{\partial u}{\partial r}\right] \tag{A.11}$$

and with $n_s = \rho_s v_s$ equation A.11 becomes:

$$\left(\frac{\partial u}{\partial t}\right)_r + v_s\left(\frac{\partial u}{\partial r}\right)_t = \frac{1}{\rho_s r^v}\frac{\partial}{\partial r}(\rho_s r^v D\frac{\partial u}{\partial r})_t \tag{A.12}$$

Transforming the space coordinate.

The solids based space coordinate z is defined as:

$$dz = \rho_s r^v dr \tag{A.13}$$

or

$$z = \int_{R_1}^{r} \rho_s r^{\upsilon} dr \qquad (A.14)$$

and its maximum value:

$$z_{max} = \int_{R_1}^{R_2} \rho_s r^{\upsilon} dr \qquad (A.15)$$

Transforming the right hand side of equation A.12 into a form, using the solids based space coordinate z, is quite simple, but for the left hand side this transformation is somewhat more demanding. Consider $u = u(t,z)$, from which follows:

$$du = (\frac{\partial u}{\partial t})_z \, dt + (\frac{\partial u}{\partial z})_t \, dz \qquad (A.16)$$

and thus:

$$(\frac{\partial u}{\partial t})_r = (\frac{\partial u}{\partial t})_z + (\frac{\partial u}{\partial r} \frac{\partial r}{\partial z})_t \, (\frac{\partial z}{\partial t})_r \qquad (A.17)$$

From equation A.13:

$$(\frac{\partial r}{\partial z})_t = \frac{1}{\rho_s r^{\upsilon}} \qquad (A.18)$$

From equation A.14:

$$(\frac{\partial z}{\partial t})_r = \int_{R_1}^{r} (\frac{\partial \rho_s}{\partial t})_r \, r^{\upsilon} dr \qquad (A.19)$$

Substitution of equation A.6 in A.19 and assuming a non moving internal boundary, it follows:

124

$$\left(\frac{\partial z}{\partial t}\right)_r = -r^{\nu} n_s = -r^{\nu} \rho_s v_s \qquad (A.20)$$

Equations A.17, A.18 and A.20 now give:

$$\left(\frac{\partial u}{\partial t}\right)_r = \left(\frac{\partial u}{\partial t}\right)_z - v_s \left(\frac{\partial u}{\partial r}\right)_t \qquad (A.21)$$

and equation A.12 written in the solids based space coordinate z finally reads:

$$\left(\frac{\partial u}{\partial t}\right)_z = \frac{\partial}{\partial z}\left(D\rho_s^2 \ r^{2\nu} \ \frac{\partial u}{\partial z}\right)_t \qquad (A.22)$$

Making the partial differential equation dimensionless.

Introducing the dimensionless parameters m, D_r, τ and $\phi = z/z_{max}$ (see Chapter III) into the partial differential equation A.22 gives:

$$\boxed{\left(\frac{\partial m}{\partial \tau}\right)_\phi = \frac{\partial}{\partial \phi}\left(D_r X^2 \ \frac{\partial m}{\partial \phi}\right)_\tau \qquad (A.23)}$$

in which the dimensionless X-parameter is defined as:

$$X = \frac{r^{\nu} d_{s,ap} R_s}{z_{max}} \qquad (A.24)$$

Working out the X-parameter.

Separation of variables in equation A.13 gives:

$$r^{\nu} dr = \frac{dz}{\rho_s} \qquad (A.25)$$

Integration between the limits $r = R_1$ and $r = r$ and substituting $dz = z_{max} d\phi$ gives the following expression:

$$r^{v} = \left[R_1^{v+1} + (v+1)z_{max} \oint_0 \frac{d\Phi}{\rho_s} \right]^{\frac{v}{v+1}}$$

(A.26)

For z_{max} holds:

$$z_{max} = \int_{R_1}^{R_2(t)} \rho_s r^{v} dr = \int_{R_1}^{R_1+R_s} d_{s,ap} r^{v} dr$$

(A.27)

In fact equation A.27 is the mass balance of the solids; executing the integration of the most right member gives:

$$z_{max} = \frac{d_{s,ap}}{v+1} \left[(R_1+R_s)^{v+1} - R_1^{v+1} \right]$$

(A.28)

From equations A.24, A.26, A.28 and the hollowness factor λ (eqn. 3.18) the following expression for the X-parameter can be derived:

$$X = (v+1)\frac{1-\lambda}{1-\lambda^{v+1}} \left[\lambda^{v+1} + (1-\lambda^{v+1})d_{s,ap} \cdot \oint_0 \frac{d\Phi}{\rho_s} \right]^{\frac{v}{v+1}}$$

(A.29)

From the shrinkage model follows (eqn. 3.26):

$$\frac{d_{s,ap}}{\rho_s} = 1+\sigma v$$

(A.30)

and the expression for the X-parameter now becomes:

$$X = (v+1)\frac{1-\lambda}{1-\lambda^{v+1}} \left[\lambda^{v+1} + (1-\lambda^{v+1}) \oint_0 (1+\sigma v)d\Phi \right]^{\frac{v}{v+1}}$$

(A.31)

Transforming the initial and boundary conditions.

It will be clear that the initial condition reads:

$$\tau = 0 \qquad 0 \leq \phi \leq 1 \qquad m = 1 \qquad (A.32)$$

For the external boundary condition the flux equation

$$j^s_{mi} = -D\rho_s \frac{\partial u}{\partial r} \qquad (A.33)$$

can rather easily be transformed into a dimensionless form via the intermediate expression:

$$j^s_{mi} = -D\rho_s^2 \frac{r^\nu}{z_{max}} \frac{\partial u}{\partial \phi} \qquad (A.34)$$

and by next applying equation 3.14 for the flux-parameter and equation A.24 for the X-parameter, the dimensionless flux equation becomes:

$$F = -D_r X_i \frac{\partial m}{\partial \phi} \qquad (A.35)$$

where parameter X_i follows from equation A.31 by putting $\phi = 1$.

After transformation the external boundary condition for a known surface concentration reads:

$$\tau > 0 \qquad \phi = 1 \qquad m = m_i \qquad (A.36)$$

or for a known surface flux:

$$\tau > 0 \qquad \phi = 1 \qquad -D_r X_i \frac{\partial m}{\partial \phi} = F \qquad (A.37)$$

In a similar way the internal boundary condition reads:

$$\tau > 0 \qquad \phi = 0 \qquad X \frac{\partial m}{\partial \phi} = 0 \qquad (A.38)$$

APPENDIX B

Analytical Solutions of Diffusion Equation with Constant Boundary Flux ($D_r = 1$, $\sigma = 0$).

The diffusion equation is given by (see §4.1):

Partial differential equation:

$$\frac{\partial m}{\partial \tau} = \frac{1}{[\lambda + (1-\lambda)y]^\nu} \frac{\partial}{\partial y}([\lambda + (1-\lambda)y]^\nu \frac{\partial m}{\partial y}) \qquad (B.1)$$

Initial condition:

$$\tau = 0 \qquad 0 \leq y \leq 1 \qquad\qquad m = 1 \qquad\qquad (B.2)$$

Boundary conditions:

$$\tau > 0 \qquad\qquad y = 0 \qquad\qquad \frac{\partial m}{\partial y} = 0 \qquad\qquad (B.3)$$

$$\qquad\qquad y = 1 \qquad\qquad -\frac{\partial m}{\partial y} = F_{ca} = \text{constant} \qquad (B.4)$$

For all geometries the solutions can be described by:

$$\frac{E'}{F_{ca}} = X_{i,\sigma=0} \left[\tau + f + \sum_{k=1}^{\infty} C_k \frac{\exp(-\mu_k^2 \tau)}{\mu_k^2} \right] \qquad (B.5)$$

The functions f and C_k and the characteristic root equations are given in the following tables.

Table B.1 *Massive systems*

geometry	f	C_k	μ_k
slab	$\frac{1}{2}y^2 - \frac{1}{6}$	$\frac{2\cos(\mu_k y)}{-\cos(\mu_k)}$	$\tan(\mu_k) = 0$ $\mu_k = k\cdot\pi$ $-\cos(\mu_k)=(-1)^{k+1}$
cylinder	$\frac{1}{4}y^2 - \frac{1}{8}$	$\frac{J_0(\mu_k y)}{-J_0(\mu_k)}$	$J_1(\mu_k) = 0$
sphere	$\frac{1}{6}y^2 - \frac{1}{10}$	$\frac{2}{3y}\frac{\sin(\mu_k y)}{-\sin(\mu_k)}$	$\tan(\mu_k) = \mu_k$

Table B.2 *Hollow cylinder*

$$f = \frac{1}{8}\frac{(2x^2-3\lambda^2-1)(1-\lambda^2) - 4\lambda^2\{(1-\lambda^2)\ln(x) + \lambda^2\ln(\lambda)\}}{(1-\lambda)^3(1+\lambda)}$$

$$C_k = -(1-\lambda^2)\frac{Z_0(\alpha_k\lambda,\alpha_k)\cdot Z_0(\alpha_k\lambda,\alpha_k x)}{Z_0^2(\alpha_k\lambda,\alpha_k) - Z_0^2(\alpha_k,\alpha_k)}$$

with : $\alpha_k = \dfrac{\mu_k}{(1-\lambda)}$

$x = \lambda+(1-\lambda)y$

$Z_n(a,b) = Y_1(a)J_n(b) - J_1(a)Y_n(b)$

$Z_0(a,a) = \dfrac{-2}{\pi a}$

$\mu_k : Z_1(\dfrac{\lambda}{1-\lambda}\mu_k,\dfrac{1}{1-\lambda}\mu_k) = 0$

Table B.3 *Hollow sphere*

$$f = \frac{\lambda^3(-5y^3+15y^2+3y-3)+\lambda^2(15y^2+6y-9)+\lambda(15y^2-6y-3)+5y^3-3y}{30(1+\lambda+\lambda^2)(\lambda+(1-\lambda)y)}$$

$$C_k = \frac{2\mu_k^2}{3} \frac{g_k\cos(\mu_k)}{h_k\sin(\mu_k)\cos(\mu_k)+i_k} \frac{(1-\lambda)\sin(\mu_k y) + \mu_k\lambda\cos(\mu_k y)}{(\lambda + (1-\lambda)y)}$$

$$g_k = -(\lambda^2+\lambda+1)\cdot[(1-\lambda)^2 + \mu_k^2\lambda^2]$$

$$h_k = \lambda^3\mu_k^4 + \lambda(1-\lambda)^3\mu_k^2 - (1-\lambda)^4$$

$$i_k = \mu_k\left[\lambda^3\mu_k^4 + \lambda(1-\lambda)^2(1+\lambda)\mu_k^2 + (1-\lambda)^4\right]$$

$$\mu_k : [(1-\lambda)^2 + \lambda\mu_k^2]\,\tan(\mu_k) - (1-\lambda)^2\mu_k = 0$$

APPENDIX C

Analytical Solutions of Diffusion Equation with Constant Boundary Concentration ($D_r=1$, $\sigma=0$).

The diffusion equation is given by (see §4.1):

Partial differential equation:

$$\frac{\partial m}{\partial \tau} = \frac{1}{[\lambda+(1-\lambda)y]^{\upsilon}} \frac{\partial}{\partial y} \left([\lambda+(1-\lambda)y]^{\upsilon} \frac{\partial m}{\partial y}\right) \qquad (C.1)$$

Initial condition:

$$\tau = 0 \qquad 0 \leq y \leq 1 \qquad m = 1 \qquad (C.2)$$

Boundary conditions:

$$\tau > 0 \qquad y = 0 \qquad \frac{\partial m}{\partial y} = 0 \qquad (C.3)$$

$$y = 1 \qquad m = m_i = 0 \qquad (C.4)$$

For all massive and hollow geometries the solutions can be described by the following relations:

$$m = \sum_{k=1}^{\infty} A_k \exp(-\mu_k^2 \tau) \qquad (C.5)$$

$$F = \sum_{k=1}^{\infty} B_k \exp(-\mu_k^2 \tau) \qquad \text{with } B_k = -\left[\frac{\partial A_k}{\partial y}\right]_{y=1} \qquad (C.6)$$

$$1-E = X_{i,\sigma=0} \sum_{k=1}^{\infty} B_k \frac{\exp(-\mu_k^2 \tau)}{\mu_k^2} \qquad (C.7)$$

The functions A_k, B_k and the characteristic root equations are given in the tables below.

Table C.1 *Massive geometries*

geometry	A_k	B_k	μ_k
slab	$\dfrac{2}{\mu_k}\dfrac{\cos(\mu_k y)}{\sin(\mu_k)}$	2	$\cos(\mu_k) = 0$ $\mu_k = (2k-1)\dfrac{\pi}{2}$ $\sin(\mu_k) = (-1)^{k+1}$
cylinder	$\dfrac{2}{\mu_k}\dfrac{J_0(\mu_k y)}{J_1(\mu_k)}$	2	$J_0(\mu_k) = 0$
sphere	$\dfrac{2}{\mu_k y}\dfrac{\sin(\mu_k y)}{-\cos(\mu_k)}$	2	$\sin(\mu_k) = 0$ $\mu_k = k\pi$ $-\cos(\mu_k) = (-1)^{k+1}$

Table C.2 *Hollow cylinder*

$$A_k = \pi\,\frac{J_1(\alpha_k\lambda)\cdot J_0(\alpha_k)}{J_1^{\,2}(\alpha_k\lambda) - J_0^{\,2}(\alpha_k)}\cdot Z_0(\alpha_k\lambda,\alpha_k x)$$

$$\text{with } \alpha_k = \frac{\mu_k}{1-\lambda}$$

$$x = \lambda + (1-\lambda)y$$

$$Z_n(a,b) = Y_1(a)J_n(b) - J_1(a)Y_n(b)$$

$$B_k = 2(1-\lambda)\,\frac{J_1^{\,2}(\alpha_k\lambda)}{J_1^{\,2}(\alpha_k\lambda) - J_0^{\,2}(\alpha_k)}$$

$$\mu_k : Z_0\!\left(\frac{\lambda}{1-\lambda}\mu_k,\frac{1}{1-\lambda}\mu_k\right) = 0$$

Table C.3 *Hollow sphere*

$$A_k = \frac{2}{\mu_k - \sin(\mu_k)\cos(\mu_k)} \frac{\sin[\mu_k(1-y)]}{\lambda + (1-\lambda)y}$$

$$B_k = \frac{2\mu_k}{\mu_k - \sin(\mu_k)\cos(\mu_k)}$$

$$\mu_k : (1-\lambda)\tan(\mu_k) = -\lambda\mu_k$$

APPENDIX D

Some Aspects of the Numerical Solution of the Diffusion Equation.

In general, the diffusion equation with $D_r = m^a$ has to be solved by
numerical methods. Only some important aspects of the numerical
approach, which may cause serious problems, will be highlighted here.
It appears that some of these problems can be dealt with by appropiate
transformations of the diffusion equation; this will be illustrated
with the generalized diffusion equation in ϕ-coordinates.

Moving external boundary

The numerical calculation of partial differential equations requires a
rectangular discretisation grid, in other words equidistant steps in
time and space should be used. However, in discretisizing the linear
r-coordinate of a shrinking system the external boundary will move
through the grid. This problem can be solved by transforming the
partial differential equation (eqn. 4.1) with a normalized linear
space coordinate:

$$y(t) = \frac{r-R_1}{R_{2,t}-R_1} \tag{D.1}$$

During every time step $R_{2,t}$ has to be calculated; this requires the
integration of the moisture flux with time or the integration of the
moisture concentration with space.

Transformation of the diffusion equation in ϕ-coordinates seems to be
a good alternative, because now a fixed external boundary is obtained.
However, the integration now emerges in the X-parameter and the
internal boundary condition for massive cylinders and spheres becomes

undetermined ($\phi=0$ and $\lambda=0 \rightarrow X=0 \rightarrow \partial m/\partial\phi=??$). This internal boundary

problem also exists for non-shrinking systems. For cylinders and

spheres with an infinite small value of λ the slope $\partial m/\partial\phi$ is clearly

zero. Therefore, it may be expected that replacing the internal boun-

dary condition of massive systems with $\partial m/\partial\phi=0$ will cause minor

errors. Indeed, by comparing the numerical solutions calculated in

ϕ-coordinates with solutions calculated in y-coordinates no detectable

errors could be traced.

Singularity of the boundary flux

If the boundary concentration m_i takes on a zero value, the diffusion

coefficient will also be zero. Because of a finite boundary flux, the

concentration gradient at the external boundary will become infinite.

This singularity causes loss of convergence and must be avoided. Also

for high values of the exponent a and low values of m_i steep

concentration gradients at the external boundary will result. Even

this non-singular situation may lead to a non-acceptable loss of

convergence. This problem can be eliminated by the following simple

transformation of the concentration: $\tilde{m} = m^{a+1}$. The generalized

diffusion equation then becomes:

Generalized partial differential equation:

$$\frac{\partial \tilde{m}}{\partial \tau} = (\tilde{m})^{\frac{a}{a+1}} \frac{\partial}{\partial \phi}(X^2 \frac{\partial \tilde{m}}{\partial \phi}) \qquad (D.2)$$

Initial condition:

$$\tau = 0 \qquad 0 \leq \phi < 1 \qquad \tilde{m} = 1 \qquad (D.3)$$

Boundary conditions:

$$\tau > 0 \qquad \phi = 0 \qquad X \frac{\partial \tilde{m}}{\partial \phi} = 0 \qquad (D.4)$$

$$\phi = 1 \qquad \tilde{m} = \tilde{m}_i \qquad (D.5)$$

$$\text{or} \qquad -X_i \frac{\partial \tilde{m}}{\partial \phi} = F(a+1) \qquad (D.6)$$

From the boundary condition at $\phi=1$ it can easily be seen that for finite values of $F(a+1)$ the gradient of the transformed concentration $\partial w / \partial \phi$ will remain finite for any value of the boundary concentration. (The same holds for $\partial w / \partial y$ and $\partial w / \partial r$).

Inconsistency of initial and boundary condition

In modelling a real drying process it may happen that the idealized boundary condition is inconsistent with the idealized initial condition; e.g. a uniform initial concentration implies a _zero_ boundary flux at t=0, whereas at t↓0 the boundary condition may impose a _non-zero_ flux. In these cases a discontinuity exists, where the external boundary condition and the initial condition should link up. This singularity tends to cause serious oscillations in the solutions and has to be dealt with.

Initially there is a drying period during which the concentration profiles are penetrating into the centre of the body. For this penetration period $(0 \leq \tau \leq \tau_{pp})$, where the drying body behaves like an infite thick body, the so-called Boltzmann transformation is most suitable to avoid this kind of singularity problems:

$$z = \sqrt{\tau}_{pp} \frac{1-\phi}{\sqrt{\tau}} \qquad (D.7)$$

Now the boundary $\phi=1$ is transformed to the origin z=0, whereas the initial condition $(\tau=0)$ is transformed to z→∞. Thus, inconsistency of conditions no longer exists. At $\tau=\tau_{pp}$ a switch back from z-coordinates to ϕ-coordinates is necessary.

136

Discretisation

At increasing values of τ the concentration profiles change more
slowly. To speed up the numerical calculations a gradually increasing
time step is required. However, to determine the convergence of the
numerical solutions, equidistant steps in space and time are required.
This problem can be solved by transforming the time variable according
to: $\tau'=\sqrt{\tau}$; equidistant steps in τ' yield growing steps in τ, because
$\Delta\tau=2\tau'\Delta\tau'$.

The transformed diffusion equation is discretisized by means of the
Crank-Nicolson scheme. Discretisation yields a set of equations which
is solved by using the Thomas-algorithm. The order of the
discretisation errors appears to be:

$(\Delta z)^2$ and $(\Delta\tau')^2$ for $0\leq\tau\leq\tau_{pp}$; $(\Delta\phi)^2$ and $(\Delta\tau')^2$ for $\tau\geq\tau_{pp}$

For non-shrinking systems with constant diffusion coefficient the
numerical calculations show excellent agreement (deviations less than
0.1%) with the analytical solutions (Chapter IV). For power law
diffusion excellent agreement exists (deviations less than 0.5%) with
the calculations of Schoeber [23] and Liou [28] and with the
calculations of regular regimes based on geometrically similar
concentration profiles [23,44].

APPENDIX E

The Initial Value $\widetilde{G}_0$ for Power Law Diffusion with Constant Boundary Flux.

In case of a power law dependence of the diffusion coefficient with concentration, the $\widetilde{G}$-parameter (see Table 5.1) is defined as:

$$\widetilde{G} = \frac{\dfrac{\widetilde{F}}{\widetilde{E}_i'} \dfrac{\widetilde{E}}{\widetilde{E}_i'}}{X_i} = \frac{F(a+1)}{X_i} \frac{1-(1-E)^{a+1}}{[1-(1-E_i')^{a+1}]^2} \qquad (E.1)$$

and the initial value:

$$\widetilde{G}_0 = \lim_{\tau \to 0} \widetilde{G} = \frac{F(a+1)}{X_i} \lim_{\tau \to 0} \left[\frac{1-(1-E)^{a+1}}{[1-(1-E_i')^{a+1}]^2} \right] \qquad (E.2)$$

If $\tau \to 0$ then also $E \to 0$ and $E_i' \to 0$ and thus:

$$\lim_{\tau \to 0} \left[\frac{1-(1-E)^{a+1}}{\{1-(1-E_i')^{a+1}\}^2} \right] = \lim_{\tau \to 0} \left[\frac{(a+1)E + \text{higher E-terms}}{[(a+1)E_i' + \text{higher } E_i'\text{-terms}]^2} \right]$$

$$= \lim_{\tau \to 0} \left[\frac{(a+1)E \cdot [1 + \text{higher E-terms}]}{(a+1)^2 E_i'^2 \cdot [1 + \text{higher } E_i'\text{-terms}]} \right]$$

$$= \lim_{\tau \to 0} \left[\frac{E}{(a+1)E_i'^2} \right] \qquad (E.3)$$

From equations E.1, E.3, and 4.35:

$$\widetilde{G}_0 = \lim_{\tau \to 0} \left[\frac{F \cdot E}{X_i E_i'^2} \right] = \lim_{\tau \to 0} G = G_0 \qquad (E.4)$$

It is assumed that the drying process with a constant boundary flux
starts with a homogeneous concentration profile. At extremely small
drying times $(\tau \to 0)$, the moisture concentration at any place in the
material, including the interface, has hardly changed from its initial
value. So, the concentration dependence of the diffusion coefficient
does not come to expression yet. Also the influence of shrinking, if
present, will be negligible at this very first drying stage. For these
reasons it can be concluded that, *irrespective of the concentration*
dependence of the diffusion coefficient and the shrinkage behaviour,
in all cases the G_0*-parameter takes on the same value*. So, the value
obtained for non-shrinking systems with constant diffusivity (eqn.
4.36) also holds in general:

$$\widetilde{G}_0 = G_0 = \frac{\pi}{4} \qquad\qquad (E.5)$$

APPENDIX F

Some Properties of Maltodextrin.

The maltodextrin (trade name: Paselli MD20) used in this study is the same as used by Kerkhof [36] and Rulkens [35].

The composition as specified by the supplier (AvéBé, Veendam, the Netherlands), is:

    1.5 wt% glucose

    4.5 wt% maltose

    9.3 wt% tri-saccharides

    6.0 wt% tetra-saccharides

    4.5 wt% penta-saccharides

    74.2 wt% poly-saccharides

The partial density of maltodextrin in aqueous solutions may be considered to be constant [36] and is 1610 kg/m^3.

The sorption-isotherm in the range $a_w \leq 0.9$ can be described very well with the G.A.B-equation [43]:

$$\frac{u}{u_1} = \frac{C_g ka_w}{(1-ka_w)\cdot(1-ka_w+C_g ka_w)}$$
(F.1)

in which,

$u_1 = 0.06343 - 8.586\cdot10^{-4}\cdot(\theta-20)$ (kg m/kg s) (F.2)

$k = 0.9132 + 3.839\cdot10^{-3}\cdot(\theta-20)$ (F.3)

$C_g = 6.394 + 2.558\cdot(\theta-20)$ (F.4)

with $15^{\circ}C \leq \theta \leq 50^{\circ}C$

The maltodextrin, used by Furuta et.al. [22], is of a different origin and has a different composition. In their paper they present the following correlation for the diffusion coefficient of water in maltodextrin solutions at $35^{\circ}C$:

$$^{10}\log(D_w^{35}) = \sum_{i=0}^{8} \frac{d_i}{(1+u)^i} \tag{F.5}$$

with $d_0 = -9.62029$, $d_1 = 3.75424$, $d_2 = -86.5335$,

$\qquad d_3 = 704.872$, $\quad d_4 = -2853.10$, $d_5 = 6354.49$,

$\qquad d_6 = -7952.04$, $\quad d_7 = 5245.81$, $\quad d_8 = -1424.05$

For the activation energy of the diffusion coefficient is given:

$$E_D = \sum_{i=0}^{5} \frac{e_i \cdot 10^4}{(1+u)^i} \tag{F.6}$$

with $e_0 = 3.32582$, $e_1 = -15.8667$, $e_2 = 151.217$,

$\qquad e_3 = -443.608$, $e_4 = 481.664$, $\quad e_5 = -146.387$

APPENDIX G-5

Experiment 5: measured and calculated drying curves of
gelled layer of maltodextrin/water.

Conditions: u_0 = 2.40 kg m/kg s $\quad\theta$ = 41.4°C

$\quad$ P = 12500 N/m2 $\qquad R_0$ = 2.50 mm

Fitting parameters: a = -0.092 $\quad D_0$ = 3.88E-10 m2/s

constant flux	penetration period	regular regime
F_{ca} = 21.563	G_0 = 0.727	Sh_d = 4.816
G_0 = 0.889	E_T = 0.524	
u_{cr} = 0.398 kg/kg	t_T = 3058 sec.	
$E'_{i,cr}$ = 0.834		
E_{ca} = 0.029	(about 70% of all data points, used in	
t_{ca} = 22 sec.	the evaluation, are represented below)	

E	time (s) meas.	time (s) calc.	% rel. error	E	time (s) meas.	time (s) calc.	% rel. error
0.020	20	15	-23.9	0.562	2888	3527	22.1
0.028	26	21	-18.6	0.570	2968	3630	22.3
0.045	38	35	-9.1	0.585	3128	3836	22.6
0.077	78	78	-0.6	0.594	3216	3952	22.9
0.098	118	120	1.4	0.605	3344	4109	22.9
0.132	198	205	3.5	0.623	3542	4365	23.2
0.146	238	247	3.9	0.633	3662	4518	23.4
0.171	318	335	5.5	0.653	3904	4821	23.5
0.182	358	381	6.4	0.662	4024	4973	23.6
0.193	398	427	7.2	0.671	4136	5114	23.6
0.215	478	523	9.5	0.689	4386	5422	23.6
0.225	518	572	10.4	0.697	4506	5560	23.4
0.243	598	669	11.9	0.713	4746	5853	23.3
0.252	638	716	12.2	0.720	4866	6002	23.3
0.261	678	765	12.8	0.728	4986	6150	23.3
0.277	758	863	13.9	0.742	5226	6443	23.3
0.285	798	912	14.3	0.752	5396	6649	23.2
0.300	878	1010	15.0	0.769	5716	7023	22.9
0.307	918	1059	15.4	0.777	5876	7210	22.7
0.314	958	1108	15.7	0.785	6036	7396	22.5
0.342	1118	1306	16.8	0.801	6396	7802	22.0
0.354	1198	1405	17.3	0.809	6596	8016	21.5
0.379	1358	1603	18.0	0.824	6996	8443	20.7
0.391	1438	1704	18.5	0.832	7236	8695	20.2
0.403	1520	1809	19.0	0.839	7476	8925	19.4
0.421	1652	1975	19.5	0.855	7998	9429	17.9
0.435	1758	2109	19.9	0.862	8318	9706	16.7
0.455	1918	2309	20.4	0.877	8996	10276	14.2
0.465	1996	2406	20.5	0.884	9394	10586	12.7
0.474	2078	2506	20.6	0.892	9846	10923	10.9
0.493	2236	2708	21.1	0.907	10924	11643	6.6
0.502	2316	2806	21.2	0.914	11604	12032	3.7
0.520	2476	3005	21.4	0.928	13476	12913	-4.2
0.529	2568	3120	21.5	0.935	14768	13402	-9.2
0.538	2648	3221	21.7	0.942	16436	13944	-15.2

APPENDIX G-6

Experiment 6: measured and calculated drying curves of
gelled layer of maltodextrin/water.

| Conditions: | u_0 = 2.40 kg m/kg s | θ = 32.8 ^{o}C |
| | P = 12450 N/m2 | R_0 = 2.50 mm |

Fitting parameters: a = 0.076 D_0 = 3.99E-10 m2/s

constant flux	penetration period	regular regime
F_{ca} = 5.951	G_0 = 0.574	Sh_d = 5.025
G_0 = 0.713	E_T = 0.482	
u_{cr} = 0.376 kg/kg	t_T = 3291 sec.	
$E'_{i,cr}$ = 0.8431		
E_{ca} = 0.0823	(about 65% of all data points, used in	
t_{ca} = 217 sec.	the evaluation, are represented below)	

E	time (s) meas.	calc.	% rel. error	E	time (s) meas.	calc.	% rel. error
0.055	160	145	-9.5	0.597	4032	5083	26.1
0.074	192	196	2.0	0.606	4144	5242	26.5
0.092	240	241	0.4	0.614	4272	5397	26.3
0.124	320	334	4.2	0.629	4496	5686	26.5
0.148	400	423	5.7	0.645	4736	5999	26.7
0.160	432	475	9.9	0.652	4848	6149	26.8
0.181	512	572	11.7	0.669	5136	6519	26.9
0.192	560	626	11.7	0.676	5248	6679	27.3
0.210	640	725	13.3	0.695	5568	7109	27.7
0.232	736	857	16.4	0.712	5888	7546	28.2
0.239	768	906	17.9	0.721	6048	7764	28.4
0.255	848	1011	19.2	0.737	6368	8198	28.7
0.269	928	1116	20.2	0.752	6688	8636	29.1
0.277	976	1171	20.0	0.759	6848	8855	29.3
0.304	1136	1383	21.7	0.776	7248	9405	29.8
0.316	1216	1486	22.2	0.784	7456	9677	29.8
0.339	1376	1694	23.1	0.799	7856	10224	30.1
0.361	1536	1902	23.8	0.814	8304	10828	30.4
0.371	1616	2008	24.3	0.822	8544	11154	30.5
0.391	1776	2214	24.7	0.837	9056	11842	30.8
0.410	1936	2418	24.9	0.851	9584	12543	30.9
0.419	2016	2523	25.1	0.859	9904	12966	30.9
0.437	2176	2727	25.3	0.873	10560	13802	30.7
0.445	2256	2830	25.5	0.881	10928	14271	30.6
0.462	2416	3036	25.6	0.896	11776	15319	30.1
0.478	2576	3240	25.8	0.910	12768	16523	29.4
0.485	2656	3343	25.8	0.917	13376	17212	28.7
0.500	2816	3549	26.0	0.932	14784	18774	27.0
0.522	3056	3859	26.3	0.946	16736	20766	24.1
0.532	3168	4013	26.7	0.953	18016	21946	21.8
0.552	3424	4323	26.2	0.975	23344	27305	17.0
0.561	3536	4473	26.5	0.982	26032	30337	16.5
0.571	3664	4635	26.5	0.989	30688	35028	14.1

APPENDIX G-7

Eperiment 7: measured and calculated drying curves of
gelled layer of maltodextrin/water.

Conditions: u_0 = 2.40 kg m/kg s θ = 26.4 °C

P = 12400 N/m2 R_0 = 2.50 mm

Fitting parameters: a = 0.292 D_0 = 5.03E-10 m2/s

constant flux		penetration period	regular regime
F_{ca} = 3.888		G_0 = 0.440	Sh_d = 5.248
G_0 = 0.555		E_T = 0.436	
u_{cr} = 0.362 kg/kg		t_T = 2854 sec.	
$E'_{i,cr}$ = 0.849			
E_{ca} = 0.082		(about 60% of all data points, used in	
t_{ca} = 262 sec.		the evaluation, are represented below)	

E	time (s) meas.	calc.	% rel. error	E	time (s) meas.	calc.	% rel. error
0.021	80	66	-18.1	0.566	4496	4823	7.3
0.047	160	150	-6.4	0.581	4736	5098	7.6
0.060	192	192	-0.1	0.589	4864	5236	7.6
0.085	272	268	-1.3	0.605	5136	5562	8.3
0.109	352	336	-4.6	0.620	5392	5863	8.7
0.121	400	373	-6.8	0.628	5552	6053	9.0
0.141	480	448	-6.6	0.645	5872	6435	9.6
0.151	512	487	-4.8	0.653	6032	6627	9.9
0.169	592	570	-3.6	0.669	6352	7014	10.4
0.186	672	655	-2.6	0.684	6688	7418	10.9
0.194	720	697	-3.1	0.692	6848	7618	11.2
0.209	800	786	-1.8	0.709	7248	8119	12.0
0.224	880	874	-0.7	0.725	7648	8624	12.8
0.237	960	963	0.3	0.733	7840	8878	13.2
0.262	1120	1138	1.6	0.748	8240	9392	14.0
0.274	1184	1225	3.4	0.755	8448	9653	14.3
0.296	1360	1403	3.1	0.771	8960	10311	15.1
0.316	1520	1574	3.5	0.786	9440	10936	15.8
0.325	1584	1662	4.9	0.794	9712	11305	16.4
0.345	1760	1847	4.9	0.809	10272	12042	17.2
0.362	1920	2018	5.1	0.824	10880	12851	18.1
0.370	2000	2104	5.2	0.832	11232	13318	18.6
0.386	2160	2273	5.2	0.846	11952	14274	19.4
0.394	2240	2359	5.3	0.854	12352	14797	19.8
0.409	2400	2529	5.4	0.868	13216	15928	20.5
0.427	2608	2738	5.0	0.882	14240	17215	20.9
0.437	2720	2863	5.3	0.890	14832	17963	21.1
0.454	2928	3088	5.5	0.904	16192	19625	21.2
0.473	3168	3349	5.7	0.918	17888	21622	20.9
0.483	3296	3488	5.8	0.926	18928	22793	20.4
0.501	3536	3750	6.0	0.949	23616	27915	18.2
0.510	3664	3882	5.9	0.956	25712	30140	17.2
0.527	3904	4149	6.3	0.971	31728	36692	15.6
0.543	4144	4415	6.5	0.985	41616	49962	20.1
0.551	4256	4548	6.9	0.992	54224	65396	20.6

APPENDIX G-8

Experiment 8: measured and calculated drying curves of
gelled layer of maltodextrin/water.

Conditions: u_0 = 4.85 kg·m/kg s $\quad\theta$ = 35.8 ^{o}C

$\qquad\qquad\qquad$ P = 12400 N/m2 $\qquad\qquad$ R_0 = 2.50 mm

Fitting parameters: a = -0.087 $\quad$ D_0 = 9.27E-10 m2/s

constant flux	penetration period	regular regime
F_{ca} = 4.254	G_0 = 0.721	Sh_d = 4.824
G_0 = 0.882	E_T = 0.523	
u_{cr} = 0.383 kg/kg	t_T = 1411 sec.	
$E'_{i,cr}$ = 0.921		
E_{ca} = 0.175	(about 80% of all data points, used in	
t_{ca} = 277 sec.	the evaluation, are represented below)	

E	time (s) meas.	calc.	% rel. error	E	time (s) meas.	calc.	% rel. error
0.021	38	33	-14.5	0.620	1988	1951	-1.9
0.049	78	78	0.1	0.632	2068	2030	-1.8
0.077	118	122	3.1	0.644	2148	2108	-1.9
0.101	156	161	3.0	0.656	2228	2188	-1.8
0.156	246	248	0.7	0.679	2388	2349	-1.6
0.178	286	283	-1.0	0.691	2468	2431	-1.5
0.199	326	319	-2.0	0.702	2548	2514	-1.3
0.218	366	356	-2.7	0.711	2616	2584	-1.2
0.254	446	436	-2.2	0.732	2786	2762	-0.9
0.267	478	468	-2.0	0.742	2866	2848	-0.6
0.287	530	519	-2.0	0.751	2940	2926	-0.5
0.302	570	560	-1.7	0.761	3030	3022	-0.3
0.329	650	641	-1.4	0.779	3190	3196	0.2
0.342	690	682	-1.1	0.788	3270	3285	0.5
0.355	730	724	-0.8	0.796	3350	3374	0.7
0.367	770	764	-0.7	0.804	3430	3465	1.0
0.390	850	845	-0.6	0.819	3586	3637	1.4
0.401	890	885	-0.6	0.827	3678	3739	1.6
0.411	930	925	-0.6	0.834	3758	3831	1.9
0.421	970	964	-0.6	0.844	3878	3968	2.3
0.441	1050	1043	-0.7	0.863	4122	4247	3.0
0.450	1090	1082	-0.8	0.872	4242	4384	3.3
0.459	1130	1120	-0.9	0.880	4362	4523	3.7
0.468	1170	1159	-0.9	0.887	4482	4656	3.9
0.486	1250	1237	-1.1	0.904	4802	5008	4.3
0.494	1290	1276	-1.1	0.913	5002	5215	4.3
0.502	1330	1313	-1.3	0.921	5182	5392	4.1
0.510	1370	1351	-1.4	0.928	5380	5592	3.9
0.528	1460	1439	-1.4	0.943	5908	6066	2.7
0.536	1500	1478	-1.5	0.951	6268	6358	1.4
0.543	1540	1517	-1.5	0.958	6694	6662	-0.5
0.550	1580	1555	-1.6	0.965	7272	7019	-3.5
0.573	1708	1679	-1.7	0.979	9794	8000	-18.3
0.580	1748	1719	-1.7	0.986	13260	8751	-34.0

APPENDIX G-9

Experiment 9: measured and calculated drying curves of
gelled layer of maltodextrin/water.

Conditions: u_0 = 4.85 kg m/kg s θ = 26.7 ^{o}C

P = 12200 N/m2 R_0 = 2.50 mm

Fitting parameters: a = 0.075 D_0 = 1.00E-09 m2/s

constant flux	penetration period	regular regime
F_{ca} = 2.187	G_0 = 0.575	Sh_d = 5.024
G_0 = 0.714	E_T = 0.482	
u_{cr} = 0.362 kg/kg	t_T = 1634 sec.	
$E'_{i,cr}$ = 0.925		
E_{ca} = 0.273	(about 70% of all data points, used in	
t_{ca} = 779 sec.	the evaluation, are represented below)	

E	time (s) meas.	time (s) calc.	% rel. error	E	time (s) meas.	time (s) calc.	% rel. error
0.032	80	92	15.1	0.589	2486	2292	-7.8
0.044	122	126	3.7	0.601	2566	2373	-7.5
0.070	202	200	-0.7	0.621	2726	2522	-7.5
0.099	276	281	1.8	0.631	2806	2596	-7.5
0.126	356	360	1.2	0.649	2966	2746	-7.4
0.140	396	400	1.0	0.660	3046	2836	-6.9
0.154	436	440	0.9	0.669	3126	2912	-6.8
0.182	516	518	0.3	0.687	3292	3071	-6.7
0.195	556	557	0.2	0.695	3372	3146	-6.7
0.222	636	633	-0.5	0.711	3532	3306	-6.4
0.235	676	671	-0.8	0.718	3612	3384	-6.3
0.260	756	741	-2.0	0.734	3772	3547	-6.0
0.272	796	776	-2.5	0.742	3864	3638	-5.8
0.284	836	810	-3.1	0.750	3956	3733	-5.6
0.305	916	880	-3.9	0.770	4196	3985	-5.0
0.316	956	917	-4.1	0.779	4316	4103	-4.9
0.336	1036	987	-4.8	0.797	4556	4352	-4.5
0.345	1076	1021	-5.1	0.805	4676	4478	-4.2
0.363	1156	1091	-5.6	0.820	4876	4719	-3.2
0.371	1192	1120	-6.0	0.827	4996	4849	-2.9
0.381	1236	1162	-6.0	0.835	5116	4980	-2.7
0.400	1326	1241	-6.4	0.853	5434	5337	-1.8
0.408	1366	1276	-6.6	0.861	5594	5523	-1.3
0.423	1446	1345	-7.0	0.876	5914	5878	-0.6
0.432	1486	1385	-6.8	0.884	6114	6090	-0.4
0.446	1566	1454	-7.1	0.899	6514	6518	0.1
0.453	1606	1488	-7.3	0.906	6714	6747	0.5
0.460	1646	1524	-7.4	0.914	6994	7034	0.6
0.487	1806	1665	-7.8	0.929	7606	7644	0.5
0.500	1886	1737	-7.9	0.936	7966	7988	0.3
0.520	2006	1852	-7.7	0.951	8950	8880	-0.8
0.532	2086	1923	-7.8	0.958	9550	9415	-1.4
0.556	2246	2071	-7.8	0.973	11276	10919	-3.2
0.567	2326	2144	-7.8	0.980	13642	11999	-12.0

LIST OF SYMBOLS

a	exponent in power relation	
a	thermodynamic activity	
a	heat diffusivity	m^2/s
a	component in binary mixture	
A	mass exchanging area	m^2
A	activation energy	$J/mol\ ^oK$
A	fitting parameter in eqn. 6.23	J/mol
b	factor in power relation	kg^2/m^4s
b	component in binary mixture	
B	fitting parameter in eqn. 6.23	kg s/ kg m
Bi	Biot number	
c	constant value	
c	molar concentration	mol/m^3
c_p	specific heat at constant pressure	$J/kg\ ^oC$
C	fitting parameter in eqn. 6.23	J/mol
d	(partial) density	kg/m^3
D	diffusion coefficient	m^2/s
D_r	reduced diffusion coefficient	
E	efficiency	
$\tilde{E}$	(see Table 5.1)	
F	dimensionless flux-parameter	
$\tilde{F}$	(see Table5.1)	
G	help function for penetration processes	
$\tilde{G}$	(see Table 5.1)	
H	shrinkage factor	
j	diffusive mass flux	kg/m^2s
J	Bessel functions	
k	mass transfer coefficient	m/s
k"	modified mass transfer coefficient	$kg\ m^2/s$
l	characteristic dimension	m
L	latent heat of evaporation	J/kg
m	exponent in Sherwood correlation (gas phase)	
m	dimensionless mass concentration	
m	moisture	
$\tilde{m}$	(see Table 5.1)	
n	mass flux in stationary coordinate system	kg/m^2s

n	exponent in Sherwood correlations (gasphase)	
N	molar flux	mol/m^2s
Nu	Nusselt number	
P	pressure	N/m^2
Pr	Prandtl number	
q	heat flux	J/m^2s
q	parameter to account for influence of dynamic radius on mass transfer coefficient k'	
r	space coordinate	m
R	radius of cylinder and sphere or thickness of one-sided drying slab	m
Re	Reynolds number	
s	solid(s)	
s	modified shrinkage coefficient	
Sc	Schmidt number	
Sh	Sherwood number	
t	time	s
T	absolute temperature	^{o}K
u	solids based mass concentration	kg m/kg s
v	ratio of volume fractions of moisture and solids	
v	velocity	m/s
V	volume	m^3
x	molar fraction on total basis	mol/mol
X	dimensionless parameter	
y	dimensionless linear space coordinate	
z	solids based space coordinate	$kg\ s/m^{2-v}$

GREEK SYMBOLS

α	heat transfer coefficient	$J/m^2s\ ^{o}C$
α	correlation parameter in eqns. 4.37 and 5.60	
$\tilde{\alpha}$	correlation parameter in eqn. 5.52	
β	correlation parameter in eqns. 4.65 and 5.7	
γ	slope of linearized sorption-isotherm	
$\tilde{\gamma}$	correlation parameter in eqn. 5.52	
δ	thickness film layer in gas phase	m
ϵ	porosity	
ϵ	(see Table 5.1)	
ϕ	generalized space coordinate	
λ	hollowness factor	
λ	heat conductivity	$J/ms\ ^{o}C$

μ_k roots of characteristic equations

υ geometry parameter

υ kinematic viscosity m^2/s

ω mass fraction on total basis kg/kg

θ temperature $^o C$

ρ mass concentration kg/m^3

σ shrinkage coefficient

τ dimensionless time

SUBSCRIPTS

a   air
ap   apparent
ca   constant activity
cr   critical
d   dispersed phase
D   diffusion
e   value at zero critical surface concentration
eff   effective
f   film
F   flux
H   heat
i   interface
i   component in mixture
m   moisture
M   mass
p   pure component
pp   penetration period
Q   transition point (Penetration Period/Regular Regime)
r   reduced value
s   solid
sat   saturated
T   transition point (Penetration Period/Regular Regime)
v   vapour
0   value at t=0
1   first root
1   internal radius
2   external radius
✱   equilibrium value
reference value
∞   bulk of gas phase

SUPERSCRIPTS

–   average value
□   volume average value
o   molar average value
s   solid
'   gas phase
'   local value
~   (see Table 5.1)

REFERENCES

1. Bird, R.B., Stewart, W.E. and Lightfoot, E.N.
   "Transport phenomena"
   John Wiley & Sons, Inc., New York (1960)

2. Perry, R.H. and Chilton, C.H.
   "Chemical engineers' handbook 5th e.d."
   McGraw-Hill Kogakusha, Ltd., Tokyo (1973)

3. Hell, F.
   "Grundlagen der Warmeubertragung, Dritte Auflage"
   VDI-Verlag GmbH, Düsseldorf (1982)

4. *"VDI-Warmeatlas, Dritte Auflage"*
   VDI-Verlag GmbH, Düsseldorf (1977)

5. Kast, W., Krischer, O., Reinicke,H., Wintermantel, K.
   "Konvektieve Warme- und Stoffubertragung"
   Springer Verlag, Berlin (1974)

6. Rohsenov, W.M. and Hartnett, J.P.
   "Handbook of heat transfer"
   McGraw-Hill (1973)

7. Eckert, E.R.G. and Drake, R.M.
   "Analysis of heat and mass transfer"
   McGraw-Hill (1973)

8. Kast, W.
   "The change of heat transfer and mass transfer coefficient by simultaneous heat and mass transfer"
   Wärme- und Stoffübertragung $\underline{15}$ (1981); 217-222

9. Keey, R.B. and Ma Kecheng
   "On the humidity-potential coefficient"
   Chem.Eng. Res.Des. $\underline{64}$ (1986); 119-124

10. v.d. Berg, C.
    "Vapour sorption equilibria and other water-starch interactions; a physico-chemical approach"
    Ph.D. Thesis, Agricultural University, Wageningen, the Netherlands (1981)

11. Iglesias, H.A. and Chirife, J.
    "Handbook of food isotherms: water sorption parameters for food and food components"
    Academic Press Inc. (1982)

12. Fortes, M. and Okos, M.R.
    "Drying theories: their bases and limitations as applied to foods and grains"
    Advances in Drying, Vol. 1, 119-154
    Hemisphere Publ.Corp. (1980)

13. Bruin, S. and Luyben, K.Ch.A.M.
    "Drying of food materials: A review of recent developments"
    Advances in Drying, Vol 1, 155-215
    Hemisphere Publ.Corp. (1980)

14. Lozano, J.E., Rotstein, E. and Urbicain, M.J.
    "Total porosity and open-pore porosity in the drying of fruits"
    Journal of Food Science, 45 (1980); 1403-1407.

15. Ibid.
    "Shrinkage, porosity and bulk density of foodstuffs at changing
    moisture contents"
    Journal of Food Science, 48 (1983); 1497-1502.

16. Rotstein, E.
    "Advances in transport phenomena and thermodynamics in the drying
    of cellular food systems"
    Proc. 5th Int. Drying Symp., Boston, Vol. 1, 1-11
    Hemisphere Publ.Corp. (1986)

17. English, A.C. and Dole, M.
    "Diffusion of sucrose in supersaturated solutions"
    J. Am. Chem. Soc., 72 (1950); 3261

18. Gladden, L.K. and Dole, M.
    "Diffusion in supersaturated solutions"
    J. Am. Chem. Soc., 75 (1953); 3900

19. Menting, L.C.
    "Retention of volatiles during the air drying of aqueous
    carbohydrate solutions"
    Ph.D. Thesis, Eindhoven University of Technology
    the Netherlands (1969)

20. Menting, L.C., Hoogstad, B. and Thijssen, H.A.C.
    "Diffusion coefficients of water and organic volatiles in
    carbohydrate-water systems"
    J. Food Technology, 5 (1970); 111-126

21. van der Lijn, J.
    "Simulation of heat and mass transfer in spray drying"
    Ph.D. Thesis, Agricultural University, Wageningen,
    the Netherlands (1976)

22. Furuta, T. ,Tsujimoto, S. Makino, H. , Okazaki, M.
    and Toei, R.
    "Measurement of diffusion coefficient of water and ethanol in
    aquous maltodextrin solutions"
    J. Food Engineering, 3 (1984); 169-186

23. Schoeber, W.J.A.H.
    "Regular regimes in sorption processes"
    Ph.D. Thesis, Eindhoven University of Technology,
    the Netherlands (1976)

24. Schoeber, W.J.A.H.
    "A short cut method for the calculation of drying rates in case
    of a concentration dependent diffusion coefficient"
    Proc. 1st Int. Drying Symp., Montreal, 1-9
    Hemisphere Publ.Corp. (1978)

25. Luyben, K.Ch.A.M., Olieman, J.J. and Bruin, S.
    "Concentration dependent diffusion coefficients derived from
    experimental drying curves"
    Proc. 2nd Int. Symp. Drying, Montreal, Vol. 2, 233-243
    Hemisphere Publ.Corp. (1980)

26. Luyben, K.Ch.A.M., Olieman, J.J. and Bruin, S.
    "Comparison of numerical and short-cut drying calculations"
    Proc. Portland

27. Luyben, K.Ch.A.M., Liou, J.K. and Bruin, S.
    "Enzyme degradation during drying"
    Proc. Int. Symp. Food Process Engineering, Helsinki,
    Vol. 2, 192-209,
    Applied Science Publ. (1979)

28. Liou, J.K.
    "An approximate method for nonlinear diffusion applied to enzyme
    inactivitation during drying"
    Ph. D. Thesis, Agricultural Univeristy, Wageningen,
    the Netherlands (1982).

29. Liou, J.K. and Bruin, S.
    "An approximate method for the nonlinear diffusion problem with a
    power relation between diffusion coefficient and concentration.
    Part I: computation of desorption times"
    Int. J. Heat and Mass Transfer, 25 (1982); 1209-1220.

30. Ibid.
    "An approximate method for the nonlinear diffusion problem with a
    power relation between diffusion coefficient and concentration.
    Part II: computation of concentration profiles"
    Int. J. Heat and Mass Transfer, 25 (1982); 1221-1229.

31. Yamamoto, S., Hoshika, M. and Sano, Y.
    "Determination of concentration dependent diffusion coefficient
    from drying rates"
    DRYING '85, 490-497
    Hemisphere Publ. Corp. (1985)

32. Sano, Y., and Yamamoto, S.
    "Calculation method of concentration dependent mutual diffusion
    coefficient based on the assumption of similar concentration
    distribution"
    Proc. Int. Drying Symp., Boston, Vol. 1, 85-93.
    Hemisphere Publ. Corp. (1986)

33. Coumans, W.J. and Thijssen, H.A.C.
    "A simplified calculation method for the isothermal drying of
    solid and hollow systems with any degree of shrinkage"
    Proc. 5th Int. Drying Symp., Boston, 49-56
    Hemisphere Publ. Corp. (1986)

34. Thijssen, H.A.C. and Coumans, W.J.
    "Concise procedure for the calculation of isothermal drying rates
    of non-shrinking solid and hollow particles"
    Proc. World Congr. III of Chem. Eng., Tokyo, 1986

154

35. Rulkens, W.H.
    "Retention of volatile trace components in drying aqueous
    carbohydrate solutions"
    Ph.D. Thesis, Eindhoven University of Technology
    the Netherlands (1973)

36. Kerkhof, P.J.A.M.
    "A quantitative study of the effect of process variables on the
    retention of volatile trace components in drying"
    Ph.D. Thesis, Eindhoven University of Technology,
    the Netherlands (1975)

37. Crank, J.
    "The mathematics of diffusion"
    Clarendon Press, Oxford (1975)

38. Carslaw, H.S. and Jaeger, J.C.
    "Conduction of heat in solids"
    Clarendon Press, Oxford (1959)

39. Luikov, A.V.
    "Analytical heat diffusion theory"
    Academic Press, New York (1968)

40. Bosch, M.L.
    "Drying: constant activity period" (in Dutch)
    Internal Report, Eindhoven University of Technology,
    the Netherlands (1985)

41. Abramowitz, M. and Stegun, I.
    "Handbook of mathematical functions"
    Dover Publications (1970)

42. Keey, R.B.
    "Drying. Principles and practice"
    Pergamon Press, Oxford (1972)

43. Manders, A.J.G.
    "Sorption-Isotherms" (in Dutch)
    Internal Report, Eindhoven University of Technology
    the Netherlands (1983)

44. Van Schaik-Van Hoek, A.
    "Calculation of Sherwood numbers of Regular Regimes of hollow and
    massive systems" (in Dutch)
    Internal Report, Eindhoven University of Technology
    the Netherlands (1985)

STELLINGEN *behorende bij proefschrift W.J. Coumans, TUE, 29 mei 1987*

Stelling 1

Voor systemen, waarin de diffusiecoefficient volgens een machtsrelatie
afhangt van de concentratie en de grensvlakconcentratie *ongelijk nul* is,
neemt het kengetal van Sherwood (betrokken op disperse fase) géén
constante waarde aan gedurende het Regular Regime. Uit eigen onderzoek
blijkt, dat het kengetal van Sherwood als functie van de droogtijd dan
een minimum vertoont.

Liou, J.K., Proefschrift LUW, 1982

Reniers, P., Afstudeerverslag TUE, 1985

Stelling 2

De berekening van droogcurven met een empirische correlatie wordt door
Petersen ten onrechte voorspelling van droogcurven genoemd.

Petersen, J.N., Drying Technology, 4 (1986);319-330

Stelling 3

Het verlies van vluchtige aromacomponenten tijdens drogen vindt plaats
gedurende het droogstadium, waarin de grensvlakconcentratie van de
aromacomponent de waarde nul nog niet bereikt heeft. Bij rekenmodellen
voor het aromatransport is de veel gehanteerde randvoorwaarde, dat reeds
vanaf het begin de grensvlakconcentratie nul zou zijn, daarom onjuist.

Kerkhof, P.J.A.M., Proefschrift TUE, 1975

Stelling 4

Uit het vergelijken van stripexperimenten (alleen aromatransport) en
droogexperimenten (water- én aromatransport) blijkt, dat in rekenmodel-
len voor het aromatransport tijdens drogen de kruisdiffusieterm niet
verwaarloosd mag worden.

de Boer, M., Afstudeerverslag TUE, 1986

Smits, J.H.P.M., Afstudeerverslag TUE,1985

Stelling 5

De wijze waarop Gupta et. al. op basis van beschikbare correlaties voor
de warmteoverdracht een nieuwe correlatie samenstellen, leidt niet tot
een beter begrip van het warmteoverdrachtsproces.

Gupta et.al., Chem.Eng.Sci., 29 (1974), 839-843

Stelling 6

De door Furuta et.al. berekende diffusiecoefficienten voor water in maltodextrine oplossingen zijn niet in overeenstemming met de door hen gepubliceerde droogcurven.

Furuta et.al., J.Food Eng., 3 (1984); 169-186

Stelling 7

Door Van de Lijn wordt niet onderkend, dat een kleine meetfout in de sorptie-isotherm zeer kritiek is bij het voorspellen van een explosie van een drogende holle druppel in een sproeidroger.

van de Lijn, J., Proefschrift LUW 1976

Stelling 8

Ook als de algebraische oplossing bekend is, kan numerieke discretisatie van differentiaal vergelijkingen rekentechnisch grote voordelen bieden.

Bosch, M.L. ,Prakticumverslag TUE, 1985

Stelling 9

Het gebruik van een interne standaard bij de analyse van vluchtige sporencomponenten (in bijv. sinaasappelsap) m.b.v. een destillatie/ extractie methode kan tot een sterke vergroting van fouten leiden.

van Spreeuwel, M.C.W., Afstudeerverslag TUE 1984

Stelling 10

De bewering van McCathren, dat het polijsten van klarinet-rieten voor-komt dat tijdens het spelen de capillairen in het riet gevuld raken met speeksel, is onjuist. Evenmin is de bewering juist dat door polijsten de ongewenste veroudering van het riet door enzymatische afbraak van de vezels wordt voorkomen.

McCathren, D.E., The Instrumentalist, October 1985, 56-63

Stelling 11

Een gezonde muzikale ontwikkeling van amateur Harmonie- en Fanfare-orkesten wordt vaak gehinderd door het traditionele verwachtingspatroon dat de gemeenschap heeft van deze orkesten.